A FUNDAMENTAL STUDY OF THE FLOW OF DILATANT FLUIDS

by

Richard G. Green

Thesis submitted to the Graduate Faculty of the

Virginia Polytechnic Institute

in candidacy for the degree of

DOCTOR OF PHILOSOPHY

in

CHEMICAL ENGINEERING

APPROVED: _____
                        Dr. G. H. Beyer

_____   _____
Dr. R. G. Griskey   Dr. G. B. Wills

_____   _____
Prof. A. J. Metzger   Dr. J. P. Wightman

June 1966

Blacksburg, Virginia

A FUNDAMENTAL STUDY OF THE FLOW

OF DILATANT FLUIDS

by

Richard G. Green

B.S. in Chemical Engineering

Thesis submitted to the Graduate Faculty

of the

Virginia Polytechnic Institute

in candidacy for the degree of

DOCTOR OF PHILOSOPHY

in

CHEMICAL ENGINEERING

1966

Blacksburg, Virginia

TABLE OF CONTENTS

LIST OF TABLES

LIST OF FIGURES

I. INTRODUCTION

As chemical engineering matures, it becomes increasingly difficult to define its frontiers. The classical areas of heat transfer, mass transfer, and fluid flow no longer monopolize the attention of the chemical engineer---now it is process optimization, computer utilization, and the in-line use of analytical instruments that excites his imagination.

It is fortunate that the horizons of the chemical engineer are widening, for it lends an excitement to the field that might otherwise be missing; it is the misfortune of chemical engineering that such glamour fields may thrive to the neglect of the older, more traditional fields in which there still remains much work to be done.

In the realm of fluid flow technology, one area which has suffered an obvious neglect is the flow of dilatant fluids. Since the recognition of these fluids as a distinct class nearly a century ago, fewer than a score of papers dealing with their rheology have been published in the open literature. Even then, the papers have been concerned with an explanation of the phenomenon of dilatancy or with a study of its rheology, and nowhere is mention made of an attempt to study dilatant fluids in pipe-line flow.

It becomes more and more important to understand the technology of dilatant fluids as processes and products in

which these materials appear assume greater commercial importance. Examples that may be cited are: high solids content pigment slips for coatings, vinyl resin plastisols, lubricating greases, and the pumping of beach sands for erosion control.

It is in recognition of this general deficiency in chemical engineering technology that the present investigation is undertaken. The purpose of this investigation is to test dilatant fluids under pipe-flow conditions, to test proposed scale-up correlations for their applicability to dilatant fluids, to determine pressure drops across selected fittings through which dilatant fluids are flowing, and to propose a basic theory for dilatancy.

II. LITERATURE REVIEW

Before presenting the literature review of dilatant fluids it might be well to define two terms pertinent to the subject: rheology and rheologist. Rheology is that branch of science concerned with the flow behavior of fluids; investigators whose primary interest lies in this branch of science are known as rheologists. However, it should not be assumed that rheology is the exclusive domain of the rheologist, for the chemical engineer must deal with fluid rheology each time he designs or attempts to scale up a system where fluids are being handled.

The literature review of dilatant fluids will be divided into two major segments. The first segment will place dilatant fluids in their proper perspective by presenting a general treatment of the entire field of fluid rheology; the second segment will be concerned exclusively with a detailed review of the literature dealing with dilatant fluids.

General Review of Rheology

As an introduction to the literature of the general field of rheology, the various classes of fluids, equations relating flow parameters, and methods of pipeline design will be presented.

Newtonian Fluids.   By far the most common and well
known class of fluids is the class known as the Newtonians.
This class is exemplified by most pure substances such as
water and glycerine, by low viscosity oils, and by many
dilute solutions of low molecular weight materials. The
distinguishing feature of this class of materials is that
rate of shear and the resultant stress arising in these
fluids are proportional, the proportionality constant being
known as the coefficient of viscosity. For a Newtonian
fluid, the coefficient of viscosity serves to define com-
pletely its flow behavior. Newtonian fluids are rheolog-
ically simple and fortunately are very common---they are of
such common occurrence that fluids not exhibiting Newtonian
behavior are said to show 'anomalous' flow.

Non-Newtonian Fluids.   All fluids not exhibiting
Newtonian flow are classified as non-Newtonian. Unlike
the Newtonians, which have a curve of shear stress versus
shear rate that is straight and passes through the origin,
the non-Newtonians have flow curves which are either not
straight, do not pass through the origin, or are incapable
of being represented fully on a two-dimensional plot of
shear stress versus shear rate because of time, strain, or
external force dependency.

Distinguishing features of the time independent fluids
are readily seen from Figure 1:   a Bingham plastic flows
only after some finite stress level is attained and there-
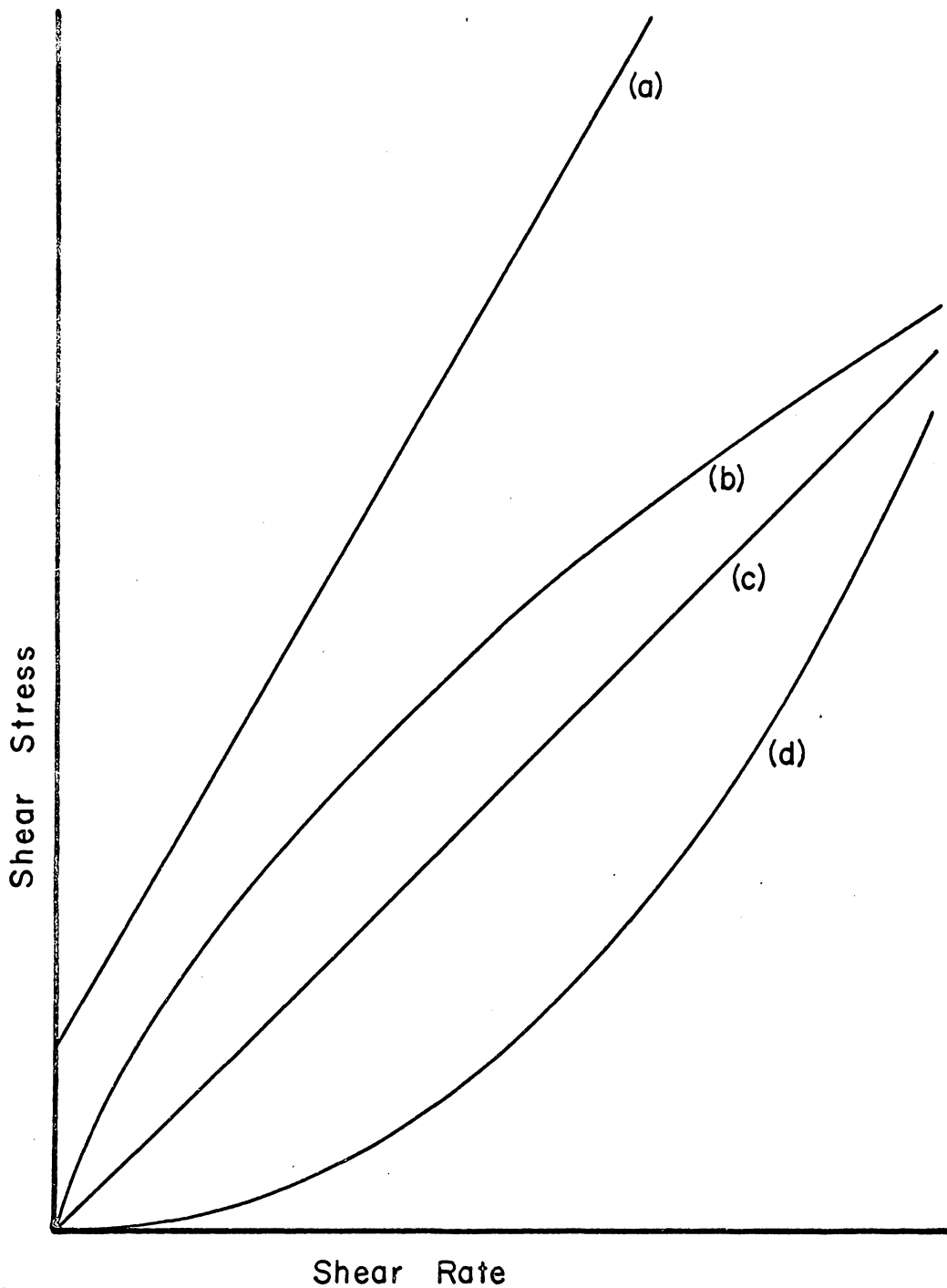
Figure 1   Typical Flow Curves for Time-Independent
            Fluids: (a) Bingham Plastic (b) Pseudo-
            plastic (c) Newtonian (d) Dilatant

after behaves as a Newtonian fluid with shear rate and shear stress proportional; a pseudoplastic flows at all stress levels but each succeeding increment of shear rate produces a smaller increment of stress(i.e., there is an apparent decrease in viscosity with increase in shear rate); a dilatant fluid also flows at all stress levels but each succeeding increment of shear rate produces an increasing increment of stress(i.e., there is an apparent increase in viscosity with increase in rate of shear). It should be mentioned that Figure 1 represents rather idealized cases.

An analogy may be drawn between the time-dependent fluids and certain of the time-independent fluids. Rheopectic and thixotropic fluids belong in the time-dependent category because they have flow properties dependent upon the rate of shear and the duration of shear. Rheopectic fluids may be considered as time-dependent counterparts of dilatant fluids while thixotropic fluids may be considered to have a similar relationship to the pseudoplastics.

Other rheological classifications that may be mentioned are the viscoelastic fluids, the external force-dependent fluids, and the two-phase fluids. The viscoelastic fluids are distinguished by an ability to partly recover their original shape when shearing stresses are removed(much as would be expected of a solid) and, further, the rate of shear is dependent upon both shear stress and strain. The fluids showing flow behavior dependent upon externally

applied fields, such as electrical or magnetic fields, are of rather limited interest to the chemical engineer. The problems of the flow of discontinuous or two-phase fluids are becoming more and more important but are ill-defined at the present time.

Constitutive Equations. The mathematical expression relating the state of stress of a fluid and its flow behavior may be called a 'constitutive equation' or even a 'rheological equation of state'. Constitutive equations are of the utmost practical importance, for they serve as bases for the utilization of viscometric data for pipeline design purposes.

By far the most important constitutive equation is that of Newton[1] which describes the flow of a Newtonian fluid:

$$\tau = \mu \dot{\gamma}$$

where: τ = shear stress, lb_f/ft^2

μ = coefficient of viscosity, $lb_f\text{-}sec/ft^2$

$\dot{\gamma}$ = shear rate, sec^{-1}

Because this equation describes the flow properties of the most simple rheological case, it also has the most simple form of all the constitutive equations proposed to date and contains only one constant. Table 1 presents a partial list of constitutive equations that have been proposed, with some of the constitutive equations being

Table 1

Constitutive Equations

ORIGINATOR(S)	EQUATION	RHEOLOGICAL CLASSIFICATIONS FOR WHICH APPLICABLE	ARBITRARY CONSTANTS
Eyring	$\tau_{yx} = A \ \text{arcsinh}\left(-\dfrac{1}{B}\dfrac{dv_x}{dy}\right)$	Newtonian, pseudoplastic	A, B
Ellis	$-\dfrac{dv_x}{dy} = \left(\varphi_0 + \varphi_1\lvert\tau_{yx}\rvert^{\alpha-1}\right)\tau_{yx}$	time-independents	$\varphi_0, \varphi_1, \alpha$
Reiner-Philipoff	$-\dfrac{dv_x}{dy} = \left(\dfrac{1}{\mu_\infty + \dfrac{\mu_0 - \mu_\infty}{1+(\tau_{yx}/\tau_s)^2}}\right)\tau_{yx}$	time-independents	$\tau_s, \mu_0, \mu_\infty$
Bingham	$\tau_{yx} = -\mu_0\dfrac{dv_x}{dy} \pm \tau_0$	Bingham plastics	μ_0, τ_0
Ostwald-deWaele	$\tau_{yx} = -m\left\lvert\dfrac{dv_x}{dy}\right\rvert^{n-1}\dfrac{dv_x}{dy}$	time-independents	m, n

Bird, R.B., et. al.: "Transport Phenomena," pp.11-13. John Wiley & Sons, New York, N.Y., 1960. 1 ed.

applicable only to special rheological classes. A somewhat fuller treatment will be given to one of the constitutive equations, namely the power law, in the following paragraphs.

The Power Law. Although a large number of equations have been proposed to cover the general case of the flow of time-independent fluids, perhaps the equation that has been shown to have more utility than any other for design purposes is the power law of Ostwald-deWaele[47]:

$$\tau = K(\dot{\gamma})^n$$

where K and n are arbitrary constants.

This equation has been popular because of its simplicity and its ability to fit the data relatively well[62]. However, the equation has come under criticism by Reiner[51] for its failure at very low and very high shear rates. The constant K is a consistency index, indicating the fluidity of the material, while the constant n is known as the flow behavior index and is a measure of the degree of divergence of the fluid from Newtonian behavior. For values of $n > 1$, the equation predicts dilatant behavior; for values of $n < 1$, the equation predicts pseudoplastic behavior; the equation reduces to that of Newton for $n = 1$.

The power law has been used as the basis of design by a number of investigators[37,39,60,etc.]. Numerous design equations based on this law will be reviewed in the following section.

Pipeline Flow. Of paramount importance to the chemical engineer is a knowledge of the design criteria for the flow of fluids in conduits. Since there have been virtually no investigations reported in the open literature concerning the flow of dilatant materials in conduits, the more general approach of using the power law fluid as a basis of design will be presented.

Using a relationship originally presented by Rabinowitsch[49] and later modified by Mooney[44], Metzner and Reed[39] showed how the determination of the two power law constants, K and n, could lead to the necessary information for pipeline design. The utility of their approach was demonstrated by experimental investigations with pseudoplastic materials.

The method of Metzner and Reed consists of substituting their value of $D \Delta P/4L$ from the expression:

$$\frac{D \Delta P}{4L} = K' \left(\frac{8V}{D}\right)^{n'}$$

which was derived by rearrangement and substitution of the Mooney expression, into the expression for the Fanning friction factor:

$$f = \frac{D \Delta P}{4L} \Big/ \frac{\rho V^2}{2g_c}$$

where: f   = Fanning friction factor, dimensionless

           D   = diameter conduit, ft

ΔP = pressure drop, lb_f/ft^2

L = length of conduit, ft

ρ = density of fluid, lb_m/ft^3

V = average bulk velocity, ft/sec

g_c = gravitational constant, $lb_m\text{-}ft/lb_f\text{-}sec^2$

such that the following expression for $\underline{f}$ resulted:

$$f = \frac{16 g_c K' 8^{n'-1}}{D^{n'} V^{2-n'} \rho}$$

Then, by letting $f = 16/Re$ as is done for Newtonian fluids
in laminar flow, the generalized Reynolds number is defined:

$$Re' = \frac{D^{n'} V^{2-n'} \rho}{\sigma}$$

where $\qquad \sigma = g_c K' 8^{n'-1}$

It is easily shown that the Re' relationship converts to
the usual Newtonian expression when $\underline{n}' = 1$.

Dodge and Metzner[10] studied the flow of non-Newtonian
fluids in the turbulent region and derived an equation
analogous to von Karman's resistance formula for Newtonian
fluids. These two investigators also proposed equations
for turbulent velocity profiles in both smooth and rough
pipes. The expressions take the same form as the correspond-
ing equations for Newtonian flow except that allowance is
made for $\underline{n}$, the flow behavior index. These equations are
presented in Table 2.

Table 2

A Comparison of Flow Equations Based on the Power Law and those Based on Newtons Law of Viscosity

QUANTITY	NEWTONIAN EXPRESSION	POWER LAW EXPRESSION
Fanning Friction Factor	$f = \dfrac{D\,\Delta p g_c}{2\,\rho L V^2}$	same
Reynolds Number	$Re = \dfrac{DV\rho}{\mu}$	$Re = \dfrac{D^{n'}V^{2-n'}\rho}{g_c K' 8^{n'-1}}$
Poiseuilles Law	$Q = \dfrac{\pi r^4 \Delta P}{8\mu L}$	$Q = \dfrac{n\,\pi r^3 (r\,\Delta P/2L)^{1/n}}{(3n+1)k^{1/n}}$
Coefficient of Friction	$C_f = 16/Re$	$C_f = 16/Re$
Laminar Velocity Profile	$u = 2u_m(1 - r^2/a^2)$	$u = u_m\left(\dfrac{3n+1}{n+1}\right)\left[1 - \left(\dfrac{r}{a}\right)^{\frac{n+1}{n}}\right] + \varphi(n)$
Turbulent Velocity Profile		
a) laminar sublayer	$u^+ = y^+$	$u^+ = (y^+)^{1/n}$
b) buffer zone	$u^+ = 5.5 + 5.75\log_{10}y^+$	$u^+ = c_1 + c_2 \log_{10}y^+$

Criteria for the onset of turbulence in non-Newtonian fluids were studied by three sets of workers: Weltmann[60] integrated the power law to give a family of curves in the laminar region with parameter $\underline{n}$ such that the appropriate intersection of the laminar line and the proper turbulent friction factor line for Newtonian fluids would give the Reynolds number for the onset of turbulence. Metzner and Reed[39] suggested that the transition occurs when the friction factor falls below 0.008; Dodge and Metzner[10] found that the critical Reynolds number increased with a decrease in flow behavior index.

The problems of entrance lengths and expansion and contraction losses have been the object of much research. Bogue[2] has studied the general problem of entrance lengths and has concluded that the entrance length decreases with Reynolds number and increases with $\underline{n}$. For expansion losses in laminar flow, Wilkinson[67] has presented a purely theoretical expression relating loss of head due to expansion to the ratio of cross-sectional areas and the flow behavior index. Toms[56], Weltmann and Keller[61], and Dodge[9] all reached different conclusions regarding contraction losses.

It must be emphasized that all of the experimental work reported above dealt with pseudoplastics as the power law fluid; the correlations were postulated to hold for dilatant fluids in most cases, but no experimental evidence was advanced.

Review of Dilatant Rheology

Although there has been a general lack of experimental studies dealing with the rheology of dilatant fluids, work has been reported sporadically throughout the literature and will be reviewed in the following paragraphs.

Historical Aspects. The general phenomenon of dilatancy was observed and named by Osborne Reynolds in 1885. Reynolds[52] observed that a mixture of beach sand and water confined in a balloon would dilate if deformed; i.e., the total volume of the mixture would increase under pressure, causing the liquid level in the balloon to be lowered. In addition to the dilation, such a mixture would exhibit increasing resistance to stirring as the rate of stirring was increased, until rupture of the pseudo-solid material that resulted would occur.

A more general meaning to the term dilatant fluid was given by Freundlich and Roder[21] in 1938 when they extended it to all materials showing increasing apparent viscosity with increasing rate of shear. Williamson and Heckart[70] chose to coin another phrase, 'inverted plasticity', to differentiate between volumetric dilation versus no volumetric dilation. Dilatancy in the rheological sense has come to mean the exhibition of a concave shear stress versus shear rate curve and will be used in that context throughout this paper.

The question has been raised by Jobling and Roberts[26] as to whether dilatancy may not be a property common to all plastics and metals; they give as an example the shear hardening that can be induced in metals by the application of thermal stresses.

Dilatant Systems Studied.   In general, most workers have confined their studies on dilatancy to one or two systems. However, Fischer[16] has studied a broad range of aqueous and non-aqueous suspensions of organic and inorganic materials. No attempt will be made to comment on each dilatant system studied; instead, the dilatant systems reported in the literature are tabulated with references in Table 3. Particularly interesting systems are the vinyl resin plastisols studied by Gunnerson and Gallagher[23].

Parameters Affecting Dilatancy.   The primary conditions establishing dilatant flow have been summarized by Fischer[17] and are as follows:

1. volume concentration of the suspended phase

2. age of the dispersion

3. quantity and nature of the deflocculating agent added

4. particle size and shape of the dispersed solid.

The volume concentration of the dispersed phase has received more attention than any other factor[14,21,40,etc.] although the particle size of the dispersed phase has also received considerable attention[4,17,41]. Pryce-Jones[48]

Table 3

Dilatant Systems

DISPERSED PHASE	CONTINUOUS PHASE	REFERENCES
gum arabic	aqueous borax solution	48
corn starch	aqueous sugar solution	48
glass particles	water	4,48,52
metallic particles	organic liquids	12,58
titanium dioxide	water, sugar solution	40
Catalpo clay	water	20
gypsum, calcium carbonate, quartz	water	20,52
quartz, starch	water	21
vinyl resin	dioctyl phthalate	23
graphite	ethylene dibromide, oil	26
metallic oxide pigments	water	3,12
starch	water	70,12
starch	carbon tetrachloride	12
calcium carbonate, barium sulfate	water, formamide, carbon tetrachloride	12
starch	ethylene glycol	12

and Daniel[3] were particularly concerned with surface of properties of the dispersed phase and the use of wetting agents to acquire the proper interfacial relationships. Freundlich and Roder[21] and Freundlich and Jones[20] have proposed that low sedimentation volume is a necessary requisite for dilatancy---hence the use of wetting agents to deflocculate dilatant suspensions. Fischer[15] has presented data to show that many dilatant materials change in their degree of non-Newtonian behavior with age: a starch/water suspension increased in dilatancy with age while an iron oxide/water solution exhibited the opposite effect of decreasing in dilatancy with age.

The Mechanism of Dilatancy. An explanation of the mechanism of dilatancy was first offered by Reynolds[52]. He felt that two conditions had to exist in order for dilatancy to occur. First, the dispersed phase must be capable of settling to a condition of minimum voids, i.e., hexagonal close packing. Secondly, there must be just enough solvent present to fill the voids when the particles are in this state of close packing. Any disturbance of such a system would cause a rearrangement of the particles to a state of greater void volume, thereby permitting the solvent to be drawn into the mass. This migration of solvent would create regions of poorly lubricated particles which would offer great resistance to shear forces because of the need to overcome the surface tension of the solvent. As the rate

of shear increased, the departure of the particles from close packing would be more and more pronounced, giving rise to greater and greater resistance to shear. Such was the theory of the mechanism of dilatancy as given by Reynolds; some later investigators [18,21] have agreed in essence with this explanation.

Williamson and Heckart[70] proposed a 'concentric shell' theory to explain the results of their experiments on dilatant materials with a cup and bob viscometer. They proposed that concentric shells of material form around the bob and that part of the shells move with the bob while the rest remain motionless with the cup. As the shear rate increases, more and more of the shells are seized by the bob with the result that the drag on the bob increases.

More recently, Metzner and Whitlock[42] have proposed an explanation for the shape of the flow curves of concentrated suspensions, which they found to be S-shaped and which exhibited a change in flow behavior with increasing shear rates, from Newtonian-to-pseudoplastic-to-Newtonian-to-dilatant. According to these investigators, Newtonian behavior occurs at very low shear rates because of the absence of forces sufficiently large to affect either the alignment or the size of the particles. But at higher shear rates pseudoplasticity manifests itself because the particles either start to align, or are broken down if in a loosely aggregated form. At still higher rates of shear the part-

icles have formed streamlines so that momentum interchange
between particles actually involves not just two particles
at a time, but two streamlines of many particles, thus giving
rise to dilatancy. It is the necessity of overcoming the
pseudoplastic tendency that gives the second Newtonian region,
for at this point the pseudoplastic and dilatant tendencies
will just offset one another.

III. EXPERIMENTAL

This section contains detailed information dealing with the materials and apparatus used, as well as the experimental procedure. In addition, the experimental data and the calculated results are presented, with an illustrative example of each type of calculation given.

Plan of Experimentation

The method of approach used in this investigation is presented in the following paragraphs.

Literature Review. A search of the open literature was made to determine what had been done in this specific field or in related fields. In particular, rheological data on dilatant fluids was of interest, as were the methods for correlating pipe-flow data for non-Newtonian fluids. A study of the literature was particularly useful in choosing the dilatant fluids to be studied.

Selection of System. Suspensions of starch in ethylene glycol, glycerine, and water were chosen for study because 1) the glycol and glycerine were available and the starch was inexpensive, 2) a broad range of fluid consistencies could be produced by varying the proportions of the solvents, 3) the materials were relatively innocuous and 4) a broad range of degrees of dilatancy at acceptable fluid consist-

encies could be produced when a combination of these materials was used.

Experimental Procedure. Considering dilatant fluids as being power law fluids, it was of interest to check postulated correlation methods for the three regions: 1) flow behavior index, $\underline{n}$, greater than 1 but less than 2, 2) $\underline{n}$ equal to 2 and 3) $\underline{n}$ greater than 2. The correlation was checked by collecting pressure drop versus flow rate data in pipeline flow, calculating friction factors and modified Reynolds numbers, and comparing these friction factors with those obtained by considering $f = 16/Re'$. The power law constants were obtained from viscometric data.

Additional information was gained from measuring the pressure drop across three fittings, a globe valve, an elbow, and a coupling, and comparing the equivalent diameters obtained with those obtained from Newtonian flow. The degree of dependency of the power law constants on temperature and concentration of the suspended phase was also studied.

The acquisition of knowledge and experience from the study of these materials was used to postulate a basic mechanism for dilatancy.

Materials

A complete and detailed description of all materials used in this investigation is given below.

Beta 58-1. 620.1 centistokes at 100 °F, 32.20 centistokes at 210 °F. Available from American Petroleum Institute. Used as an absolute viscosity standard.

Carbon Tetrachloride. Technical Grade. Lot No. 745531. Obtained from Fisher Scientific Co., FairLawn, N. J. Used as a manometer fluid.

Corn Starch. Keever Pearl 210, Victor Mills Starch. Manufactured by Keever Starch Co., Columbus, Ohio. Used as the dispersed phase for the dilatant fluids.

Ethylene Glycol. Technical Grade. Lot No. C1/2298/JG. Obtained from Union Carbide Chemical Co., Charleston, W. Va. Used as a component for preparing dilatant fluids.

Glycerine. U.S.P. Grade. Lot No. 750592. Obtained from Fisher Scientific Co., Fair Lawn, N. J. Used to calibrate the cone/plate viscometer.

Glycerine, "Star". U.S.P. Grade. Lot No. 5091. Obtained from Proctor and Gamble, Cincinnati, Ohio. Used to calibrate flow apparatus.

Ink, Red Recorder. Obtained from Varian Associates, Palo Alto, Calif. Used in manometer lead water to provide contrast to interface with manometer fluid.

Mercury. Technical Grade. Lot No. 4576. Obtained from J. T. Baker Chemical Co., Philipsburg, N. J. Used as a manometer fluid.

Tetrabromoethane (Acetylene Tetrabromide). Purified

Grade. Lot No. 731122. Obtained from Fisher Scientific

Co., Fair Lawn, N. J. Used as a manometer fluid.

Water, Distilled. Obtained by distillation of Virginia

Polytechnic Institute tap water in a tin lined, steam heated

distillation unit. Used to calibrate Westphal balance.

Water, Tap. Obtained from Virginia Polytechnic Insti-

tute-Radford Water Authority, Radford, Va. Used to prepare

dilatant fluids and to flush out flow apparatus.

Apparatus

A complete list of the apparatus used in this investi-

gation is given on the following pages. Where a piece of

equipment is of novel design or is not commercially available,

its description is supported with a sketch or drawing.

Bucket. Galvanized, 10 qt. Obtained from the Unit

Operations Laboratory, Virginia Polytechnic Institute. Used

to transfer dilatant fluids between weighing station and

storage tank.

Heater, Immersion. Fisher, 300 watts, 115v, 50/60

cycle. Obtained from Fisher Scientific Co., Chicago, Ill.

Used for heating test fluid in flow apparatus to the desired

temperature.

Hydrometer. Fisher, sp gr 1.000-2.000, 0.002 sub-

divisions. Obtained from Fisher Scientific Co., Chicago,

Ill. Used to determine specific gravities of the dilatant fluids.

Manometer. Meriam, U-tube, 50 in., 1/10 in. graduations. Manufactured by Meriam Instrument Co., Cleveland, Ohio. Used to measure pressure drops on flow apparatus.

Mixer. Lightnin', model no. CV2, serial no. 50093Z, 1/8 hp, 115v, 3.4 amp, 100-1800 rpm. Manufactured by Mixing Equipment Co., Inc., Rochester, N.Y. Used in storage tank to agitate test fluid.

Mixer. Alsop, Hy-Speed, type 23V5, serial no. 82476, ¼ hp, 4 amp, 60 cycle, 115v, 500-1800 rpm. Manufactured by Alsop Engineering Corp., Milldale, Conn. Used to prepare the dilatant fluids.

Pump, Moyno. Robins and Meyers, type CDO, serial no. AS9019, 3-13 gpm, 350 psi nominal discharge pressure, tool steel chromium plated rotor, neoprene housing. Manufactured by Robins and Meyers, Inc., Springfield, Ohio. Used to pump dilatant slurry through piping loop.

Piping Loop. Galvanized, 1-¼ in. Schedule 40. Fabricated by the author. Used for studying flow characteristics of dilatant fluids. See Figure 2, page 25.

Pulsation Dampener. Fabricated by author. Used to damp pulsating flow from Moyno pump. See Figure 3, page 26.

Scale. Howe, upright, 0-250 lb, ¼ lb graduation. Available in Unit Operations Laboratory, Department of Chemical Engineering, Virginia Polytechnic Institute. Used

LEGEND

A   MANOMETER
B   MIXER
C   STORAGE TANK
D   LEADS' FLUID RESERVOIR
E   PULSATING FLOW DAMPENER
F   MOYNO PUMP
G   THERMOMETER
H   HEAT EXCHANGER

COOLING WATER

COOLING WATER OUT

COOLING WATER IN

TO SCALES
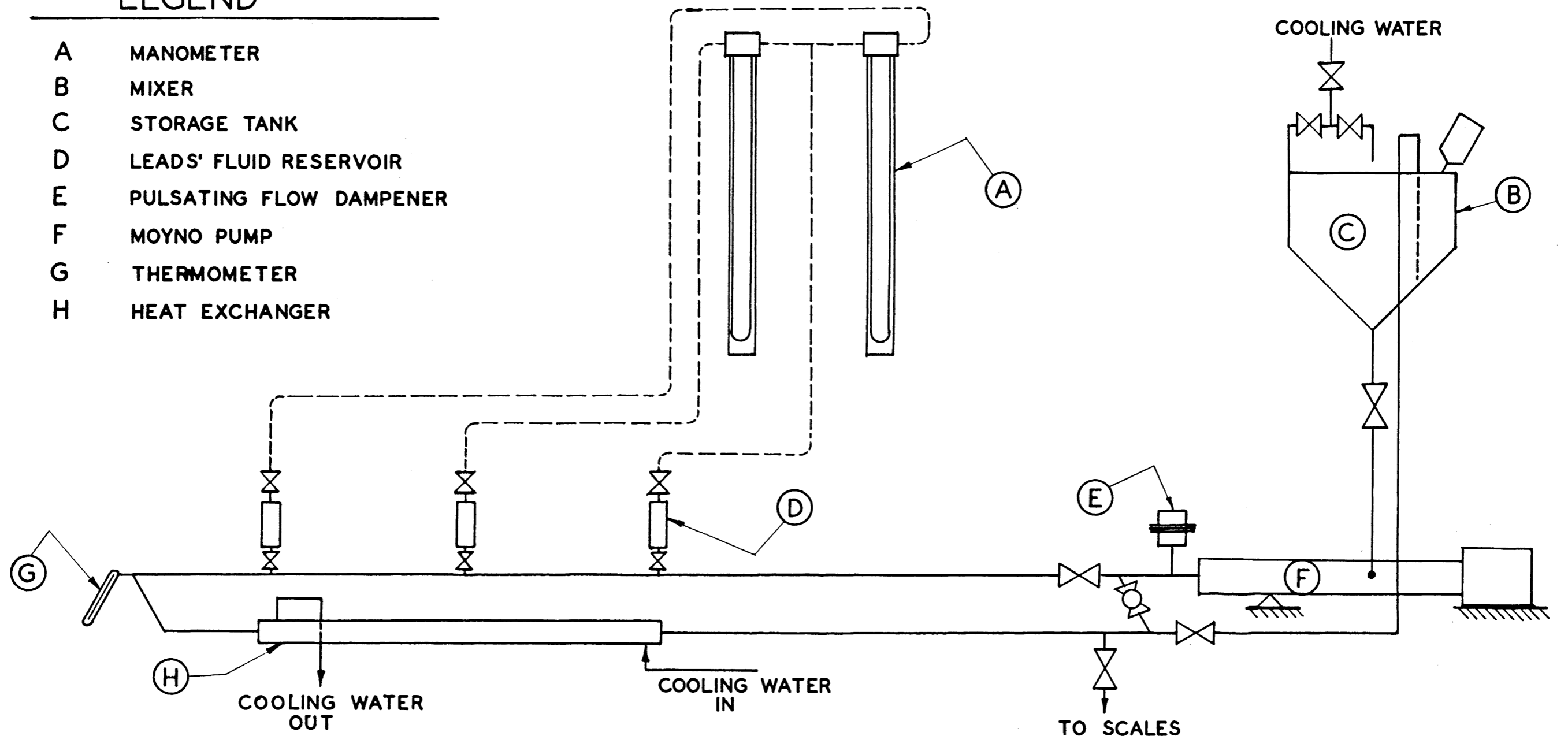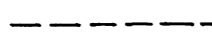
GATE VALVE
GLOBE VALVE
3/8" TUBING

FIGURE 2   FLOW TEST EQUIPMENT

DRAWN BY: RGG
APPROVED BY:
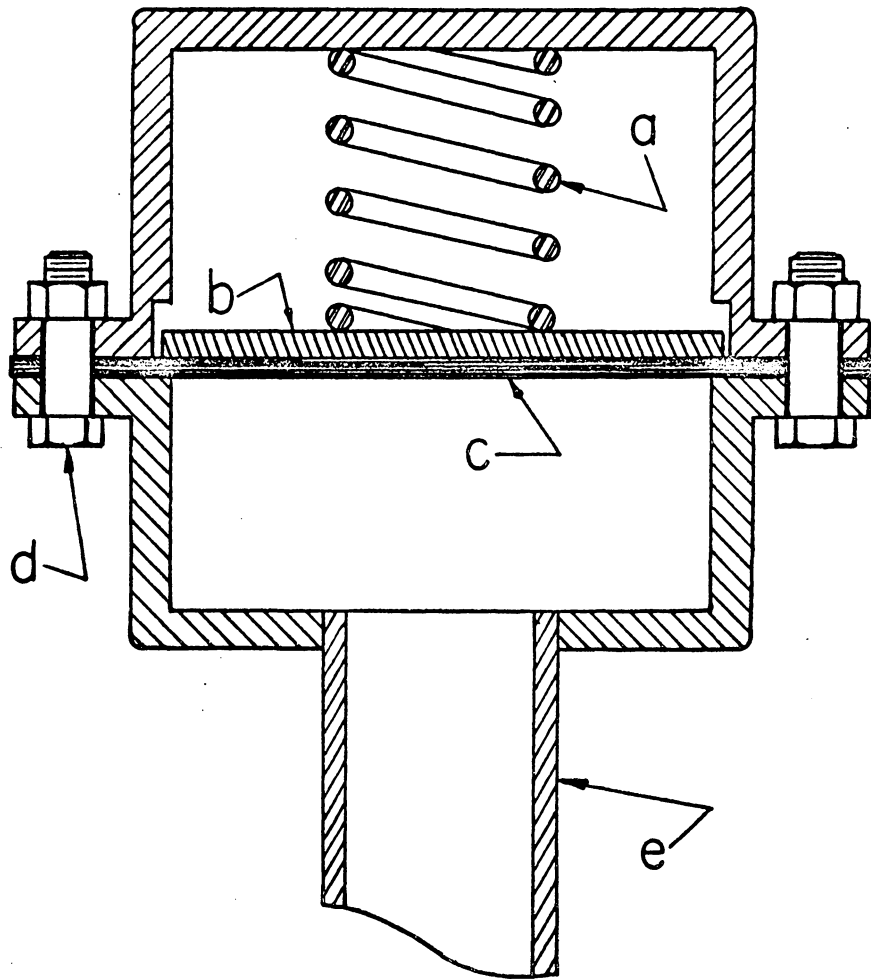
Figure 3   Pulsating Flow Dampener. (a) spring
            (b) rupture disk   (c) rubber diaphragm
            (d) flange bolt   (e) to process line

to prepare test fluids and to measure flow rates during tests.

Switch, Relay. Fisher transistor, model 32, serial no. 101, 115v, 15 amp., 60 cycle. Obtained from Fisher Scientific Co., Chicago, Ill. Used in conjunction with thermoregulator and immersion heater to control the temperature of the test fluid.

Tank, Mixing. Fabricated in Department of Chemical Engineering Shops, Virginia Polytechnic Institute, by cutting off upper third of 55 gal drum. Used for preparing dilatant fluids.

Tank, Storage. Designed by author and fabricated in Department of Chemical Engineering Shops, Virginia Polytechnic Institute. Used to store test fluid and to control test fluid temperature. See Figure 4, page 28.

Thermoregulator. Fenwal, serial no 105886, 70-130 °F. Manufactured by Fenwal, Inc., Ashland, Mass. Used in conjunction with relay switch and immersion heater to regulate temperature of test fluid.

Tub. Galvanized, 20 gal. Obtained from the Unit Operations Laboratory, Department of Chemical Engineering, Virginia Polytechnic Institute. Used to collect fluid during flow test for the determination of fluid flow rates.

Timer. Time-It, precision electric, 0-10,000 sec, 155v, 60 cycle, 5 watt. Obtained from Fisher Scientific Co., Chicago, Ill. Used with the cone/plate viscometer to

WATER INLET

TEST FLUID
RETURN

JACKET
FILL

STORAGE
TANK

A

B

C

D

WATER
OUTLET

JACKET DRAIN

TO REGULATOR

TO MOYNO PUMP
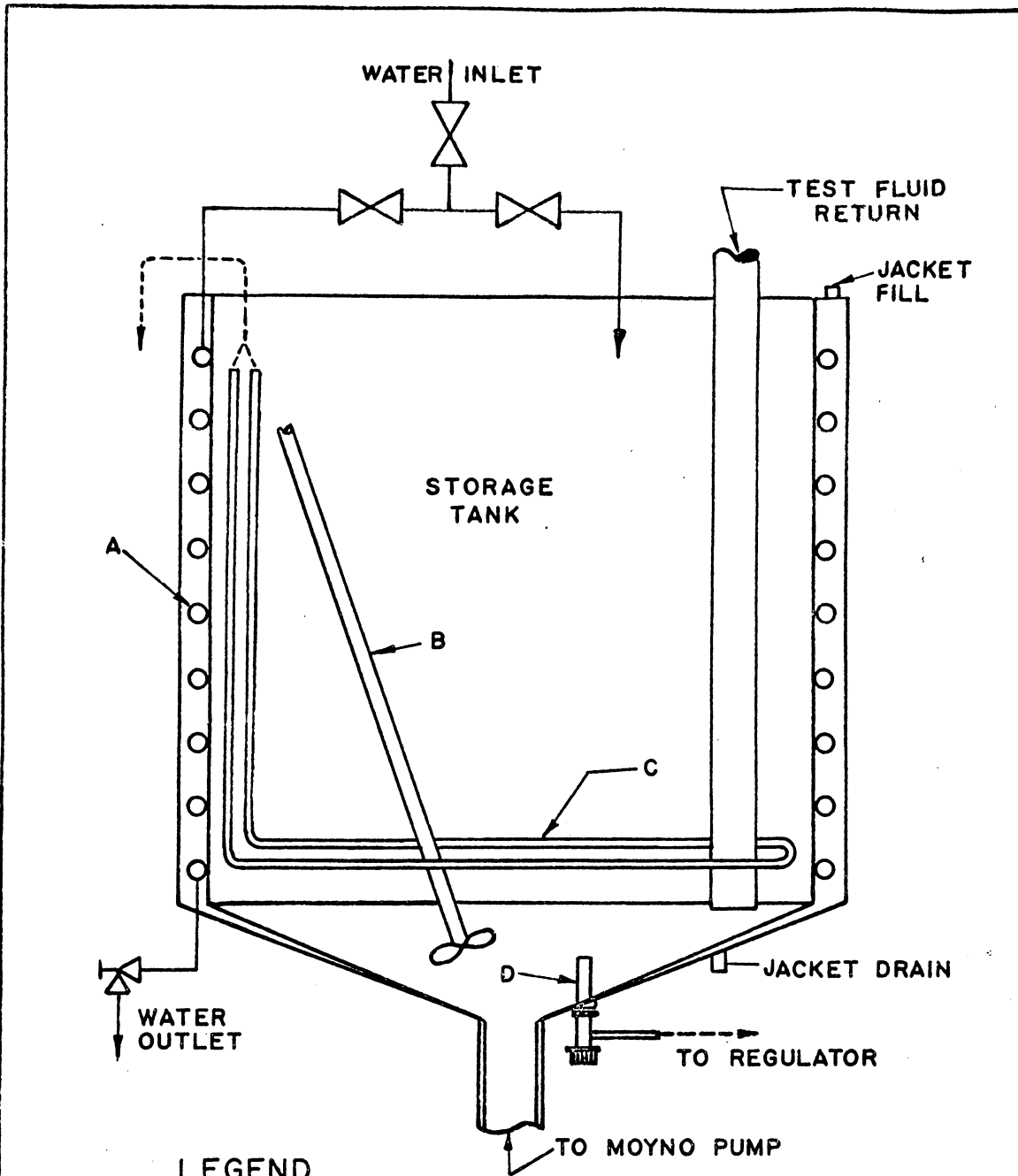
LEGEND

A   3/8" COOLING COILS

B   AGITATOR

C   HEATING ELEMENT

D   THERMOREGULATOR

FIGURE 4   TEST FLUID
STORAGE TANK

SCALE: 3/16"= 1"
DRAWN BY: RGG
APPROVED BY:

determine rotational speeds of the viscometer spindle and with the flow apparatus to determine fluid flow rates.

Viscometer, Cone/Plate. Designed by author and fabricated in Chemical Engineering Shops, Virginia Ploytechnic Institute. Used to determine flow curves of dilatant fluids. See Figure 5 , page 30 for details.

Viscometer, Ostwald-Fenske. Number 300, serial no. 974. Obtained from Fisher Scientific Co., Chicago, Ill. Used to determine the viscosity of the glycerine/water solution used to calibrate the flow apparatus.

Weights. Stormer, auxiliary 25-100.0 g., with 50 g weight hanger. Obtained from Fisher Scientific Co., Chicago, Ill. Used to extend the shear rate range of the cone/plate viscometer.

Wesphal Balance. Number 2-150, sp. gr. 0-2.000. Obtained from Fisher Scientific Co., Chicago, Ill. Used to measure specific gravity of the carbon tetrachloride used as a manometer fluid.
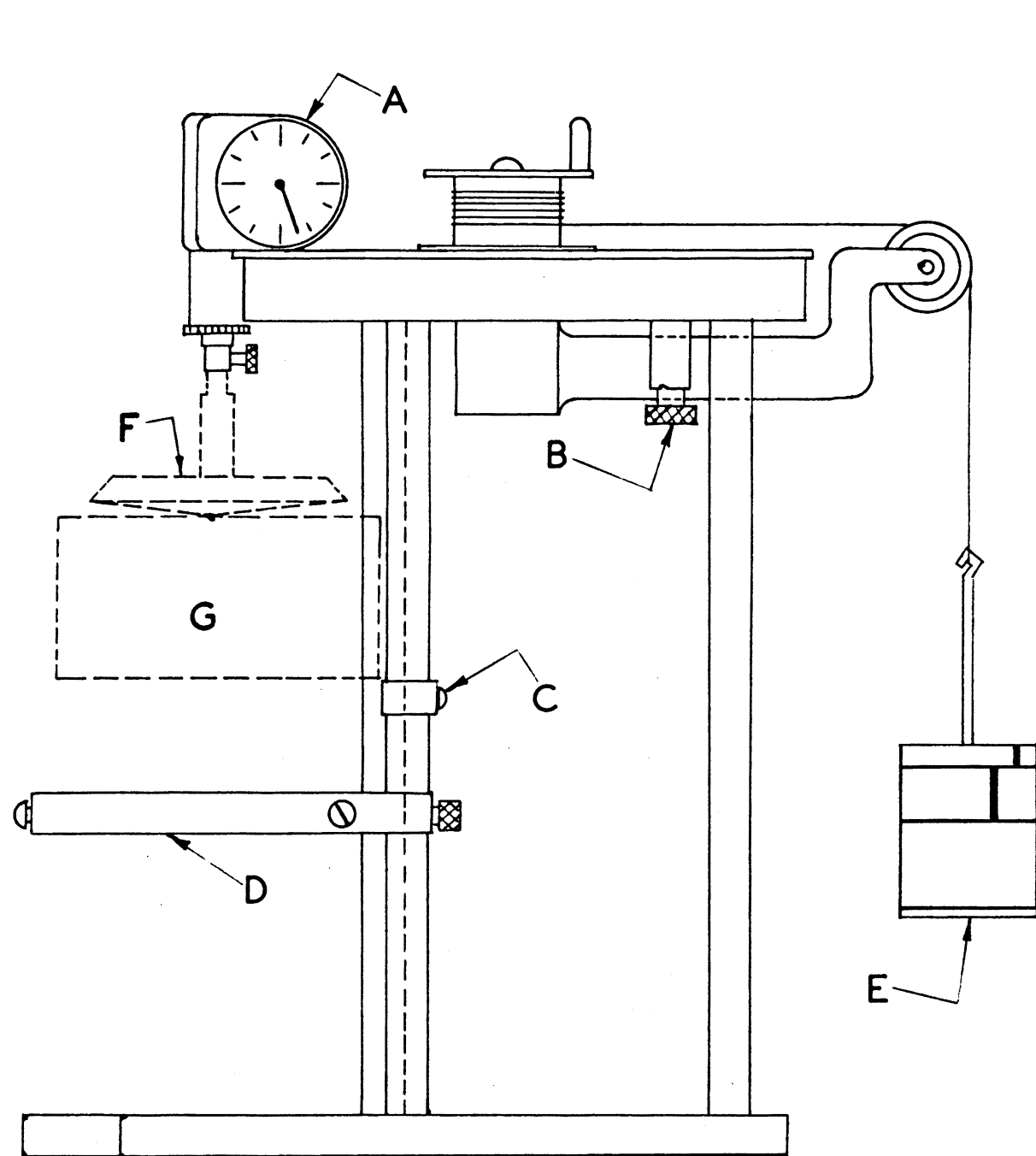
STORMER VISCOMETER
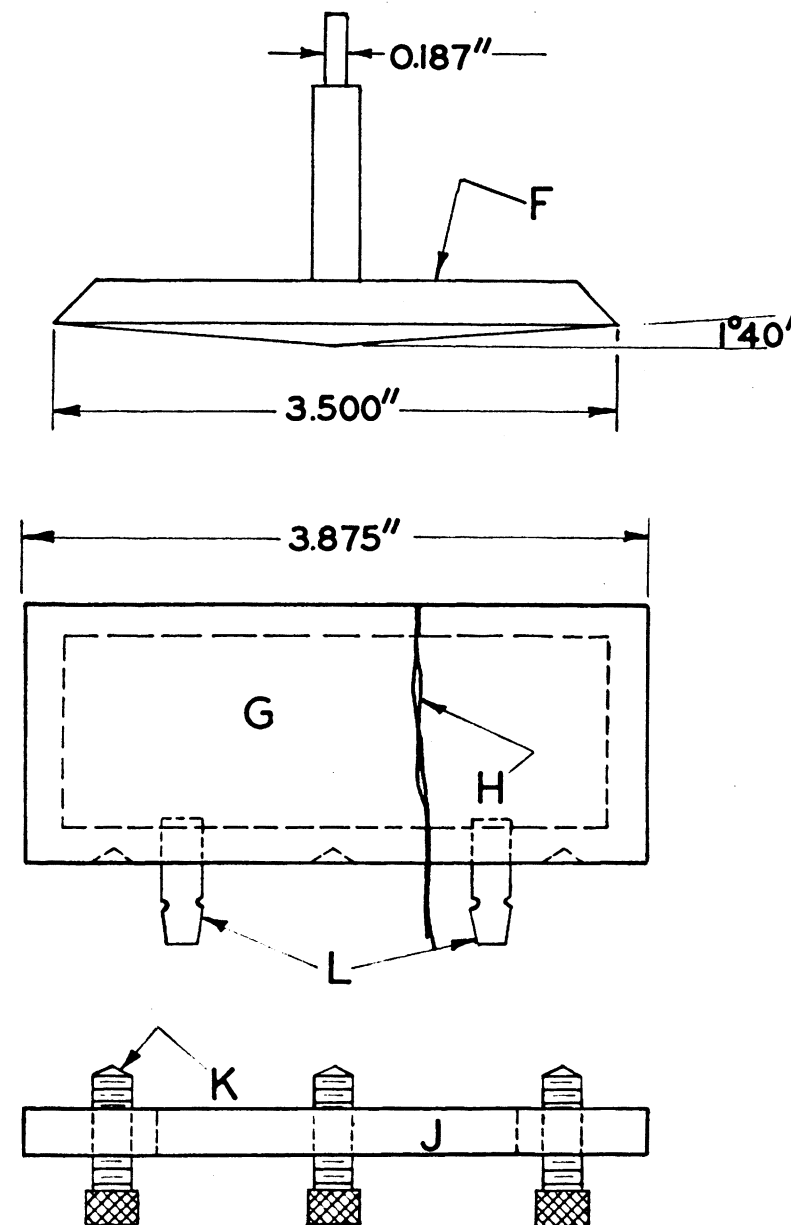
CONE/PLATE ASSEMBLY

LEGEND

A   REVOLUTION COUNTER
B   CLUTCH
C   CARRAIGE STOP
D   CARRAIGE
E   DRIVING WEIGHTS
F   CONE
G   PLATE
H   THERMOCOUPLE
J   SUPPORT ASSEMBLY
K   LEVELING SCREW
L   HEAT TRANSFER PORTS

FIGURE 5: STORMER
VISCOMETER AND CONE
PLATE ATTACHMENT

DRAWN BY: RGG
APPROVED BY:

Method of Procedure

The method of procedure for fabricating special equipment and for collecting data in support of this experimental investigation is outlined in the following paragraphs.

Collection of Flow Curve Data. In order that the power law parameters n and K might be evaluated, it was necessary to procure viscometric data for the construction of a flow curve. Operation of the viscometer proceeded as follows.

The bath for the ice junction was prepared and the junction immersed in the bath. The potentiometer was calibrated by standard techniques. The circulating water bath was set at the desired temperature and the water was allowed to circulate through the plate cavity. The gap between the cone and the plate was filled with water and the temperature of the water followed with the potentiometer. When the desired temperature was reached, the plate was lowered, the cone removed, and both were wiped dry.

Approximately twenty milliliters of test fluid were then poured carefully onto the center of the plate, the cone replaced and the plate raised until it was nearly to the test position. At this point the viscometer clutch was released and a small weight allowed to drop. This served to rotate the cone and draw the fluid evenly into the gap. The plate was again raised until the traveling platform rested against the platform stop. Fluid was then either

added to the periphery of the gap or cleaned away so that the fluid filled the gap just to the edge of the cone.

After the potentiometer indicated that the sample had reached test temperature, the test was started. This temperature equilibration took less than two minutes, the time being small because of the thinness of the sample. The smallest weight to be used was then placed on the weight hanger, the clutch released, and after a few revolutions the time to make a given number of revolutions, as indicated on the revolution counter, was recorded. The largest weight was used next, followed by intermediate weights until seven or eight points were determined. A flow curve could then be prepared from this data by converting the load readings to shear stresses, as shown in the Sample Calculations Section, page 60, and the revolutions per minute reading to shear rate as shown on page 61.

Test Fluid Preparation. The dilatant fluids used for this investigation were suspensions of starch in water, in ethylene glycol, in glycerine, or in combinations of these liquids. After preliminary studies with a viscometer to determine what fluid compositions were desired, the test fluids were prepared in the following manner.

The correct amount of liquid was weighed into the lower half of a fifty-five gallon drum used as a mixing tank. The mixer was started and starch was slowly added until the required amount was incorporated into the mixture. The

mixture was than allowed to agitate for about two hours, at the end of which time the mixer was turned off and the mixture allowed to digest at least overnight. Immediately before the flow test was to be performed, the mixer was again started and the starch re-suspended and agitated for an additional two hours.

Determination of Operating Conditions. The choice of operating temperature was dictated by the following requirements: 1) the temperature had to be great enough that it could be controlled rapidly with the heat exchangers, 2) the temperature had to be low enough that an appreciable pressure drop existed across the test section for the flow rates of interest, and 3) the temperature had to be low enough so that the starch would not cook.

Operating pressures were limited by the ability of the pump to continuously move the test fluid around the piping loop.

Three manometer fluids, mercury, tetrabromoethane, and carbon tetrachloride were used in conjunction with water as the fluid filling the leads to enable operation over the different ranges of pressure drop encountered.

Collection of Pipe-Flow Data. Before loading the test fluid into the storage tank, the pump and pipe-loop were evacuated to remove most of the water remaining in the system from the clean-up of the previous test. The test fluid was then loaded into the tank with buckets, the mixer at the

storage tank started, and the Moyno pump allowed to circulate the fluid around the entire loop. The manometer lead valves were closed to prevent test fluid from entering that section. Water was allowed to circulate freely through the two heat exchangers.

While the test fluid was equilibrating, the fluid reservoirs and the manometer leads were filled with water colored with red recorder's ink. It was necessary to siphon water into the leads to fill them. The manometers were removed from their stand and were cleaned and refilled with the appropriate fluid, usually carbon tetrachloride, up to the zero reading. The colored water was used to fill them to the top of the manometer. By using this procedure to fill the fluid reservoirs, leads, and manometers, the time needed to bleed air from the system was appreciably reduced.

After the pressure indicating system was reassembled, the flow rate to the test section was minimized by fully opening the recycle valve, and the valves between the taps and reservoirs opened, allowing the fluid pressure to act on the manometer system. The recycle valve was then slowly closed to determine whether the manometer could read the pressure drop at maximum flow rate. If it could not, then the temperature of the test fluid was allowed to rise by cutting down the rate of cooling water to the heat exchangers until a reading at maximum flow rate could be taken. The air was then bled out of the manometer leads and the

reservoirs. Since the manometer leads were made of a clear vinyl tubing, the presence of air was readily detected.

At the conclusion of this start-up period, which generally took 3-6 hours, the flow tests were begun. Pressure drop and mass rates of flow were recorded at maximum flow rates for the system, i.e., with the recycle valve fully closed, at minimum flow rates, i.e., with the recycle valve fully open, and at several intermediate points. Between each set of readings the test fluid was allowed to come back to the proper temperature, as evidenced by the temperature readings at the test section thermometer, and by the pressure drop readings on both manometers with the test fluid recycling around the test loop at maximum flow rate.

Generally, ten to thirty pounds of fluid were collected for each test, the collection being timed only after several pounds of fluid had been allowed to flow into the container so that a constant flow rate had been attained. This fluid was returned to the storage tank after each test. Introduction of air into the test system from pouring these viscous materials back into the storage tank made it imperative that the manometer leads be checked periodically for air bubbles.

At the end of the test a 300 milliliter sample of test fluid was collected to be used for determining its flow curve and density.

Specific Gravity of Test Fluids. The specific gravity
of the test fluids was determined at the test temperature by
the use of a hydrometer. The hydrometer was calibrated
initially against water and glycerine.

Specific Gravity of Manometer Fluids. The specific
gravity of the carbon tetrachloride was measured with a
Westphal balance, the Westphal balance being calibrated by
standard techniques.

Handbook values for the specific gravities of tetra-
bromoethane (sp gr = 2.98) and mercury (sp gr = 13.6) were
used.

Density of Starch. A pycnometer bottle was used to
measure the density of the starch. The tare weight of the
pycnometer bottle was first recorded. The volume of the
bottle was then found by weighing it filled with distilled
water at a known temperature. A starch sample was placed in
the bottle and the sample weight recorded. The remainder
of the bottle's volume was filled with water and the bottle
reweighed. With this information, the density of the starch
could be calculated by knowing the volume of the water dis-
placed by the starch sample and the weight of the starch
sample.

Data and Results

The data and results of this investigation are presented in the following paragraphs.

Development of the Rheological Apparatus. Initially, a Stormer viscometer(Couette type) was investigated as a rheometer for studying dilatant fluids. In order that the Stormer viscometer might be suitable for measuring extremely viscous materials, a special cup was machined from brass to eliminate the thermometer well located in the standard Stormer cup. The discovery that end effects in this type of viscometer gave rise to dilatant flow curves for Newtonian materials of less than about 600 centipoise led to its abandonment, since its use would have entailed calibration for effective bob length at numerous shear rates with materials of known viscosity.

The next device constructed for the determination of flow curves was a capillary rheometer. Construction details of the capillary rheometer are shown in Figure 6 , page 38 . This apparatus was constructed from a 12 inch section of a three inch nominal brass pipe threaded at both ends to accommodate standard three inch brass pipe caps. The lower cap was tapped to receive an one half inch plug, through which the precision stainless steel capillary tube was extended and brazed. Nitrogen pressure was introduced through the top of the chamber and was measured with 18 inch, 0-300
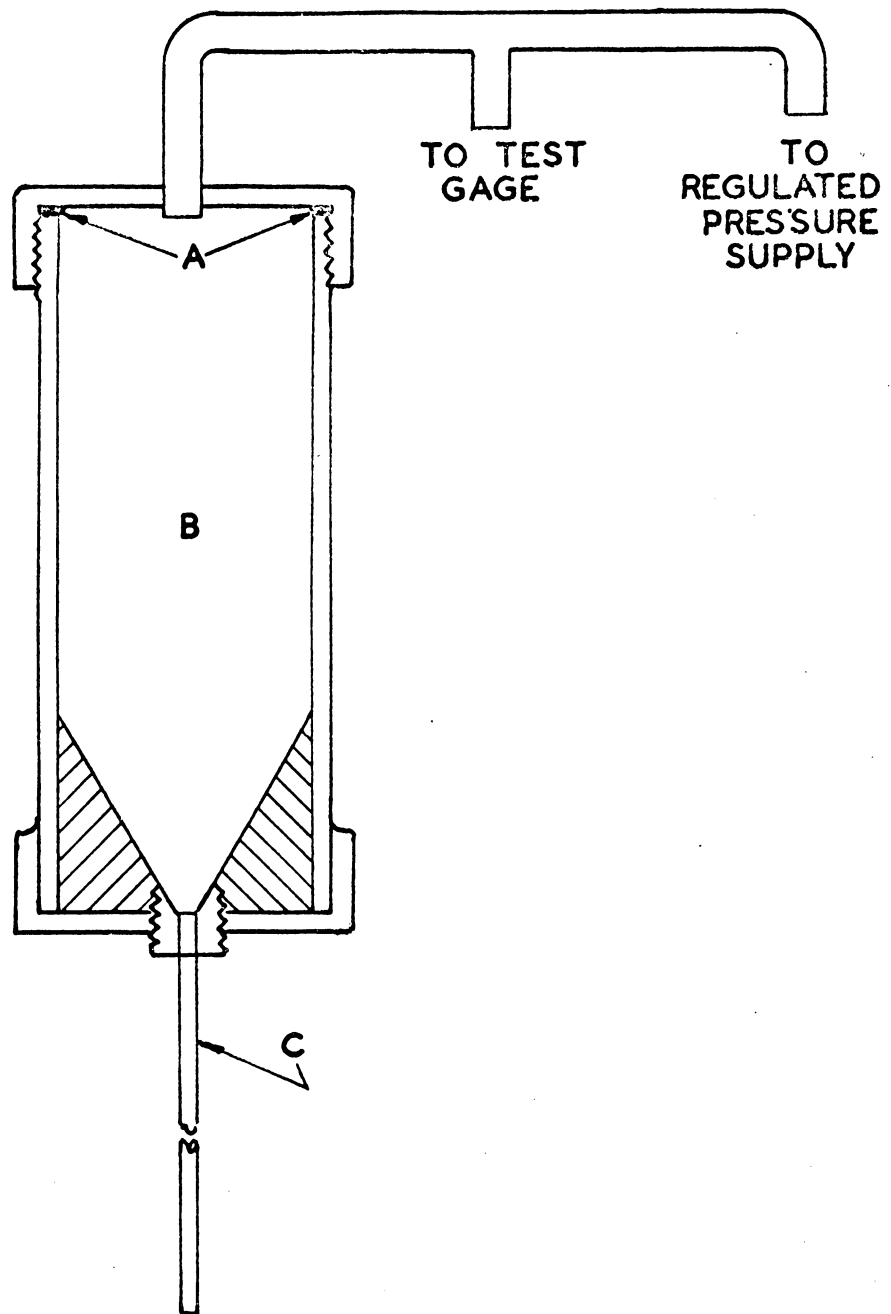
Figure 6   Capillary Rheometer.   (A) chamber
gasket   (B) capillary chamber
(C) capillary tube

pound per square inch test gauges. The capillary chamber was wrapped with an electrical tape for heating the samples. The bottom of the chamber was beveled to aid in preventing the build-up of starch sludges at the bottom of the chamber. However, this rheometer failed to perform satisfactorially with highly dilatant fluids because of preferential exudation of a solvent rich phase through the fine capillary tubes.

Finally, a cone and plate viscometer was fabricated by utilizing the Stormer apparatus. For this purpose, a cone and a plate were machined from four inch aluminum bar stock. The cone was machined in one piece, with a shank to fit in the chuck of the rotating Stormer spindle. The shank portion of the cone was machined to within one half mil of the chuck size to insure a tight sliding fit and proper vertical alignment of the cone. The semi-vertical angle of the cone was measured and found to be $1^{\circ}40'$. The surfaces of the cone and the plate contacting the sample were smoothly polished.

The plate portion of the assembly was provided with a cavity for the circulation of water for temperature control. Piercing the cavity was a copper-constantan thermocouple which was exposed at its junction to the test fluid. Epoxy resin glue was used to seal the two holes provided in the cavity walls for the thermocouple to pass through. The thermocouple was provided with an ice point reference junction and was connected to a standard potentiometer galva-

nometer for potential readings. Temperature readings were taken at each shear rate for a given flow curve.

A support ring machined from aluminum and sized to be clamped in the traveling platform of the Stormer viscometer completed its conversion to a cone and plate viscometer. Three screws with knurled heads passed through the ring and supported the plate assembly; these same screws also functioned as a leveling device for the plate. For a detailed drawing of the cone/plate viscometer, see Figure 5 , page 30.

It was necessary to adjust the alignment of the cone/ plate assembly in three respects: (1) for vertical positioning of the cone axis with respect to the plane of the plate, (2) for vertical positioning of the cone with respect to the plate surface, and (3) for the levelness of the overall assembly. The vertical positioning of the cone axis with respect to the plane of the plate surface was checked by allowing the plate to barely touch the tip of the cone and then measuring the gap around the periphery of the cone with a spacer; adjustments were made with the three leveling screws until a constant gap width all around was achieved. The vertical positioning of the cone with respect to the plate surface was set by adjusting the vertical position of the traveling platform. By sighting between the cone and the plate against a bright background light and comparing the width with a one mil foil strip, the separation between cone tip and plate was set at less than five ten-thousandths of

an inch. The platform stop was then set at this position, insuring the same gap width for subsequent tests. The alignment of the overall assembly was checked with a bubble level placed on the plate surface. Shims were inserted under the viscometer's base to attain a level position.

Calibration of the Cone/Plate Viscometer. Calibration of the cone and plate viscometer was accomplished by testing materials of known viscosity, chosen to cover the range of fluid consistencies of interest. For this purpose, a glycol/water mixture and a standard calibrating oil, Beta 58-1, were used. The viscosity of the glycol/water mixture was determined by Ostwald-Fenske capillary viscometry, while the designated value of the viscosity of the oil was accepted. The values measured by the cone and plate viscometer were found to be sufficiently close to the true viscosities that a correction factor was unnecessary. The viscometric data for these two fluids is presented in Figure 7.

The viscosity of the glycol/water mixture as determined by capillary viscometry was 5.47 centipoise at 80 °F. The indicated kinematic viscosity of 620 centistokes for Beta 58-1 at 80 °F was converted to absolute viscosity and was found to be 553 centipoise. The cone/plate viscometer gave values of 5.47 and 547 centipoise, respectively, for the two fluids at 80 °F. The complete calibration data is given in Table A29, page 29 of Appendix A.
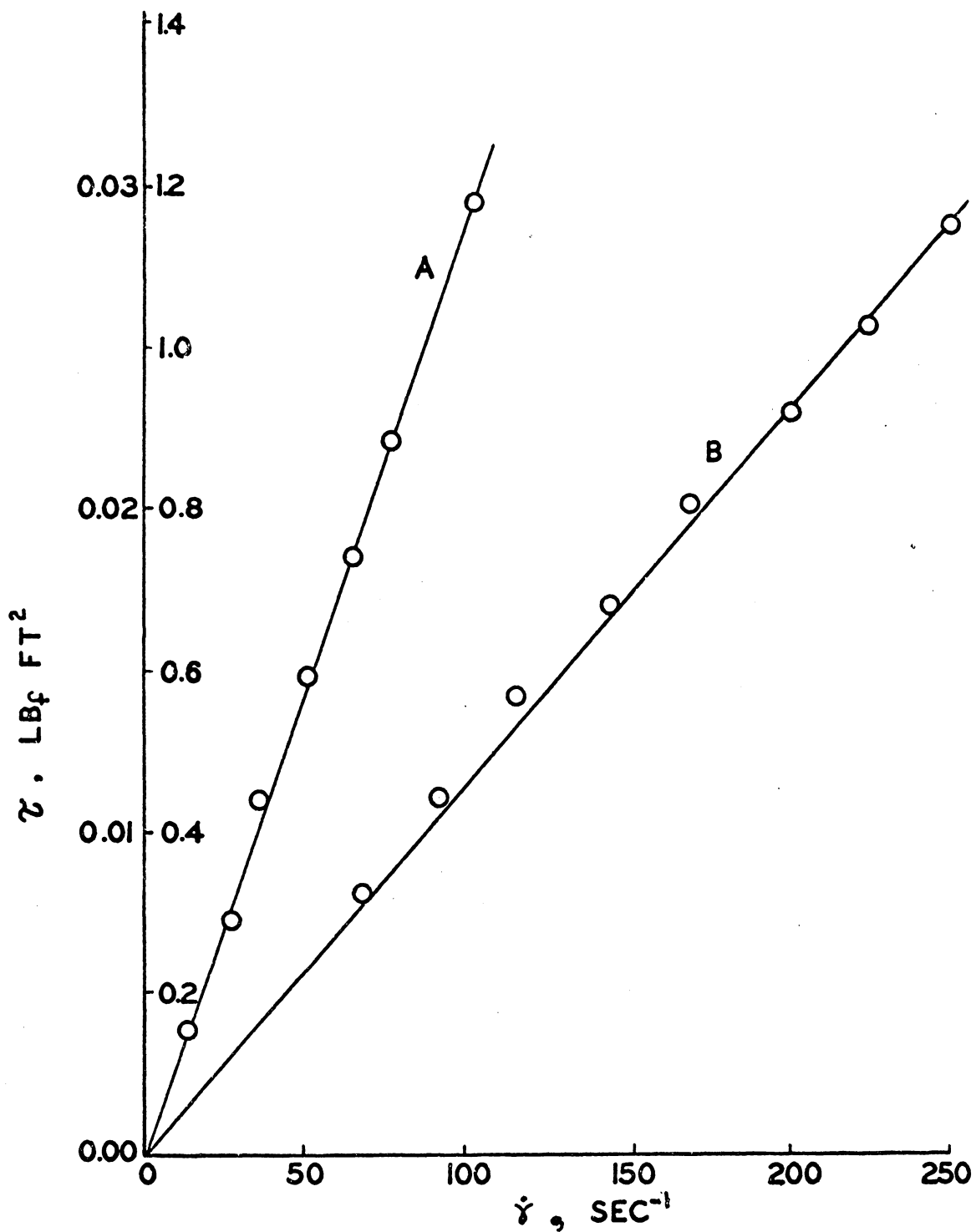
Figure 7   Calibration of Cone/Plate Viscometer:
Viscometric Data.   (A)   Beta 58-1
(B)   ethylene glycol/water mixture

Development of Flow Apparatus. A flow apparatus was developed for the procurement of data relating pressure drop and flow rate. A schematic diagram of the apparatus is presented in Figure 2, page 25 .

The piping loop was constructed from 1-¼ inch galvanized pipe with calming sections preceding and following the test section. Temperature indication was previded with a mercury thermometer installed three feet downstream from the test section. Heating and cooling of the test fluid was controlled by 1) a 300 watt immersion heater in the storage tank, 2) eight feet of double pipe heat exchanger employing water as the transfer fluid and 3) cooling coils in the storage tank, also employing tap water as the transfer fluid. The immersion heater was controlled through a relay which was actuated by a bimetallic temperature sensing element exposed to the test fluid. The two heat exchangers were controlled by adjusting the cooling water valves.

The storage tank was of special construction to provide storage, temperature regulation, and agitation of the test fluid. See Figure 4, page 28. Three pressure taps at the test section enabled the pressure drop over five and ten foot sections of pipe to be measured with the fifty inch manometers. Special fluid reservoirs were provided at each tap to store water for use in purging air from the manometer leads. A globe valve was provided on the recycle line to enable the rate of fluid flowing through the test section to

be varied. Flow rate data was found by timing the collection of test fluid as it effluxed into a bath tub placed on upright scales.

A novel flow dampener was devised to damp the surging flow of fluid from the Moyno pump; this surging flow caused difficulties in reading the manometers. The flow dampener is presented in Figure 3, page 26.

The flow dampener is primarily an elastic, spring loaded membrane against which surges of liquid are allowed to expend their energy. The elastic membrane (c) was cut from one eighth inch rubber sheet stock and was clamped in place by eight machine bolts (d) spaced evenly around the flanged cylindrical damping chamber. A metal plate (b) just small enough to move vertically in the upper damping chamber was fastened to the spring (a) to distribute the effect of the spring over the entire membrane, and to reenforce the membrane. A reduction in cross section of the upper chamber at a small distance above the diaphragm prevented the diaphragm from being distended to its rupture point. The flow dampener was connected to the piping loop via a tee placed immediately after the pump discharge.

Calibration of the Flow Apparatus. A mixture of glycerine and water of known Newtonian character was used to calibrate the flow apparatus. The viscosity of this fluid was determined at the operating temperature with an Ostwald-Fenske viscometer. Results of the calibration are presented

as a plot of friction factor versus Reynolds number in Figure 8, page 46. The data used to construct this plot are given in Table A3, page A3 of Appendix A. The data shows satisfactory agreement between experimental and theoretical values.

Flow Data. An object of this investigation was to determine whether the methods of correlation used for Newtonian fluids could be extended to dilatant fluids by using the technique of Metzner and Reed[39]. Flow data were collected which covered a range of modified Reynolds numbers from 12-400; the dilatant fluids studied had flow behavior indexes between 1.15 and 2.50. Table 4, page 47 summarizes the dilatant systems studied. The flow data is presented in Tables A1-A29, page A1-A29 of the Appendix.

Two dilatant fluids were used to study the pressure drop across selected fittings. Pressure drop and flow rate data are presented in Tables 5-6, pages 48-49. In addition, the data has been treated in the traditional manner and has been presented as equivalent pipe diameters of added conduit length; these values have been compared to published values for Newtonian fluids.

Temperature Dependency of Power Law Parameters. As a piece of information of ancillary interest, the power law parameters $\underline{n}$ and $\underline{K}$ were investigated for their temperature dependency. The flow behavior index, $\underline{n}$, was found not to
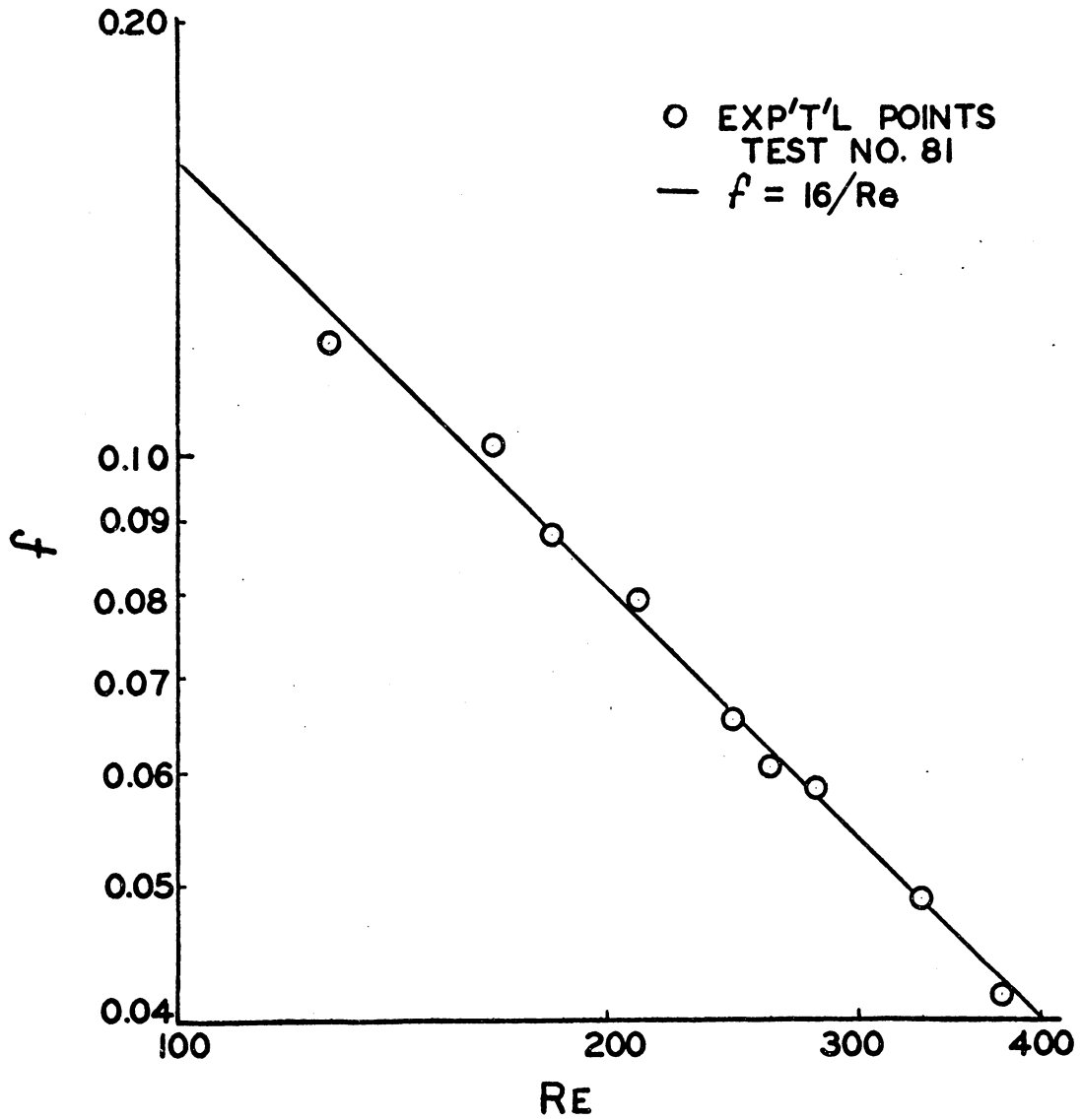
Figure 8   Plot of $\underline{f}$ versus Reynolds Number for Calibration of Flow Apparatus

Table 4

Dilatant Starch Systems Studied

test no.	continuous phase	type of test	$K, lb_f\text{-}sec^n/ft^2$	n,dimensionless
101-109	eth.glycol/glycerine	n,K vs. temp.	$0.7\text{-}6.0 \times 10^{-3}$	1.38
110	ethy.glycol	n,K vs. conc.	1.10×10^{-3}	1.29
111	"	"	8.85×10^{-4}	1.51
112	"	"	6.42×10^{-4}	1.75
113	"	"	1.45×10^{-4}	2.43
75	eth.glycol/H_2O	flow	1.84×10^{-4}	1.60
86	"	"	5.22×10^{-4}	1.18
87	"	"	10.22×10^{-5}	1.78
88	"	"	9.60×10^{-5}	1.79
89	"	"	8.72×10^{-5}	1.82
90	"	"	5.99×10^{-5}	1.87
93	"	"	3.15×10^{-4}	1.45
116	"	"	2.85×10^{-6}	2.00
117	"	"	4.38×10^{-6}	2.50
98	eth.glycol/H_2O/glycerine	"	3.08×10^{-3}	1.37
99	"	"	1.83×10^{-3}	1.35
100	"	"	1.08×10^{-3}	1.29
114	"	fittings	1.19×10^{-3}	1.15
115	"	"	7.51×10^{-4}	1.36

TABLE 5

The Flow of Dilatant Fluids
Through Fittings

Test No.	type of fitting	fluid velocity ft/sec	resistance to flow equivalent pipe diameters	
			dilatant	Newtonian
114-2	globe valve	1.810	29.1	300
-4	"	0.685	17.8	
-6	"	1.516	31.8	
-8	"	1.314	32.2	
-10	"	1.190	27.1	
-12	"	1.031	23.5	
-14	"	0.916	28.6	
-16	"	0.850	26.6	↓
-21	coupling	1.825	0	0
-23	"	0.667		
-25	"	1.573		
-27	"	1.230		
-29	"	1.000	↓	↓
-34	90° elbow	1.850	10.2	30
-36	"	0.641	33.0	
-38	"	0.875	25.5	
-40	"	1.397	16.3	
-42	"	1.060	23.3	
-44	"	0.632	39.8	↓

TABLE 6

The Flow of Dilatant Fluids
Through Fittings

Test No.	type of fitting	fluid velocity ft/sec	resistance to flow equivalent pipe diameters	
			dilatant	Newtonian
115-22	globe valve	1.742	24.8	300
-23	"	0.389	33.0	
-25	"	1.233	23.6	
-26	"	1.050	15.8	
-28	"	0.674	27.8	
-29	"	0.463	34.4	
-30	"	1.460	21.7	↓
-12	coupling	1.760	0	0
-13	"	0.612		
-15	"	1.593		
-16	"	1.560		
-18	"	1.153		
-19	"	0.794		
-20	"	0.564	↓	↓
-2	90° elbow	1.792	0.8	30
-3	"	0.571	24.4	
-5	"	1.568	1.3	
-6	"	0.987	6.3	
-8	"	1.387	1.5	
-9	"	1.106	5.2	↓

vary with temperature over the 50° F temperature range investigated. The flow consistency index, $\underline{K}$, was found to decrease with increasing temperature in a non-linear fashion. The values of $\underline{n}$ and $\underline{K}$ as a function of temperature are plotted in Figure 9, page 51.

Concentration Dependency of Power Law Parameters. Sufficient rheological data was collected to relate concentration of the dispersed phase and the power law parameters. A plot is presented for $\underline{n}$ and $\underline{K}$ as a function of starch volume concentration in Figure 10, page 52. The flow behavior indexes varied from 1.29 at 33.0 per cent starch to 2.43 at 38.1 per cent starch while the values of flow consistency index varied from 1.42×10^{-3} to 9.00×10^{-6} $lb_f\text{-}sec^n/ft^2$ respectively. This indicates that the flow consistency index actually decreases in value as the starch concentration (or $\underline{n}$ value) increases. This point will be considered further in a following section.

Theory of Dilatancy. The original concept of dilatancy, as introduced by O. Reynolds, involved the idea of a mechanical interaction between dispersed particles as being the primary cause for dilatancy. Although the term dilatancy was later given a broader rheological meaning, the mechanical interaction model was still accepted as an explanation of dilatancy.
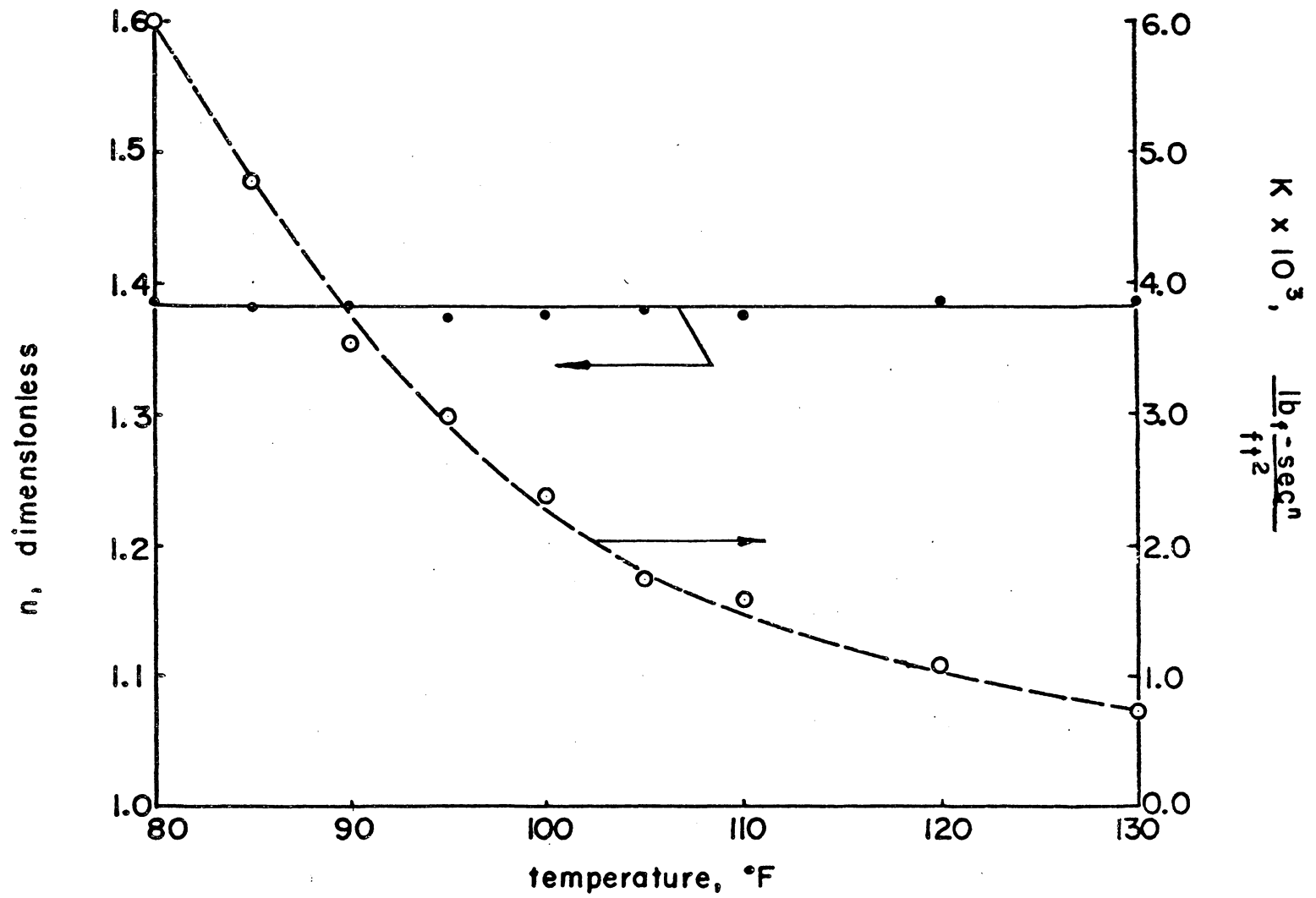
Figure 9   The Power Law Parameters, n and K, as a Function of Temperature
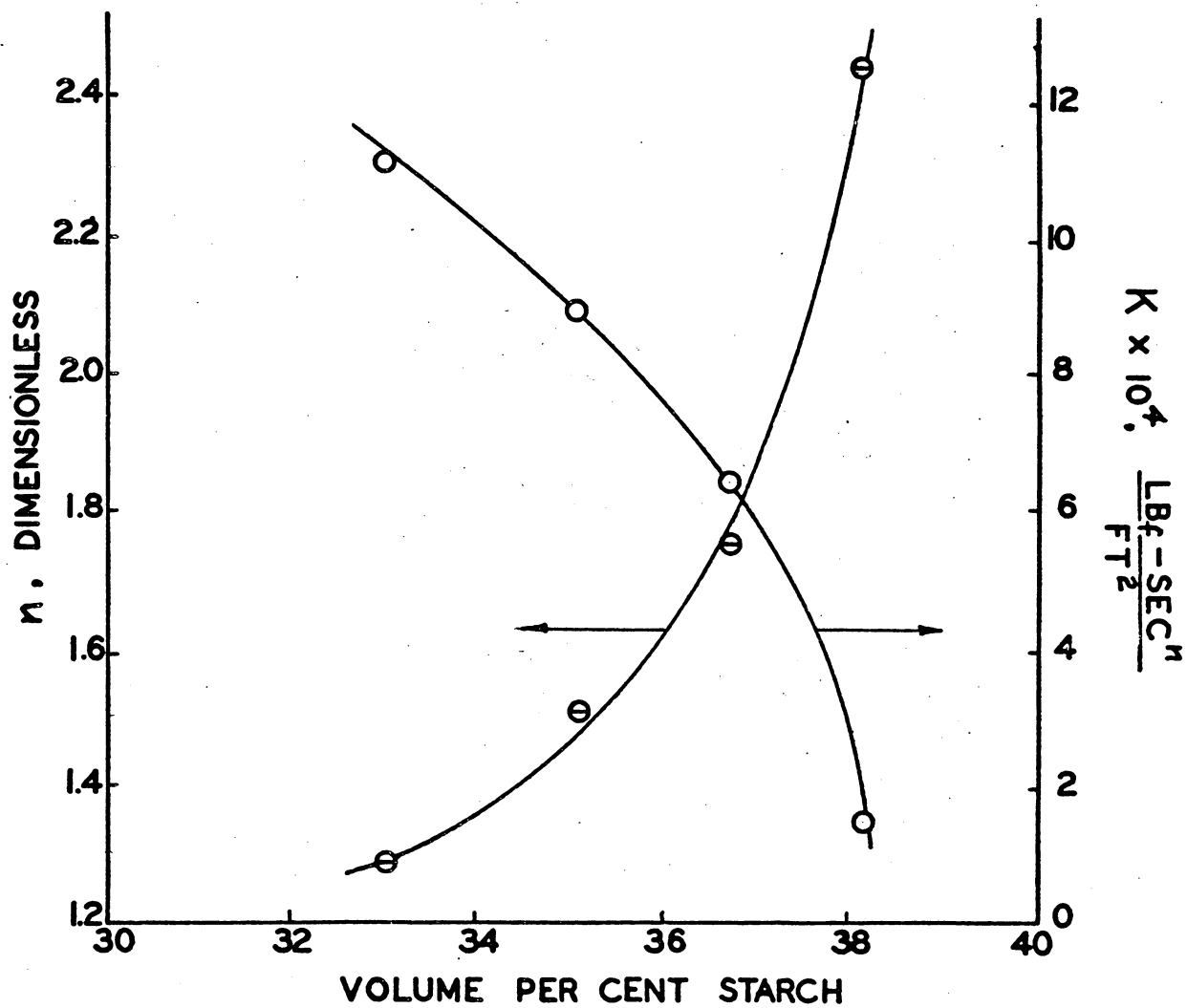
Figure 10   The Power Law Parameters as a Function of Starch
             Volume Concentration

Metzner and Whitlock[43] have carried the mechanical interaction model a step further by attributing the phenomenon to a momentum interaction between 'rows' of aligned particles. According to this momentum interaction model, the laminae of particles become progressively more perfectly aligned as the shear rate is increased, thus increasing the effective mass of the particles which experience momentum transfer with adjacent laminae whenever a single particle moves h terally. This model has an underlying discrepancy with the mechanical interaction model. In the latter case perfect alignment is initially present but decays to some less perfectly aligned configuration: the momentum interaction model assumes more perfect alignment of particles as the shear rate is increased. Metzner and Whitlock have intimated that there may be no actual physical conatact between dispersed particles, but that momentum transfer may be accomplished through a thin liquid film.

In the present work the phenomenon of dilatancy is treated only from a physico-chemical standpoint. To establish this concept, we must begin by examining a solid particle, spherical in shape and surrounded by a medium composed of a mobile, Newtonian fluid. It has been well established that such a solid particle would exert a field of force radially from its surface and for a distance into the suspending medium. This field would tend to be neutralized by the suspend-

ing medium, the amount of neutralization per unit mass of suspending medium depending on the polarity of the suspending medium. If the medium were water, for example, the force field would extend only a short distance through the medium, and so only a relatively thin layer of 'associated' water would insulate the effects of one particle from that of another particle. On the other hand, this layer of water would be expected to be tightly held, and great forces would be necessary to remove it.

The data of Harkins and Jura[25] gives some idea of the magnitude of the forces holding a film of water on titanium dioxide powders. The following data gives the energy of desorption of molecular layers of water as they are removed from the surface of the solid:

number of molecular layer	energy of desorption minus energy of vaporization, cal/mol
1	6550
2	1380
3	450
4	80
5	40
sum of all above 5	~30

DeWaele and Lewis[8] found that the thickness of the adsorbed layer depended on the force of adhesion between the liquid and the solid; plasticity was found to be proportional to the thickness of the adsorbed layer, with poorly wetting fluids giving plastic suspensions. DeWaele[7] found that poorly wetting oils represent poor lubricants because the slightest force applied normal to the solid-liquid

interface was sufficient to remove the lubricating layer and expose the solid to friction.

While studying boundary lubrication, Needs[45] found that the minimum thicknesses that could be attained between polished solid surfaces depended upon the viscosity of the entrained liquid but was of an order of magnitude of only a few microns. For one case, the viscosity of a 1.2 micron film was five times the fluid's bulk viscosity in the direction of flow at a load of 300 pounds per square inch. Furthermore, loads of up to 800 pounds per square inch could not appreciably change the film's thickness.

In studying air pressures needed to blow liquids from between 0.177 millimeter slits, Deryagin et. al.[6] found that liquids capable of wetting the slit walls showed an increase in viscosity(about ten times) extending to a distance of 0.5 microns from the solid walls. Hardy[24] and Freundlich[19] have both asserted that the force field at a solid surface must extend through many molecular dimensions.

Volkova[59] measured the rate of capillary movement of both water and toluene through quartz powder and found the rate of movement of the water to be small campared to that of toluene when the quartz grains were smaller than 40 microns. Immobile layers of water have been assumed to account for this discrepancy; values of film thickness of one micron have been calculated. Deryagin[5] also found that the pressure needed to thin down a film beneath a bubble

entrapped between two plates was small up to a film thickness of two microns, but increased tremendously when the film thickness decreased to 1.5 microns. Additional evidence for an adsorbed layer was furnished by Williams[69] when he found that the sedimentation rate for materials in a wetting medium were slower than that predicted by Stoke's Law. He concluded that the apparent density of the solids were decreased by an adsorbed layer.

Another factor must be considered concerning the behavior of suspensions: the rotational speed of the dispersed particles. Mason and Bartok[30] have experimentally verified that the angular velocity of a suspension of sheared, rigid spheres is:

$$\zeta = \dot{\omega}/2 \tag{1}$$

where:

ζ = angular velocity of sphere, rad/sec

$\dot{\omega}$ = shear rate at sphere surface, sec^{-1}

These same two investigators found that the two-body collision frequency per unit volume is[31]:

$$F = \frac{24\ c^3\ \dot{\omega}}{\pi^3\ a^3} \tag{2}$$

where:

F = two-body collision frequency per unit volume, $sec^{-1}ft^{-3}$

c = volume fraction particles in suspension

$\dot{\omega}$ = average shear rate, sec^{-1}

a = diameter of sphere, ft

And now a picture of the dilatant system can be form-
ulated: a relatively crowded dispersion of particles in-
sulated from the effects of one another by an adsorbed
layer of the continuous phase, each particle being small
enough so that the adsorbed layer is of appreciable thick-
ness compared to the particle diameters. As the system is
suddenly set into motion through the application of an
external force, the dispersed particles with their adsorbed
layers move rotationally and translationally. As they do so,
collisions between adsorbed layers on the particles occur
and energy is expended in "shearing off" a portion of the
adsorbed shell. As the rate of shearing is increased, not
only is the number of collisions increased, but the impact
of collision causes the shearing action to affect a lower,
more tightly held layer of adsorbed liquid. In addition,
the particles rotate at greater speeds, giving rise
to local turbulence and local areas of shear. It is the sum
of the effects of increased number of collisions, harder
impacts, and local turbulence with shear that gives rise to
the peculiar shape of the dilatant flow curve.

For particles of large size ($> 100\mu$) the dilatant
effect would be small because the frequency of collision is
reduced drastically, a consequence of the cube of the part-
icle diameter being in the denominator of equation 2. For
small particles (submicron range) the dilatant effect
would be suppressed, since the collisions due to Brownian

motion would be of more importance[32] than those caused by shearing the suspension and the suspension would be in a constant state of apparently high viscosity. This is in accord with the observations of Sweeney and Geckler[55] who found that the viscosity of suspensions of particles of diameter less than five microns increased as the particle size decreased. This effect was not apparent when non-wetting liquids were used. With these small particle-sized suspensions, dilatancy might be expected to be observed only at extremely high rates of shear. For solids dispersed in a non-wetting medium, the spherical shells of fluid would be extremely easy to remove and Brownian motion would provide the necessary force to allow mutual adhesion of the particles to occur. The result would be typical plastic behavior, a conclusion supported by the extensive data of Fischer[12].

Sample Calculations

The following section contains examples of the calculations made to derive the results of this investigation.

Conversion of Kinematic Viscosity to Absolute Viscosity. Since the standard viscometric oil was given in centistokes, the cgs system was used to convert that value to centipoise. Absolute and kinematic viscosities are related through density, as follows:

$$\mu = \rho \eta$$

μ = coefficient of viscosity, g/cm-sec

η = kinematic viscosity, cm^2/sec

The specific gravity of the oil was given as 0.895 and the kinematic viscosity was given as 620.1 centistokes at 80°F. Knowing that the density of water at 80°F is 0.997 g/ml gives:

$$\mu = (0.997)(0.895)(620.1)$$

$$\mu = 553 \text{ centipoise}$$

Absolute Viscosity from Capillary Data. The Ostwald-Fenske capillary viscometer measures kinematic viscosities by comparing the efflux time of a sample of the test fluid with the efflux time of some fluid of known kinematic viscosity, the efflux times being directly proportional to kinematic viscosities. Once the kinematic viscosity was known and the specific gravity was determined, the absolute viscosity was calculated as shown above.

Moment Acting on Viscometer Cone. In order that shear
stresses could be calculated for the determination of flow
curves, it was necessary to calculate the moment acting on
the viscometer cone as a function of the driving weight em-
ployed. The relationship is as follows:

$$M = F \times L$$

where: M = moment, ft-lb$_f$

F = force, lb$_f$

L = lever arm, ft

For the Stormer viscometer, the lever arm was measured to be
0.57 inches with a gear reduction of 11/1. Therefore, for
a driving weight of 100g:

$$M = \frac{(100)(1)(0.57)}{(453.6)(11)(12)} \cdot \frac{g}{g_c}$$

$$M = 0.951 \times 10^{-3} \text{ ft-lb}_f/100g \text{ of driving weight}$$

where: 453.6 = factor to conver grams to lb$_m$

g/g_c = factor to convert lb$_m$ to lb$_f$ = 1

The moment for other weights would then be incremental
fractions or multiples of the moment for 100 grams.

Shear Stress. Shear stresses were calculated from a
knowledge of the moment acting on the cone and from the
dimensions of the cone[64]:

$$\tau = \frac{3M}{2\pi a^3}$$

where: τ = shear stress at cone surface, lb$_f$/ft^2

M = moment acting on cone, ft-lb$_f$

π = circular measurement constant

a = radius of cone, ft

Since of the radius of the cone was determined as 1.75 inches and the moment per 100 grams of driving force was calculated as 0.951×10^{-3} ft-lb$_f$, the shearing stress per 100 grams of driving force was:

$$\tau = \frac{3(0.951 \times 10^{-3})}{2\ \pi\ (1.75/12)^3}$$

$\tau = 0.1464$ lb$_f$/ft^2 per 100 g of driving weight

The shear stresses for other driving loads were fractions or multiples of this value. For example, for Test 100-34, page A19, the weight involved was 300 grams, so:

$$\tau = 300/100 \times 0.1464$$

$$\tau = 0.439 \text{ lb}_f/\text{ft}^2$$

Shear Rate. For a cone and plate viscometer, shear rate has been found to be constant throughout the sample for Newtonian fluids and approximately constant throughout the sample for non-Newtonian fluids, providing the cone angle is small. According to Oka[46]:

$$\dot{\gamma} = \frac{\Omega}{\tan \alpha}$$

where:

$\dot{\gamma}$ = shear rate, sec^{-1}

Ω = angular velocity of cone, radian/sec

α = cone angle, degrees

From the data of Test 100-34, page A19, and knowing that the cone angle is $1°40'$, shear stress can be calculated:

$$\dot{\gamma} = \frac{\frac{2\pi}{60}(29.0)}{\tan(1°40')}$$

$$\dot{\gamma} = 104 \text{ sec}^{-1}$$

The factor $2\pi/60$ was inserted to convert revolutions per minute to radians per second. Also, $\tan(1°40') = 0.0291$.

Flow Behavior Index, n. The assumption of a power law fluid allows n to be determined from a plot of $\log \tau$ versus $\log \dot{\gamma}$, the slope of such a plot equalling n. When such a plot is non-linear, n varies with shear rate. However, all of the dilatant fluids studied evidenced constant values of n over the shear rate ranges of interest.

The Constant n'. For the calculation of modified Reynolds numbers, the constant n' was of interest, rather than the flow behavior index, n. The definition of n' comes from consideration of shear stresses at the wall of a circular conduit and the average shear rate in the conduit. According to Mooney[44], n' is defined as the slope of the log-log plot of shear stress at the wall and the average shear rate:

$$n' = \frac{d(\log D \Delta P/4L)}{d(\log 8V/D)}$$

where: D = diameter conduit, ft

$\Delta P/L$ = pressure drop per unit lingth of conduit, lb_f/ft^3

$$\bar{V} = \text{average fluid velocity in conduit, ft/sec}$$

$$D \Delta P/4L = \text{shear stress at conduit wall, } lb_f/ft^2$$

$$8\bar{V}/D = \text{average shear rate in conduit, } sec^{-1}$$

Metzner[37], however, has shown that the two constants n and n' may be considered equal; they were considered so throughout this dissertation.

Flow Consistency Index, K. Once the other quantities of the Power Law equation have been measured or calculated, the equation may be rearranged and solved for K. A mathematical statement of the Power Law is:

$$\mathcal{T} = K(\dot{\gamma})^n$$

which can be rearranged to give:

$$K = \frac{\mathcal{T}}{(\dot{\gamma})^n}$$

where: $\mathcal{T} = \text{shear stress, } lb_f/ft^2$

$\dot{\gamma} = \text{shear rate, } sec^{-1}$

$n = \text{flow behavior index, dimensionless}$

$K = \text{flow consistency index, } lb_f\text{-}sec^n/ft^2$

This calculation can be illustrated by substituting the data of Test 100-34, page A19 , with $\mathcal{T} = 0.439$, $\dot{\gamma} = 104$ and $n = 1.29$ to give:

$$K = \frac{(0.439)}{(104)^{1.29}}$$

$$K = 1.08 \times 10^{-3} \; lb_f\text{-}sec^n/ft^2$$

The Constant K'. Analogously to the case of $\underline{n}$ and $\underline{n}'$, the parameter $\underline{K}'$ is of interest, rather than the flow consistency index, $\underline{K}$. A method for converting $\underline{K}$ to $\underline{K}'$ is given by Wilkinson[65]:

$$K' = K \left(\frac{3n'+1}{4n'}\right)^{n'}$$

where:

K' = constant used in calculation of modified Reynolds number and pertaining to pipe flow, $lb_f\text{-sec}^n/ft^2$

K = flow consistency index, $lb_f\text{-sec}^n/ft^2$

n' = constant used in calculation of modified Reynolds number and pertaining to pipe flow, dimensionless

Substitution of the data from Test 100-34, page A19, gives:

$$K' = (1.08 \times 10^{-3})\left[\frac{3(1.29) + 1}{4(1.29)}\right]^{1.29}$$

$$K' = 1.00 \times 10^{-3} \; lb_f\text{-sec}^n/ft^2$$

Pressure Drop in Pipeline. The calculation of friction factors dictated the conversion of observed manometer readings to pressure drops. The manometric equation is:

$$\Delta P = h \, \rho_w (\sigma_B - \sigma_A) \, g/g_c$$

where:

ΔP = pressure drop, lb_f/ft^2

h = height of manometer reading, ft

ρ_w = density of water, lb_m/ft^3

σ_B = specific gravity of manometer fluid, dimensionless

σ_A = specific gravity of fluid filling man-
ometer leads, dimensionless

g = acceleration of gravity, ft/sec^2

g_c = gravitational constant, $lb_m\text{-}ft/lb_f\text{-}sec^2$

Substitution of the data of Test 100-24, page A20, gives:

$$\Delta P = \frac{8.8}{12}\,(62.35)(2.964 - 1.000)\,\frac{32.2}{32.2}$$

$$\Delta P = 89.8 \ lb_f/ft^2$$

Fluid Velocity in Pipeline. The average fluid velocity
in the pipeline was found by dividing the mass flow rate of
the fluid by the product of the density and the cross sect-
ional area of the pipe:

$$\bar{V} = \frac{W}{\rho A}$$

where:

$\bar{V}$ = average fluid velocity, ft/sec

W = mass flow rate, lb_m/sec

ρ = density of fluid, lb_m/ft^3

A = cross sectional area of duct, ft^2

The cross sectional area of an 1-¼ inch Schedule 40 pipe is
0.0104 ft^2[33]. Using the data of Test 100-24, page A20,
gives for $\bar{V}$:

$$\bar{V} = \frac{(0.930)}{(1.260 \times 62.35 \times 0.992)(0.0104)}$$

$$\bar{V} = 1.151 \ ft/sec$$

The density of water at the test temperature, 102°F, is
(0.992 x 62.35) lb_m/ft^3.

Fanning Friction Factor, f. From a knowledge of the pressure drop over a length of conduit, the geometry of the conduit, and the fluid density, the friction factor can be calculated.

$$f = \frac{\Delta P \; D \; g_c}{2 \; \rho \; L \; \bar{V}^2}$$

where: f = friction factor, dimensionless

$\Delta P/L$ = pressure drop per length of conduit, lb_f/ft^3

D = diameter of conduit, ft

g_c = gravitational constant, 32.2 lb_m-ft/lb_f-sec^2

ρ = density fluid, lb_m/ft^3

$\bar{V}$ = average fluid velocity, ft/sec

From the data of Test 100-24, page A20, f may be calculated:

$$f = \frac{(89.8)(0.115)(32.2)}{2(0.992 \times 62.35)(10)(1.325)^2}$$

$$f = 0.159$$

Modified Reynolds Number. For the case of the flow of incompressible fluids in conduits, the modified Reynolds number takes the following form[36]:

$$Re' = \frac{D^{n'} \; \bar{V}^{2-n'} \rho}{g_c \; K' \; 8^{n'-1}}$$

where: Re' = modified Reynolds number, dimensionless

D = diameter conduit, ft

$\overline{V}$ = average fluid velocity, ft/sec

ρ = fluid density, lb_m/ft^3

g_c = gravitational constant, $lb_m\text{-}ft/lb_f\text{-}sec^2$

$\underline{K}'$ = constant, related to $\underline{K}$, $lb_f\text{-}sec^n/ft^2$

$\underline{n}'$ = constant, related to $\underline{n}$, dimensionless

The data from Test 100-24, page $_{A20}$, may be utilized to illustrate the calculation:

$$Re' = \frac{(0.115)^{1.29}(1.151)^{0.71}(62.35 \times 0.992 \times 1.260)}{(32.2)(1.00 \times 10^{-3})(8)^{0.29}}$$

$$Re' = 91.6$$

<u>Modified Friction Factor, f'.</u> The modified friction factor arises from the analogy between Reynolds number and and modified Reynolds number. The equation is:

$$\underline{f}' = 16/Re'$$

where: $\underline{f}'$ = modified friction factor, dimensionless

Re' = modified Reynolds number, dimensionless

<u>Pressure Drop Through Fittings.</u> Because the pressure taps for measuring the pressure drops across fittings were located one foot upstream and one foot downstream from the fittings, the equivalent pressure drop for this two feet of conduit had to be subtracted from the observed pressure drop for the fitting.

The calculational procedure for determining the expected pressure drop per foot of conduit consisted of (1)

using viscometric and flow rate data to solve for modified
Reynolds numbers, (2) determining $\underline{f}'$ from the relation
$\underline{f}' = 16/Re'$, and (3) rearranging the friction equation to
solve for the pressure drop per unit length of conduit, or
$\Delta P/L$.

Using the data of Test 115-2, page A24:

$$(1) \quad Re' = \frac{(0.115)^{1.36}(1.792)^{0.64}(62.35 \times 1.243)}{(32.2)(6.86 \times 10^{-4})(8)^{0.36}}$$

$$Re' = 132.0$$

$$(2) \quad \underline{f}' = 16/(132.0)$$

$$\underline{f}' = 0.1211$$

$$(3) \quad \frac{\Delta P}{L} = \frac{2(62.35 \times 1.243)(0.1211)(1.792)^2}{(0.115)(32.2)}$$

$$\frac{\Delta P}{L} = 16.30 \ lb_f/ft^2 \text{ per foot of conduit}$$

Multiplying this number by 2 and subtracting from the ob-
served pressure drop, gives for Test 115-2, page A24 :

$$\Delta P = (34.1) - 2(16.30)$$

$$\Delta P = 1.5 \ lb_f/ft^2$$

Equivalent Pipe Diameters of Resistance.   In order
that the data of pressure loss through fittings might con-
veniently be compared with published values for Newtonian
fluids, the pressure drops were expressed as equivalent dia-
meters of added pipe length. The relationship is:

$$D_{eq} = \frac{\Delta P}{(\Delta P/L)\ D}$$

where: D_{eq} = equivalent diameters of pipe length, dimensionless

ΔP = observed pressure drop over fitting only, lb_f/ft^2

$\Delta P/L$ = calculated pressure drop per unit length of conduit, lb_f/ft^3

D = diameter of conduit, ft

The calculation is illustrated by using the data of Test 115-2, page A20:

$$D_{eq} = \frac{(1.5)}{(16.30)(0.115)}$$

D_{eq} = 0.8 pipe diameters of resistance

<u>Activation Energy for K.</u>   An activation energy for the change of <u>K</u> with temperature may be determined from a plot of log K versus 1/T. The Arrhenius relationship is:

$$K = K_o\ e^{-\Delta E/RT}$$

where: K = flow consistency index, $lb_f\text{-}sec^n/ft^2$

K_o = constant, $lb_f\text{-}sec^n/ft^2$

ΔE = activation energy, Kcal/mol

R = gas law constant, 1.987 g-cal/mol-^oR

T = absolute temperature, ^oK

Taking logarithms of both sides of the equation gives:

$$\log_e K = \log_e K_0 - \Delta E / RT$$

Therefore, a plot of $\log_{10} K$ versus $1/T$ will give a straight line with a slope equal to $\Delta E / 2.303R$. From Figure 16, page 87 , there is found:

$$\text{slope} = \frac{\log(6.0 \times 10^{-3}) - \log(7.6 \times 10^{-4})}{(1.847 - 1.693)\ 10^{-3}}$$

$$\text{slope} = 5,820$$

It is necessary for the sake of dimensional consistency to introduce a factor of 1.8 to change the $1/^{\circ}R$ readings to $1/^{\circ}K$ readings. Then there is found:

$$\Delta E = \frac{(1.987)(5.820)(2.303)}{(1.8)}$$

$$\Delta E = 14,800 \text{ g-cal/g-mol}$$

$$\Delta E = 14.8 \text{ Kcal/g-mol}$$

IV. DISCUSSION

Contained in this section is a discussion of the literature of dilatant fluids, the experimental procedures used, and the results of this study to characterize the behavior of dilatant fluids. In addition, recommendations for further work and limitations of this investigation are outlined.

Discussion of Literature

The literature of dilatant fluids is discussed in the following paragraphs. Particular note is made of the discrepancies existing between the conclusions drawn by various investigators.

Mechanism of Dilatancy. A hydrodynamical approach to the mechanism of dilatancy, as postulated by Reynolds in 1885, enjoys an almost universal acceptance. This approach is illustrated by a quantity of rigid, spherical particles dispersed in sufficient concentration in some liquid such that the particles are hexagonally close-packed, with only enough of the liquid phase to fill the voids between particles. Any disturbance of this system, as by some externally applied force, leads to a disturbance of the hexagonal array; since hexagonal packing represents maximum packing for spheres, and since there is only sufficient fluid to fill the voids at maximum packing, any change will tend to create

a deficiency of liquid. According to the postulated mechanism, it is this deficiency in lubricating liquid that gives rise to increasing resistance to flow as shearing rates are increased.

Hexagonal close-packing is represented by a void volume of approximately 28 percent. Therefore, it would be expected that in order to be consistent with this postulated mechanism, the volume concentration of dispersed, spherical particles must approach 72 percent for dilatancy to occur. However, dilatancy has been observed in suspensions with solid phase concentrations as low as 12 percent[17].

Other shortcomings of this theory are evident. For example, it has been noted by several investigators that the wetting characteristics of the liquid for the dispersed solid is of paramount importance[48, 58, 70]. This dependency on wettability is not predicted from the postulated mechanism, since the approach is based on a purely physical interaction between particles. The postulated mechanism also fails to account for the experimentally observed fact that suspensions of large particle size do not show dilatancy[40], while the effect was also not noted when the average particle size of the dispersed solid was less than five microns[40]. Finally, all previous published data on dilatant fluids dealt with suspensions with liquid phase viscosities of 50 centipoise of less. This has led to conjecture by Freundlich and Roder[21] that low liquid viscosities

may be a prerequisite for the manifestation of dilatancy. Once again, the postulated mechanism fails to predict such a dependency.

It can be seen that the accepted mechanism for the phenomenon of dilatancy is inadequate to explain observed properties of these materials; the need for a new theory is clearly indicated.

Methods of Correlation. Two methods for the correlation of pipe flow data have been advanced which might have utility for correlating the data for the flow of dilatant fluids.

In the first method, Weltmann[60] made use of the familiar friction factor diagram by defining the Reynolds number as:

$$Re = \frac{D V \rho}{\mu_a}$$

where μ_a is the apparent viscosity of the dilatant fluid, measured at the prevailing flow conditions (i.e., the shear rate) in the conduit. The friction factor, f, is then defined as:

$$f = \frac{16}{Re} \left(\frac{3n + 1}{4n} \right)$$

where n is the flow behavior index. A typical friction factor plot for dilatant fluids, according to this concept, is shown in Figure 11, page 74. This method of correlation suffers from three major disadvantages.
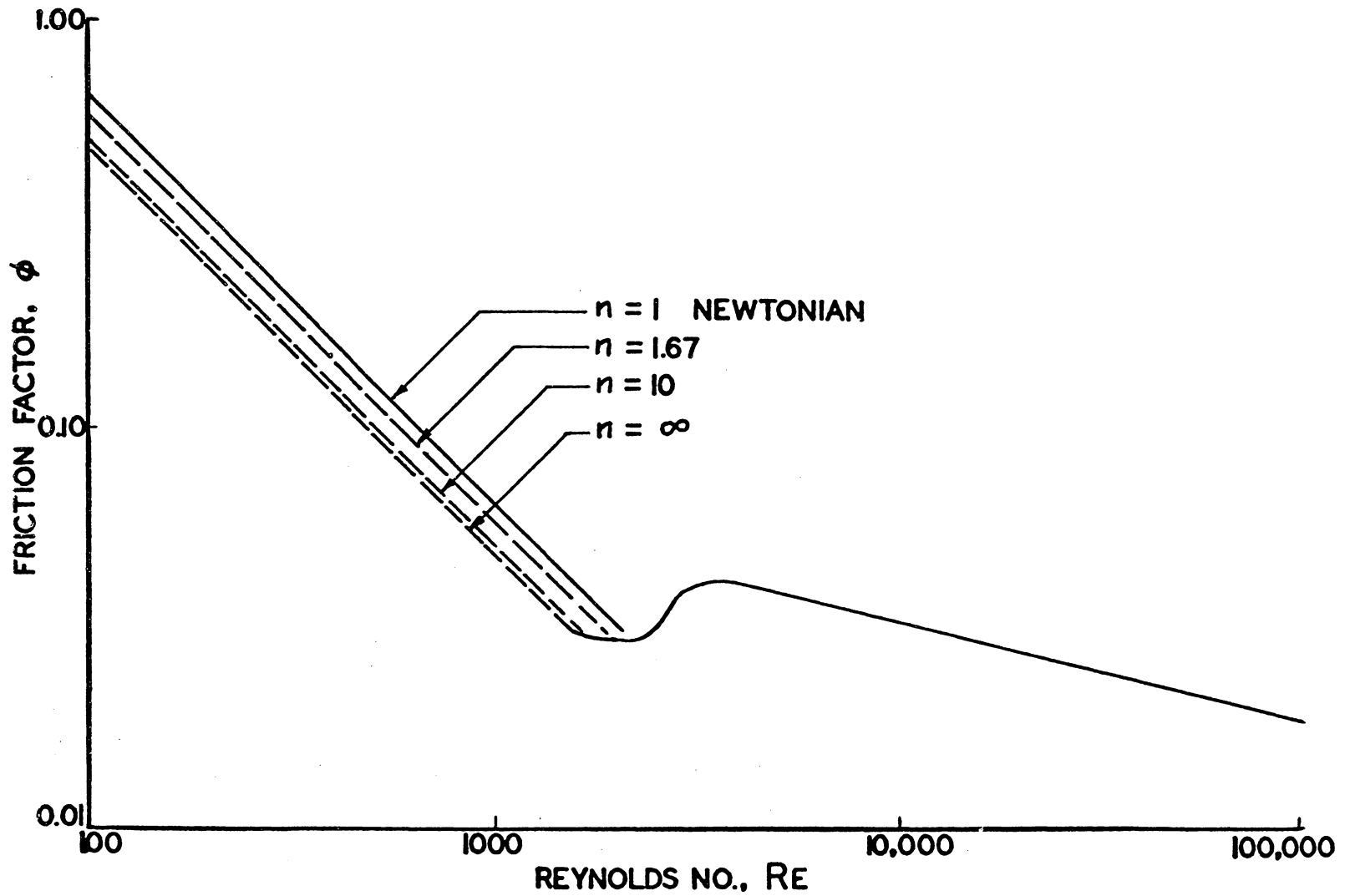
Figure 11   Friction Factor Reynolds Number Correlation According to Technique of Weltman

Limitations of this method are: it is applicable only if the dilatant fluid is of the ideal, power law fluid type; it gives rise to a family of curves in the laminar region with the flow behavior index, $\underline{n}$, as a parameter, rather than correlating to a single curve; and it makes it necessary to measure apparent viscosities at specific shear rates, thus requiring as many apparent viscosity determinations as there are friction factors desired.

The second method was proposed by Metzner and Reed[39] and also involves use of the friction factor diagram, but defines the Reynolds number in such a manner that a single line in the laminar region suffices to correlate all dilatant data, and without the limitation that the fluid must obey the power law. Dodge and Metzner[10] extended the analogy to the turbulent regime where they found separate curves for each flow behavior index. This method of correlation is illustrated in Figure 12, page 76.

Neither method of correlation was experimentally verified for the case of dilatant fluids previous to this investigation.

Discussion of Procedure and Results

It is instructive to discuss the special procedures followed in this investigation, as well as to critically discuss the experimental results; the following paragraphs serve that purpose.
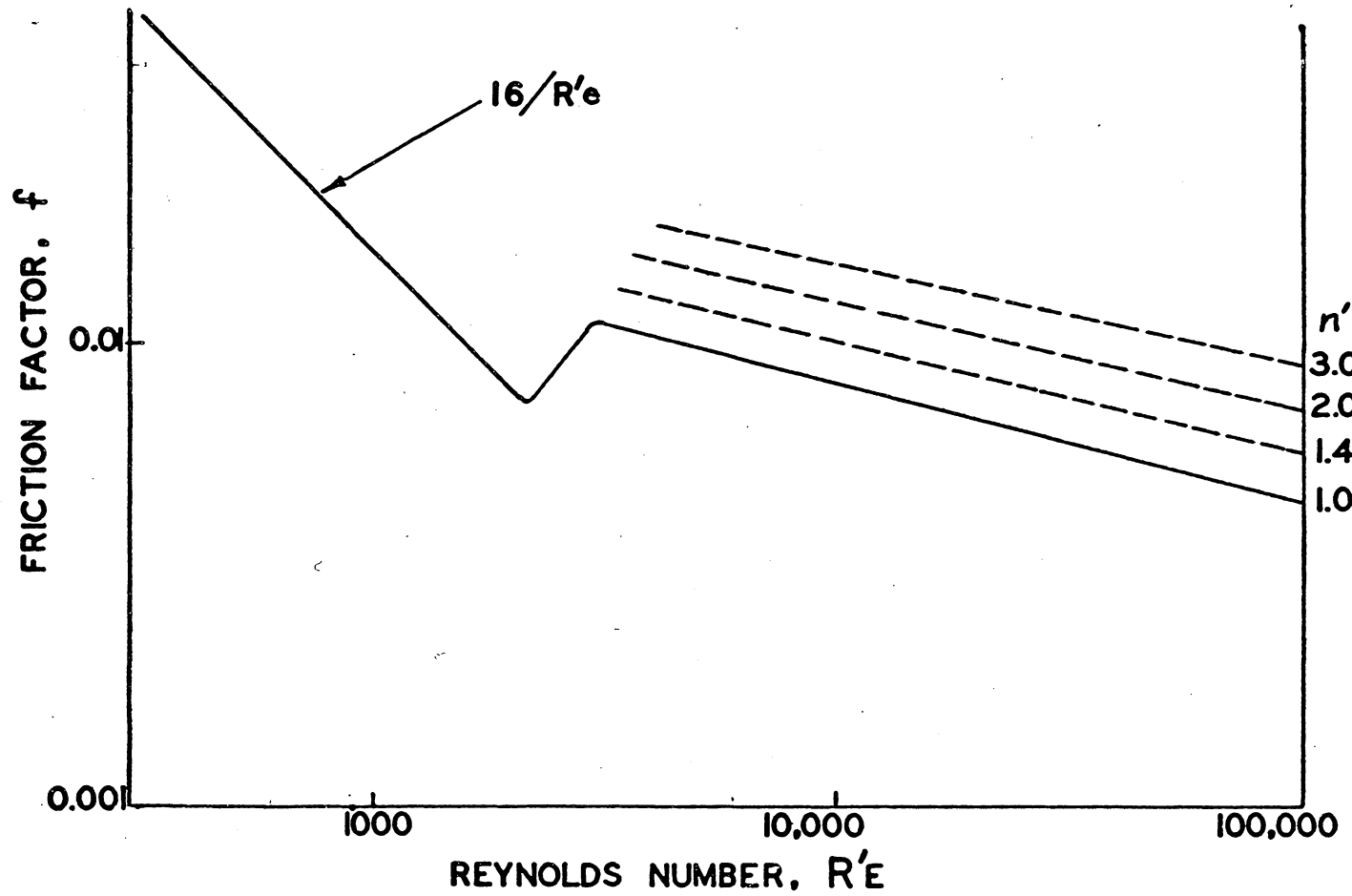
Figure 12   Friction Factor Reynolds Number Correlation According to
Technique of Metzner and Reed

Rheological Equipment. The original intention was to construct and use a capillary rheometer for the characterization of the test fluids. Had it been sucessful, it would have allowed the power law parameters to be determined at flow conditions identical in character and magnitude to those encountered in the pipe flow equipment. To this end, a capillary rheometer was built in the manner described by Wilkinson[68] and was tested for its ability to characterize dilatant fluids. This instrument was found not to be suitable because of its propensity to retain the starch and to exude a solvent-rich material. Extensive attempts to overcome this shortcoming by altering the viscometer's geometry failed, and its use was abandoned.

Since Fischer[13] had published extensive data on dilatant fluids obtained using a modified Stormer viscometer, it was decided to make similar modifications on an available Stormer viscometer and to attempt to use such an instrument. The modification consisted simply of machining a cylindrical cup from brass with internal dimensions of 1.844 inches in diameter by 2.200 inches in height. The standard bob with a diameter of 1.233 inches was used. The clearance between cup and bob was then approximately 0.5 centimeters, the clearance recommended by Fischer[13] to prevent excessive crawling of the viscous dilatant fluids at high shear rates.

The modified Stormer viscometer was found to have three serious limitations: (1) it lacked good temperature control,

(2) the dilatant suspensions settled badly during a flow curve determination, and (3) an extensive and tedious calibration was necessary to correct for end effects. Evidence for settling of the starch particles is shown in Figure 13, page 79 , which gives the flow curves for a single material which was tested in three consecutive replications. The flow curves indicate that the fluid near the periphery of the bob was gradually being depleted of starch, the starch settling to the bottom of the cup and decreasing the separation between bob and cup bottom, thereby creating a larger and larger end effect. After a test such as this, a thick layer of starch could be found in the cup bottom.

That the end effect is important in the Stormer viscometer is shown in Figure 14, page 80, where the flow curves of several low viscosity materials as determined by this viscometer are shown. It can be seen that the slope of the log-log curves diverge further and further from the predicted value of 1.0 for a Newtonian fluid as the fluid viscosities decrease; this phenomenon has been attributed to end effects[13]. For liquid viscosities below 500 centipoise, the instrument must be calibrated for 'effective' bob lengths at small intervals of viscosity with liquids of known viscosity. This difficulty in calibration, lack of temperature control, and inability to prevent settling made the modified Stormer viscometer seem unattractive for characterizing dilatant fluids.
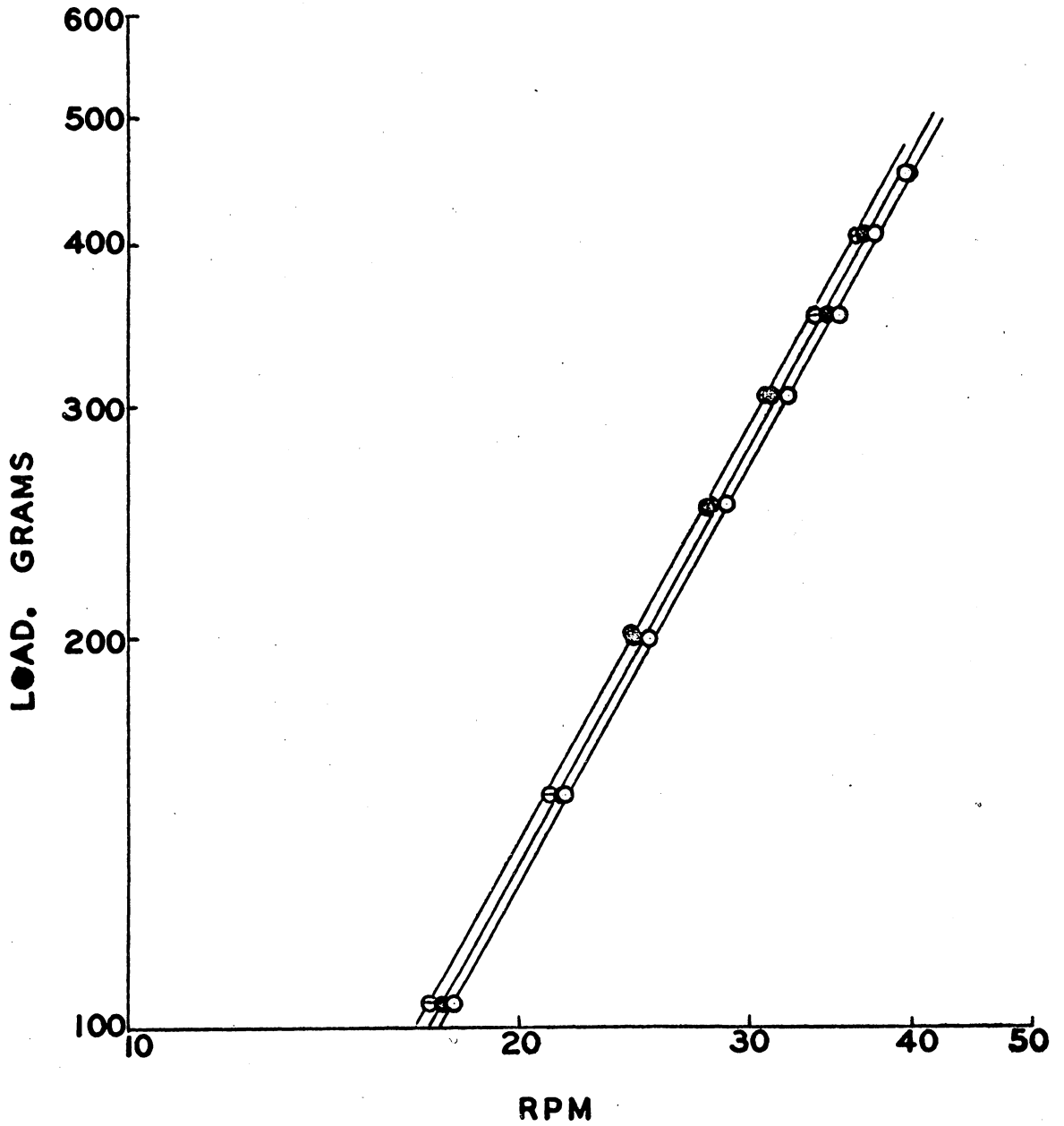
Figure 13   Effect of Starch Settling on the Flow Curves
of a Dilatant Suspension
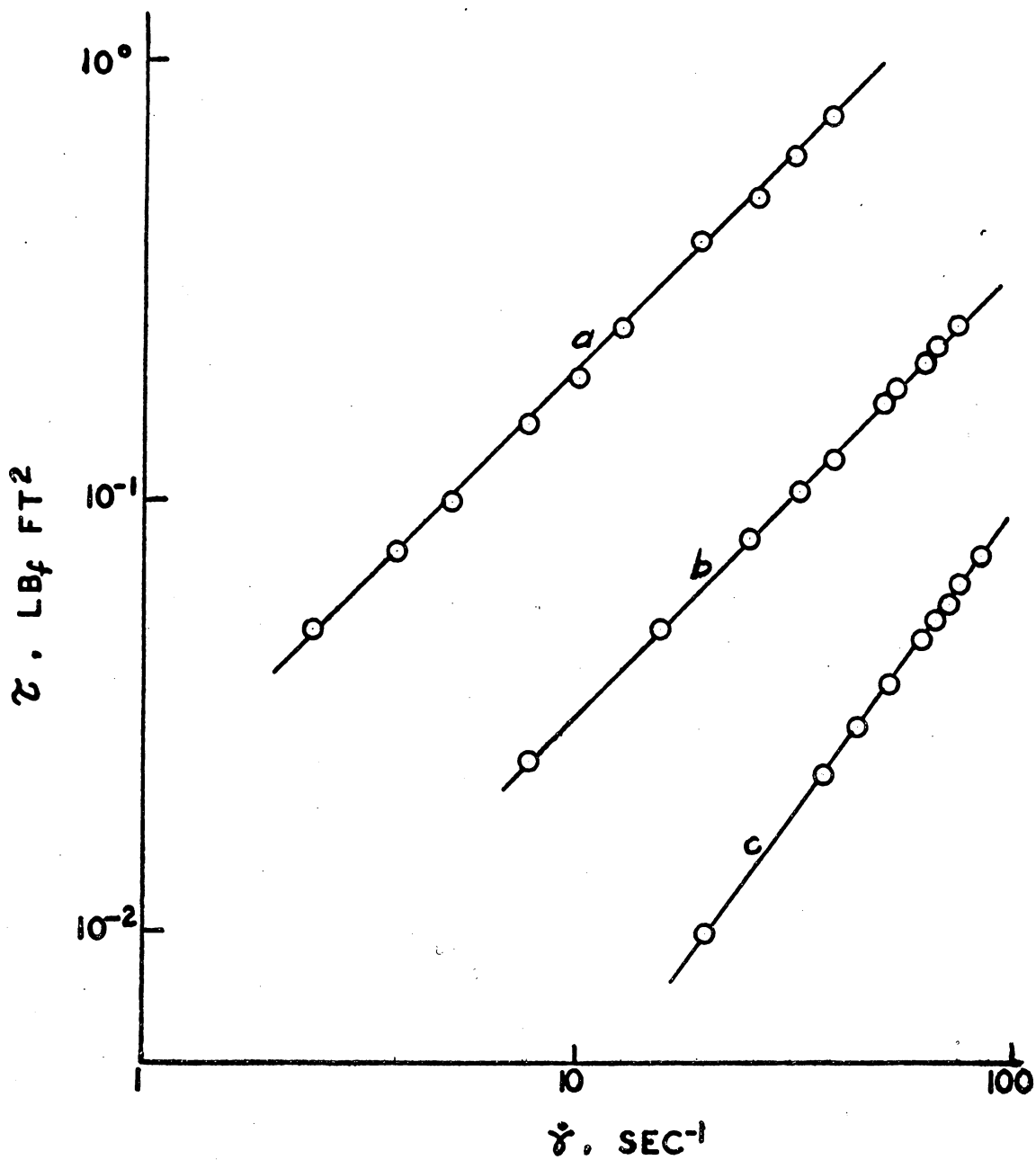
Figure 14   The End Effect for Fluids of Diverse Consistency. (a) glycerine   (b) ethylene glycol/water   (c) water

A cone and plate assembly was fabricated to be used with the Stormer instrument. Fabrication of this assembly was described on page 39 , while the apparatus is shown in Figure 5 , page 30 . This apparatus effectively overcame the limitations of the capillary and Stormer viscometers by providing for rapid and accurate temperature control, by supplying sufficient shearing motion to prevent settling, and by not requiring tedious calibrations.

Markovitz et. al.[29] have calculated the misalignments necessary in a cone and plate viscometer of cone radius four centimeters and cone angle of two degrees such that a one per cent error is introduced. The values are:

1. error in separation of cone and plate: 0.001 cm

2. divergence from 90° of cone axis and plate surface: $0^o20'$

3. error in measuring radius of fluid sample in test cavity: 0.26 cm

4. truncation of cone, radius of truncation: 0.11 cm

In the present cone and plate design, chances of errors 3 and 4 were eliminated by always filling the fluid just to the periphery of the cone and by not truncating the cone. Separation of the cone and plate was measured to be less than one half of one mil, or about 0.001 centimeters. Error 2 was estimated to be about $0^o20'$, thus bringing the total error within the one per cent value. However, error in temperature measurement of a few tenths of a degree could introduce a relatively large error. Therefore, even though

calibration with two fluids showed the maximum error to be less than two percent, the instrument is conservatively estimated to be accurate only to five per cent.

One limitation noted with the cone and plate viscometer was its tendency to throw fluid from between the cone and the plate when extremely dilatant fluids were studied at high rates of shear. This did not pose a problem for the present investigation since the shear rates of interest were low.

Flow Curves. For fluids which obey the Power Law, flow curves are conveniently plotted on log-log coordinates to evaluate the power law parameters, n and K. Starting with the Power Law:

$$\tau = K \; (\dot{\gamma})^n$$

and taking logarithmns of both sides:

$$\log \tau = \log K + n \log \dot{\gamma}$$

It can be seen that a plot of $\log \tau$ versus $\log \dot{\gamma}$ should give a straight line with slope n and intercept log K. The linearity of the line resulting from the plot of actual flow data serves as an indication of the closeness of a real fluid to approaching the Power Law Model.

The test fluids studied in this investigation were found to closely fit the Power Law Model over the range of shearing rates studied. Three typical flow curves, representing slightly dilatant, moderately dilatant, and highly dilatant fluids are presented in Figure 15, page 83.
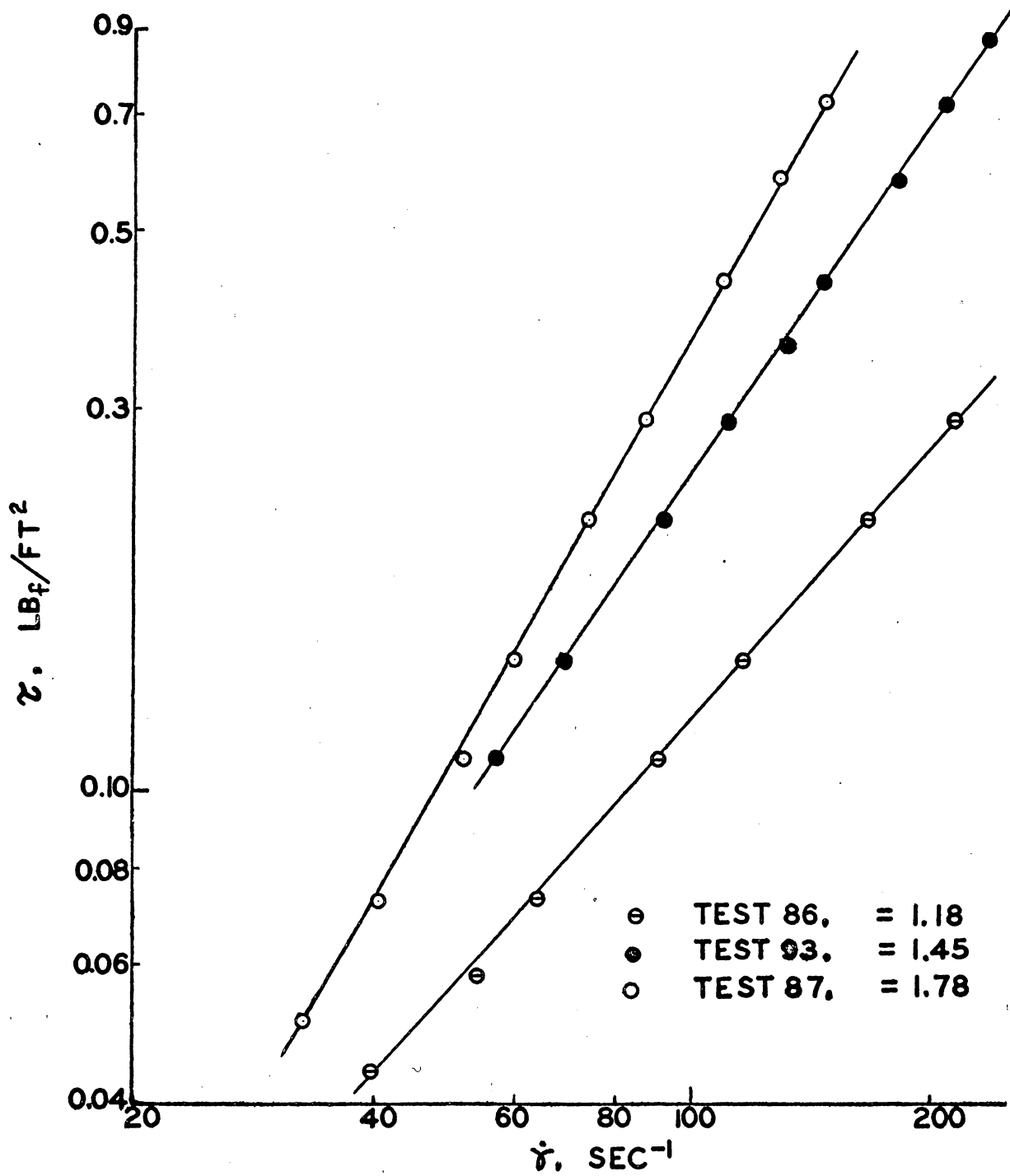
Figure 15   Typical Dilatant Flow Curves

Rheological Data. Dilatant fluids reported in the literature were critically reviewed for their applicability for studying large quantities of materials in a pilot plant size flow apparatus. The data of Fischer[14] was of particular interest because he reported a large number of fluids which were found to exhibit dilatancy. Careful consideration narrowed the field down to three systems: starch in ethylene glycol, red iron oxide in an aqueous sodium lighin sulfonate solution, and carbon black in an aqueous sodium lignin sulfonate solution. These three fluids were chosen because they were readily available, were cheap, and were relatively non-toxic.

Attempts to produce dilatancy with the latter two systems failed at the volume concentrations claimed dilatant by Fischer, and also at higher concentrations. Since the red iron oxide and the carbon black used by Fischer were not completely described as to type and particle size, there was no way of knowing whether his materials were duplicated. In view of the criticality of having proper particle surface properties and size, it follows that his experimental conditions were not attained. As a consequence, starch in ethylene glycol was adopted as the test fluid; water and glycerine were eventually added as a convenient method of varying fluid consistencies. Dilatant systems using solely water as the solvent were avoided because such systems were found to change significantly in their degree of dilatancy

with ageing; this phenomenon has been attributed to hydrolysis of the starch particles[17]. On the other hand, changes in degree of dilatancy were found to be negligible if water was present in small amounts, while glycol or glycerine as solvents did not show this phenomenon.

Data was collected to show the dependency of the power law parameters on the concentration of the dispersed phase; this dependency is shown in Figure 10, page 52. It can be seen that the flow behavior index, $\underline{n}$, increases in a nonlinear fashion with the concentration of the starch, as would be expected. However, the flow consistency index, $\underline{K}$, decreases with increasing starch concentration, a consequence of the shear stress being divided by the shear rate raised to a power greater than one:

$$K = \frac{\tau}{(\dot{\gamma})^n} \qquad \text{for } \underline{n} > 1$$

The power law parameters have been plotted as a function of temperature in Figure 9, page 51. Within experimental error, the flow behavior index is seen to be independent of temperature over the $50°F$ range of temperature studied. This observation is in line with Metzner[36] who considers $\underline{n}$ to be constant over a range of $30°C$, and Reed[50] who found a 0.04 change in $\underline{n}$ over a range of $50°F$ for pseudoplastics. Gallay and Puddington[22] found the dilatancy of an aqueous starch suspension to decrease slightly

with rise in temperature at temperatures just above the suspension's freezing point, but attributed the change to hydration of the starch particles. Thus, it may be concluded than the degree of dilatancy of a suspension is independent of temperature over moderate ranges of temperature.

The shape of the curve of $\underline{K}$ versus temperature suggests an exponential relationship between the two variables. This type of relationship is not unexpected, for Newtonian fluids have been known to have a viscosity-temperature relationship of the Arrhenius type:

$$\mu = \mu_0 \, e^{-\Delta E/RT}$$

where μ_0 is a constant, ΔE is the energy of activation, R the gas constant, and T the absolute temperature. Since, for the case of constant $\underline{n}$, $\underline{K}$ is a measure of the "viscosity" of a dilatant suspension, it might also be expected to vary with temperature according to an Arrhenius relationship:

$$K = K_0 \, e^{-\Delta E/RT}$$

This relationship, when plotted on the semi-logarithmic coordinates of log K versus 1/T would have a slope of $-\Delta E/R$. Such a plot for the data of this investigation is shown in Figure 16 , page 87 . Also plotted on this figure is the data of Segur and Oberstar[53] for glycerine. It will be noted that the lines are nearly parallel, in-
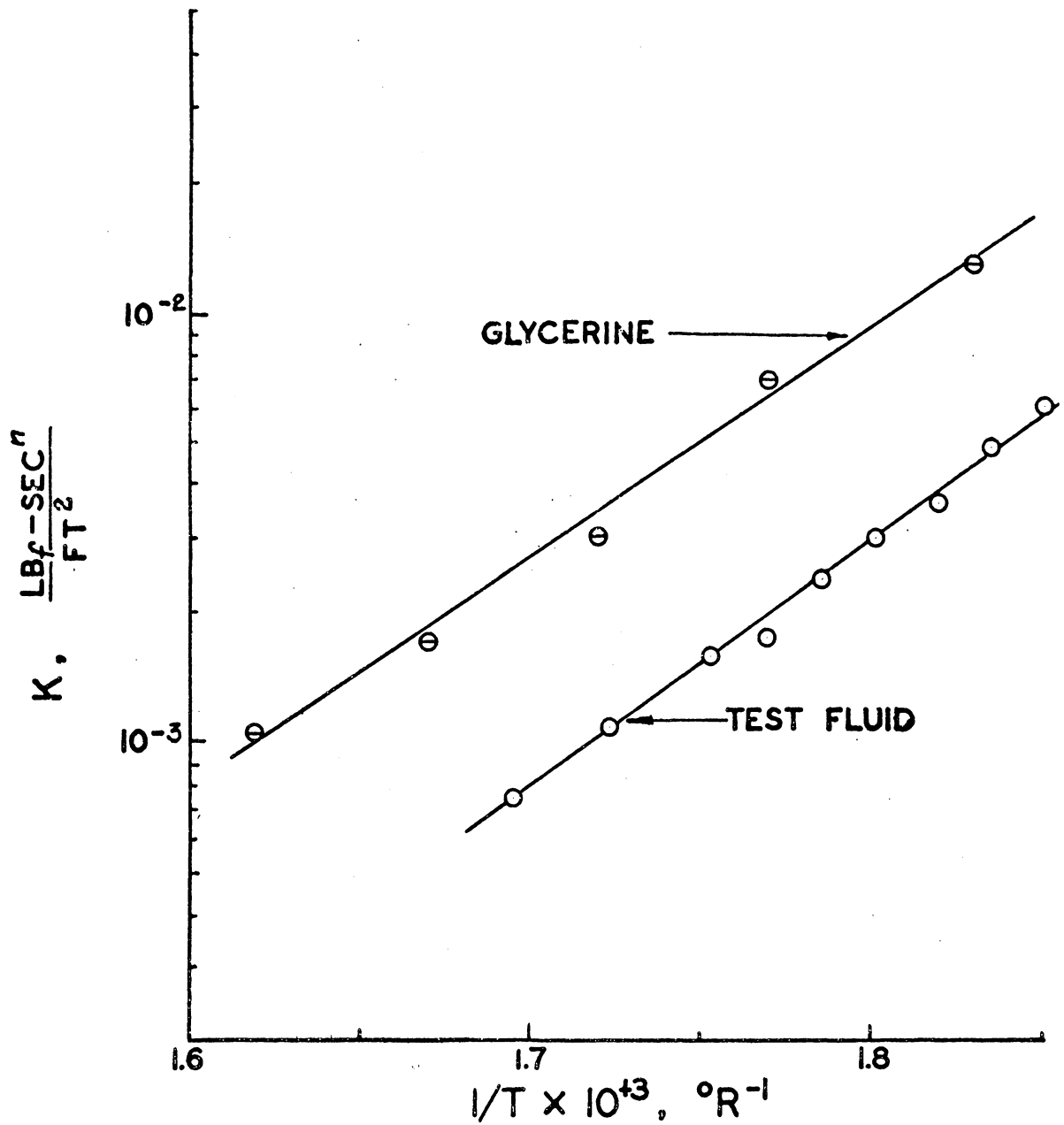
Figure 16 Determination of Activation Energy for K:
Comparison With Activation Energy for
Flow of Glycerine

dicating nearly equal activation energies for viscosity change with temperature in the two systems. This would indicate that at least at this volume concentration of starch part- icles, the activation energy depends almost entirely on the composition of the continuous phase. The value for activ- ation energy in this case is calculated to be 14.8 Kcal/mole. This value may be compared to 11.1 Kcal/mole found by Severs[54] for polyethylene and 98.0 Kcal/mole found for ethyl cellulose. Reed[50] also found that the consistency index, $\underline{K}$, changed at the same rate as the viscosity of the suspending medium for polymer solutions.

Flow Test Apparatus. Initial considerations concern- ing the design of the flow apparatus were: (1) a method for flow rate control, (2) a method for measuring flow rate, (3) a method for measuring pressure drop, (4) pro- visions for calming sections before and after the test section, (5) a method for controlling temperature, and (6) the proper sizing for the pipeline so that comparable shear rates could be realized with the cone/plate viscometer.

Since the Moyno pump that was available was not equip- ped for variable speed delivery, a recycle loop with a system of valves was used to vary the flow rates through the test section. Flow rates were determined by the direct weighing of test fluid as it effluxed from the system into a container on a scale. It was originally planned to mon- itor the flow rates with an electromagnetic flowmeter, but

this method was found unsuitable because of fouling of the sensing element by the starch slurry. Orifice meters were considered but were rejected as being too insensitive and uncertain.

Just as the thinking on flow rate measurement had to be revised, so had it to be for the measurement of pressure drop. Calculations from available data on dilatant fluids had indicated that the pressure drop over ten feet of test section would be of the order of 10 to 100 pounds per square inch. Exploratory experiments designed to indicate what fluids the Moyno pump would be able to handle showed that the pressure drop would be much smaller, and could more conveniently be measured with manometers. A critical part of the design of the manometer system was the use of a second fluid to fill the manometer leads and the provision of reservoirs to hold quantities of this fluid sufficient for purging the air from the manometer system. The manometer leads were fabricated from clear vinyl tubing so that air bubbles could easily be detected.

The need for calming sections immediately preceding and following the test section was met by providing eight feet, or nearly 70 pipe diameters, of fitting-free conduit before the test section, and three feet, or about 26 pipe diameters, following the test section. These values exceed the minimum values suggested for Newtonian fluids[34]. Several checks made to compare the pressure drop at five

and ten feet of test section indicated that the velocity profile was essentially fully developed in the length of calming section provided. The length of the test section was limited to ten feet because of the need for calming sections and from space limitations of the laboratory.

Temperature control was provided so that isothermal conditions would exist in the test section. Cumulatively, substantial quantities of heat were generated in the Moyno pump and throughout the conduit; a double pipe heat exchanger was provided to remove this heat. The storage tank wall also acted as a heat exchanger. Temperature control was effected by using these two heat exchangers to sub-cool the test fluid and then using the immersion heater to reheat it and keep it at the desired temperature. This method of control proved to be very effective in its simplicity and speed of response.

A rough estimation of the limiting value of temperature rise per pass through the Moyno pump can be made by assuming a typical fluid specific heat of 0.5 BTU/lb_m-°F with an average fluid bulk flow rate of 1.4 lb_m/sec. The pump motor was rated as five horsepower which, if an efficiency of 40 per cent is assumed, makes two horsepower available for conversion to thermal energy:

$$\Delta T = \frac{Q}{m\ C_p} = \frac{(2 \times 2.5445 \times 10^3)\ \text{BTU}}{(1.4 \times 3600)\ \text{lb/hr} \times (0.5)\ \text{BTU/lb-°F}}$$

$$\Delta T = 2.0 \, ^{\circ}F$$

This $2\,^{\circ}F$ represents the upper limit on temperature rise; the actual rise was probably $1\,^{\circ}F$ or less.

Heating effects due to viscous dissipation as a quantity greater than convection losses could be inferred form known temperatures at the storage tank and at the test section thermometers. Since these two temperatures always agreed within $1.5\,^{\circ}F$, it must be concluded that the net effect of viscous dissipation minus convection losses in the loop from the storage tank to the test section was approximately $1\,^{\circ}F$. Adding another degree for dissipation throughout the rest of the loop would give a total heating effect per pass of about $2-3\,^{\circ}F$. This heating effect was found to be cumulative and drove the temperature of the fluid to as high as $160\,^{\circ}F$ if no cooling was provided.

The size of the pipeline used in this investigation was dictated by the shear rate range that the cone and plate viscometer was able to measure. It was considered imperative that the flow curves for the test fluids cover the same range of shear rates studied in the flow apparatus. Care was taken to match the two shear rate ranges to insure that the degree of dilatancy of the test fluid was constant over the shear rates studied in the flow apparatus. Concern for this point arose from the many non-linear flow curves shown for dilatant fluids in the literature[40,38].

A problem throughout the first few flow tests was the dilution of the test fluids by water remaining in the pump and pipe loop from the cleanup of the previous test. Consequently, exact compositions were not known for the first few tests; however, compositions of the test fluids were not of primary importance. Later in the program a method was devised for removing essentially all of this residual water from the pump and pipe loop. The method consisted of evacuation of the pump and loop with the laboratory vacuum system, utilizing a storage tank that stood nearby. It was found that as much as 30 pounds of water remained in the system after simple draining, but that the vacuum removed all of the water so that no dilution of test fluid occurred. Exact test fluid compositions were known for the later runs.

The flow dampener pictured in Figure 3 , page 26 was designed to answer the need for a method to control surges, or pulses, of liquid through the test section, such surges making the measurement of pressure difficult. This dampener had the advantages over other methods of dampening such as the air piston[28] and throttling valve[57] of being completely automatic, of simple construction, and of being suitable for suspensions of large particle size. The use of a pulsation dampener is especially critical when trying to read pressure with a Bourdon gauge, since the gauge dial will oscillate wildly from the surging flow of the Moyno pump without damping. This device smoothed out downstream flow

by allowing the energy from the surges of liquid to be expended against the elastic membrane, thereby damping their effect.

Flow Tests. Dilatant fluids with flow behavior indices between 1.18 and 2.50 were studied in pipeline flow, with one test made with a fluid of $n = 2.0$. Fluids with $n > 2.50$ were found to give pressure drops of such magnitude that the Moyno pump was incapable of moving them through the pipeline. However, this did cover the ranges of interest ($1 < n < 2$; $n = 2$; $n > 2$) and probably covered the range of dilatancy that would be of commercial interest.

The advantages of the Metzner-Reed correlation over that of Weltmann have already been presented (see Methods of Correlation, page 73). The data of this investigation was used to test the Metzner-Reed correlation by plotting the coefficient of friction, c_f, versus the modified Reynolds number in Figure 17, page 93. It can be seen from this plot that the data fall closely around the theoretical line, confirming the validity of the Metzner-Reed correlation for dilatant fluids in laminar flow. The experimental and predicted coefficients of friction are compared in Figure 18; all points fall within ± 5 percent of the predicted values. This compares favorably with the non-Newtonian data of Dodge and Metzner[10] for laminar flow which cannot be contained in an interval of ± 5 per cent.

SYMBOL	TEST NO.	n'
◐	75	1.60
◑	86	1.18
⊘	93	1.45
⊟	98	1.37
⊖	99	1.35
⊘	100	1.29
●	116	2.00
○	117	2.50

$$f = 16/R'e$$

FRICTION FACTOR, f

REYNOLDS NUMBER, $R'e$
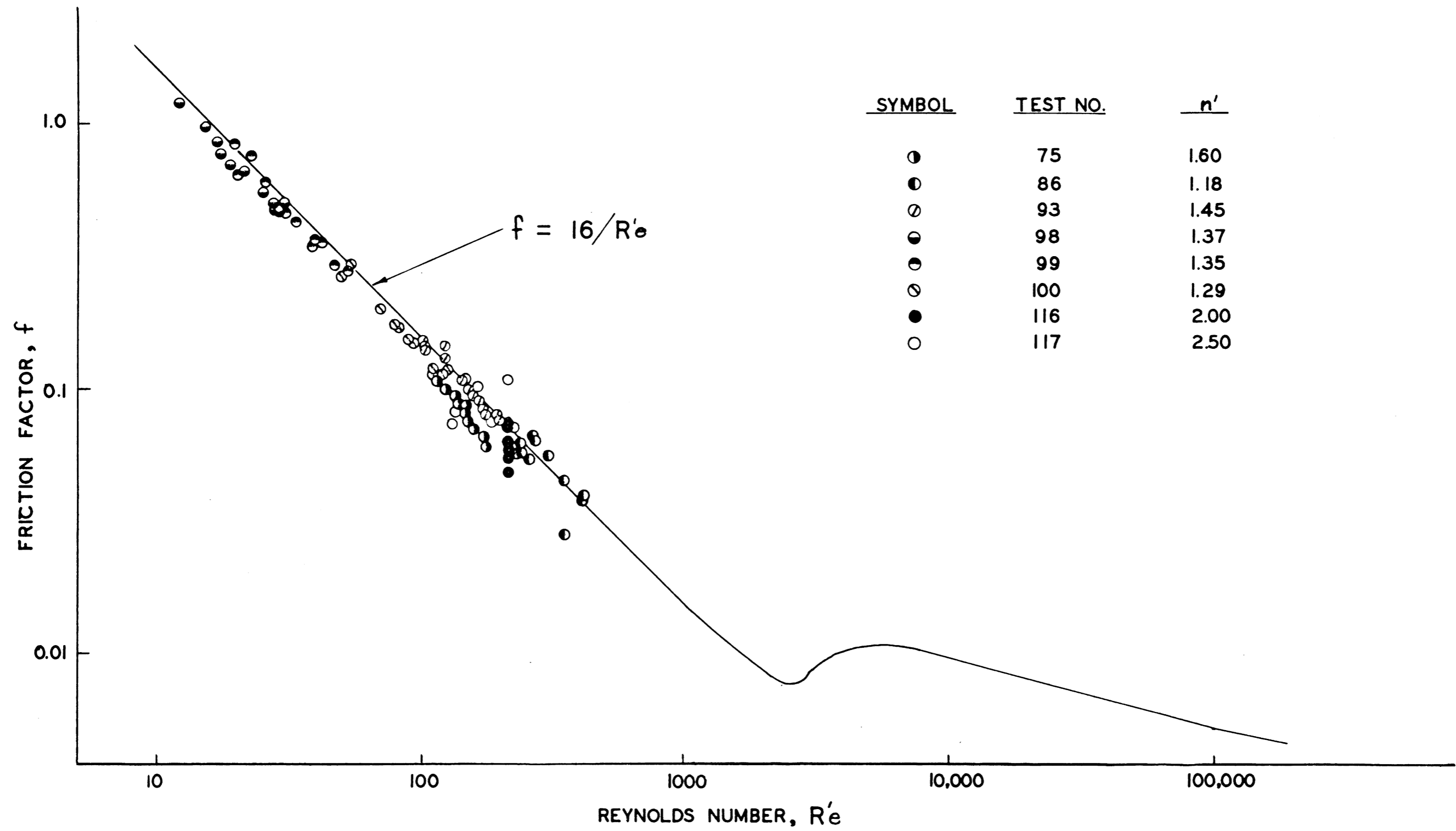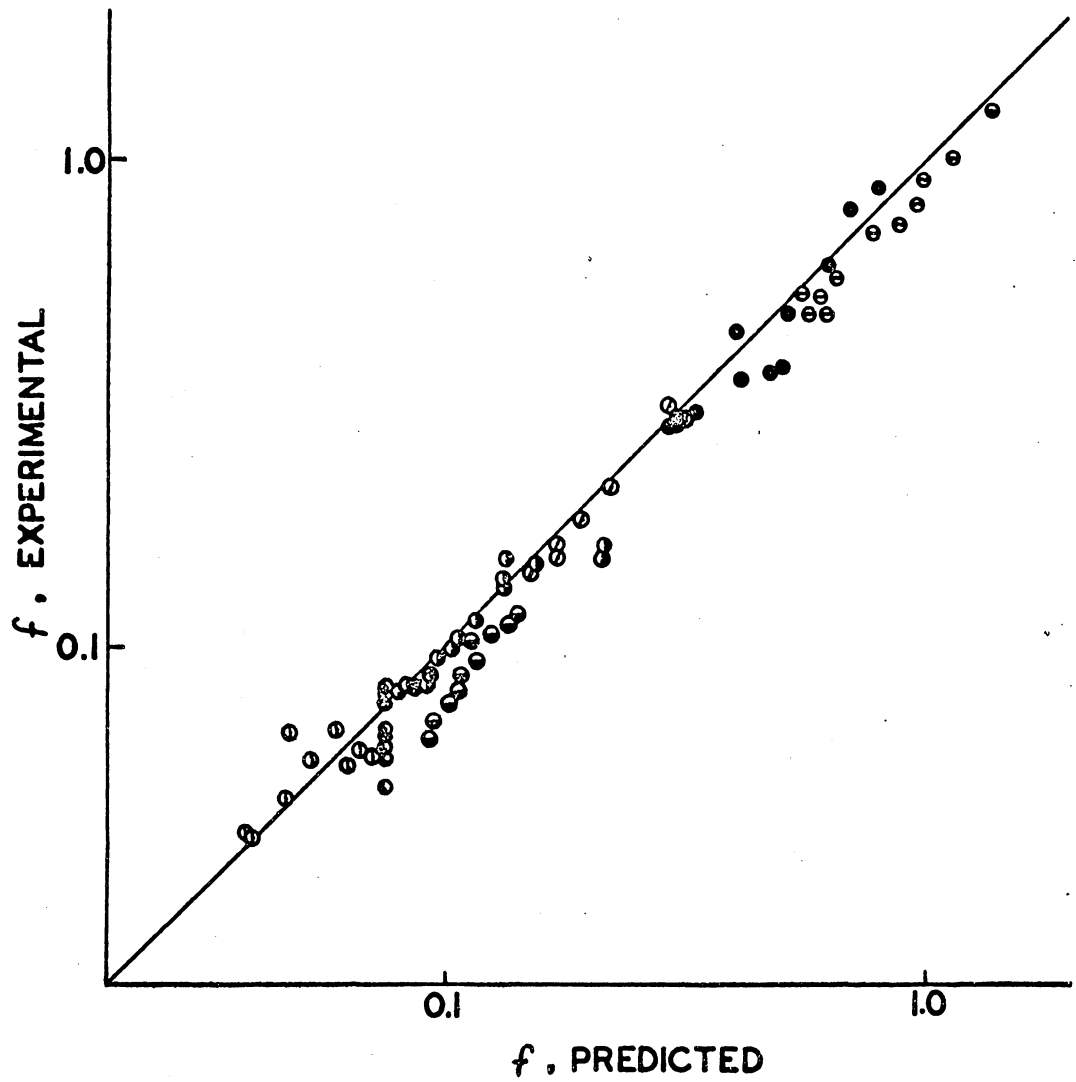
Figure 18   Comparison of Experimental and Predicted
Friction Factors

It is interesting to note that in order to fit the cor-
relation, dilatant fluids with flow behavior indices greater
than two must give rise to friction factors that increase
with increasing flow rates. This is directly opposite to
what is encountered for fluids with $n < 2$, including Newton-
ian and pseudoplastic fluids, but is a consequence of
decreasing Reynolds numbers with increasing fluid velocities.
The decreasing Reynolds numbers, in turn, are predicted from
the velocity term in the numerator of the Reynolds number,
which is $V^{2-n'}$; this term is raised to a negative power
when $n' > 2$ and serves to decrease the Reynolds number when
V increases. In addition, when $n' = 2$, the Reynolds numbers
and the friction factors are fixed at some invariable value
independent of the fluid velocity and determined by the mag-
nitude of the flow consistency index, K.

Because of equipment limitations, this investigation
was not concerned with the turbulent regime. However it is
instructive to analyze the turbulent regime correlation for
the case of $n' = 2$ and $n' > 2$. The general form of the von
Karman equation is[66]:

$$1/\sqrt{c_f} = \frac{4.0}{(n')^{0.75}} \log_{10}\left[Re \; c_f^{\,1-n'/2}\right] - \frac{0.4}{(n')^{1.2}}$$

where the coefficient of friction, c_f, is equal to $16/Re'$.
It can be seen that for $n' = 2$, and since $Re' = D^{n'}V^{2-n'}\rho/\sigma$,
both Re' and $c_f^{\,1-n'/2}$ are constants. Therefore, the coeffic-

ient of friction is also a constant independent of fluid velocity and an analogy with the laminar case results.

At values of $n' > 2$, the log term becomes smaller because Re' becomes smaller with increasing fluid velocity and c_f becomes larger---but c_f, through a now negative exponent finds itself in the denominator. As a result, the coefficient of friction finds itself becoming larger and larger as the fluid velocity increases. Here again the analogy with the laminar case exists.

Pressure Drop Across Fittings. In order that the flow behavior of dilatant and Newtonian fluids might be compared in still another respect, data was collected on the pressure drop occurring across selected fittings through which dilatant fluids were flowing. The resulting resistances to flow, expressed as equivalent pipe diameters of straight conduit, are compared to those values published for Newtonian fluids in Tables 5-6 , pages 48-49.

It can be seen that there is a rough correspondence between the values found for the two classes of fluids when pressure drop was measured across couplings and 90° elbows, with a fluid of low degree of dilatancy. However, for the 90° elbow, there seemed to be a dependency on flow rate, the equivalent resistance decreasing with increasing flow rate. For the more dilatant fluid, there was a strong dependency of equivalent resistances on flow rate, with a spread of values of 0.8 to 24.4 as the fluid velocity

changed from 1.792 feet per second to 0.571 feet per second.
Equivalent resistances found for the globe valve were very
nearly 30 for both dilatant fluids at all fluid velocities
studied.

The greatest descrepancy between resistance values
found here and those accepted for Newtonian fluids was the
resistance of the globe valve; the ratio between Newtonian
and dilatant values was approximately 300/30, or 10/1. This
difference is significant and some attempt must be made to
explain it.

First, it must be mentioned that data on the pressure
drop across fittings is extremely scanty. In addition, most
data originates from a period previous to 1930, and is ap-
plicable strictly to turbulent flow[11]. Wide variations,
especially in the case of valves, are acknowledged for equip-
ment designed by different manufacturers[35]. The data of
Wilson et. al.[71] is pertinent, for these investigators
found that the number of equivalent pipe diameters of press-
ure drop for 90° elbows varied from 2.5 at Re$\sim$10 to about
30 for Re in the turbulent regime. It seems, then, the
results found here need not be considered to vary from the
literature, but rather to extend it in an area of general
deficiency.

Theory of Dilatant Flow. The limitations of the pre-
sent theories of dilatancy were discussed in an earlier
section and a new theory was proposed. Because the Power

Law Model has been almost universally accepted as empirically describing the flow behavior of dilatant fluids, any satisfactory theory of dilatancy must conform to a degree with this model. If, in addition, the theory can be used to derive, if only semi-theoretically, the Power Law relationship, then both the theory and the relationship are strengthened.

According to the proposed theory, the model dilatant system is composed of a suspension of hard, rigid spheres in a Newtonian fluid. Figure 19, a photomicrograph of a starch suspension, shows this to be a good approximation to the real case. The surface properties for the dispersed spheres are such that a tightly bound layer of the suspending medium exists around each sphere, this bound layer effectively increasing the diameter of the spherical particles. The variables that might be expected to affect the viscosity of such a suspension are:

μ_{app} = apparent viscosity of the suspension

μ_o = viscosity of Newtonian suspending fluid

r = characteristic distance between particles

$\dot{\gamma}$ = shear rate

ρ_o = density of the suspending fluid

A dimensional analysis may be performed to group these variables in dimensionless groups. For purposes of dimensional analysis, the units are expressed in terms of mass M, distance L, and time T. The units are given below.
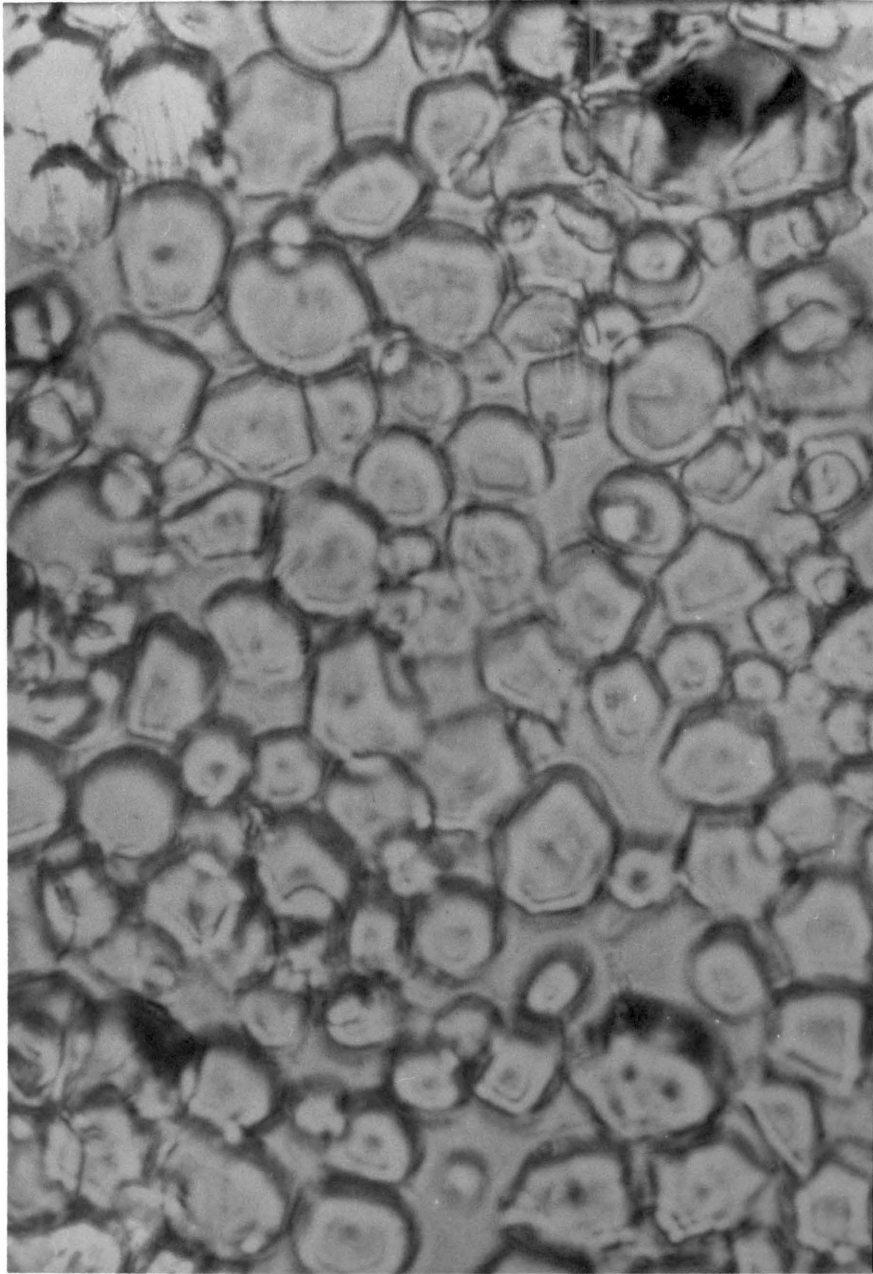
Figure 19   Photomicrograph of Starch Suspension

symbol	meaning	dimensionality
μ_{app}	apparent viscosity	$ML^{-1}T^{-1}$
μ_o	viscosity of medium	$ML^{-1}T^{-1}$
r	particle separation	L
$\dot{\gamma}$	shear rate	T^{-1}
ρ_o	density of medium	ML^{-3}

Following the procedures of dimensional analysis:

$$A = (ML^{-1}T^{-1})^{-a} (ML^{-1}T^{-1})^{b} (L)^{c} (T^{-1})^{d} (ML^{-3})^{e} \quad (1)$$

which gives the following set of equations when powers of M, L, and T are collected:

M : $0 = -a + b + e$

L : $0 = a - b + c - 3e$

T : $0 = a - b - d$

Solution of these equations for $\underline{b}$, $\underline{c}$ and $\underline{e}$ in terms of $\underline{a}$ and $\underline{d}$ yields:

$b = a - d$

$e = d$

$c = 2d$

When these values are substituted back into (1), there is found:

$$A = (\mu_{app})^{-a} (\mu_o)^{a-d} (r)^{2d} (\dot{\gamma})^{d} (\rho_o)^{d} \quad (2)$$

or:

$$A = (\mu_{app})^{-a} (\mu_o)^{a} \left(\frac{r^2 \dot{\gamma} \rho_o}{\mu_o} \right)^{d} \quad (3)$$

By taking the ath root of both sides and letting $d/a = n-1$, Equation (3) may be rearranged to give:

$$\mu_{app} = A' \mu_o \left(\frac{r^a \dot{\gamma} \rho_o}{\mu_o} \right)^{n-1} \qquad (4)$$

or alternately,

$$\mu_{app} = \left[A' (\mu_o)^{2-n} (r^a \rho_o)^{n-1} \right] (\dot{\gamma})^{n-1} \qquad (5)$$

It is now evident that Equation (5) fits the general form of the apparent viscosity term in the power law equation:

$$\tau = \mu_{app} \dot{\gamma}$$

and:

$$\tau = K (\dot{\gamma})^n = K \left[(\dot{\gamma})^{n-1} \right] (\dot{\gamma})$$

therefore:

$$\mu_{app} = K (\dot{\gamma})^{n-1} \qquad (6)$$

Comparison of Equations (4), (5) and (6) reveals that the term in brackets in Equation (5) is no more or less than the power law constant, $\underline{K}$. Since it is known that μ_{app} must equal μ_o for $\underline{n} = 1$ (Newtonian fluid), it is also known that the constant A' must be equal to one. The terms $(r^a \rho_o)^{n-1}$ and $(\dot{\gamma})^{n-1}$ disappear in this case and the Newtonian equation results.

Particular notice should also be made of Equation (4) and the fact that the dimensionless group in parentheses bears a resemblance to the Reynolds number, with the term

$r\dot{\gamma}$ representing a velocity. Such a group was given the name "internal Reynolds number" by Krieger[27] in his analysis of colloid rheology. The apparent viscosity is seen to be a function of the viscosity of the medium and this internal Reynolds number.

The dependency of the power law parameter, $\underline{K}$, on temperature and dispersed phase concentration can be predicted from inspection of Equation (4):

$$K = \mu_o\left(\frac{r^2 \rho_o}{\mu_o}\right)^{n-1} \tag{7}$$

For the case of the temperature dependency of $\underline{K}$, $\underline{r}$ and ρ_o are seen to be constant (an approximation for the case of ρ_o) which means that $\underline{K}$ becomes only a function of the viscosity of the medium, μ_o, raised to the power 2.-n. Since $\underline{n}$ has been found to be independent of temperature over small ranges of temperature, $\underline{K}$ becomes dependent only on viscosity. It is not surprising then that the activation energy for the "viscosity" of the suspension is nearly equal to this same property of the medium. The small changes in $\underline{n}$ with temperature found by some investigators over large temperature ranges[36,50] may well be the result of small changes in density, an affect that would be too small to measure over small ranges of temperature.

For the case of the concentration dependency of $\underline{K}$, the density and viscosity of the medium are fixed, but $\underline{n}$ and

the characteristic distance, $\underline{r}$, are variable:

$$K = (\eta_o)^{2-n} (\rho_o)^{n-1} (r^2)^{n-1}$$

Since the average distance between dispersed particles would decrease with concentration and $\underline{n}$ would increase, it can be seen that the magnitude of $\underline{K}$ would decrease as concentration increases. This prediction is verified by the data of Figure 9, page 51.

In summary, it has been shown that the proposed theory of dilatancy, where a characteristic average interparticle distance is assigned to each system, depending on the interfacial relationship between phases and the relative quantity of dispersed phase, leads to an expression for μ_{app} which is identical with the experimentally verified Power Law expression. Further, this expression predicts the correct variation of $\underline{K}$ with temperature and concentration but fails to predict how $\underline{n}$ would change with finite changes in concentration of the dispersed phase.

However, it is probable that $\underline{n}$ is not only a function of concentration of the dispersed phase, but is also dependent upon rate of shear. Rheologists have long believed that all fluids (and solids) are viscoelastic in behavior. As a result, the deformation of any fluid from the imposition of a stress is the sum of an elastic deformation, which is recoverable, and viscous flow which is not recoverable. For fluids of low viscosity at moderate rates

of shear, the elastic recovery is extremely rapid, and the
relaxation time is extremely short. As a result, the
elastic portion of the deformation is too small to measure,
and the fluid is considered to be simply viscous. In the
case of concentrated and well dispersed suspensions, there
is particle interference analogous to the chain entangle-
ments in solutions of amorphous polymers, and like polymer
solutions, rate of deformation becomes important in deter-
mining flow behavior.

The fracture observed by many investigators[40,26]
in highly dilatant suspensions at high rates of shear is
believed to be a manifestation of viscoelastic behavior; in
this case, the reciprocal shear rate is exceeded by the relax-
ation time with the result that the suspension behaves as a
solid, its shear strength is exceeded, and fracture occurs.
The gel-like structure resulting when more than about 50 vol-
ume per cent of starch is present in aqueous glycol or gly-
cerine solutions has pronounced viscoelastic properties even
at shear rates approaching zero. In the light of the theory
of dilatancy proposed here, this gel-like state is viewed as
resulting from interactions of adsorbed layers, with London
or Van der Waal forces giving rigidity to the structure.

Mixing of Dilatant Fluids. A short investigation of
the agitation of dilatant fluids was performed in conjunction
with this study. The results of that investigation are pre-

sented in Appendix B, together with a discussion of the
implications of the results of that investigation on the
flow of dilatant fluids.

Limitations

This investigation was performed under the following limiting conditions.

Dilatant Fluids.   The dilatant fluids studied were confined to those which employed corn starch as the dispersed phase and water, ethylene glycol, glycerine, or a combination of these liquids as the continuous phase.   The concentration of dispersed phase to continuous phase was limited to the range of 38-49 per cent by weight, inclusively.

Flow Behavior Index, n.   Flow behavior incexes between 1.15 and 2.50 were studied in pipe flow; flow behavior indexes between 1.10 and 5.30 were studied viscometrically.

Flow Consistency Index, K.   The pipe flow study included fluids with flow consistency indexes between 1.08 x 10^{-3} and 4.38 x 10^{-6} lb_f-sec^n/ft^2.   Values of flow consistency index between 1.08 x 10^{-3} and 9.00 x 10^{-6} were studied viscometrically.

Temperature.   The flow test temperatures were determined by other operating conditions and included the range of temperatures between 80-120°F.   For the study of the Power Law parameters as a function of temperature, the temperature range studied was 80-130°F.

Reynolds Numbers.   The obtainable Reynolds numbers were limited by the motive force available with the Moyno

pump, the method of varying flow rates which affected the
minimum flow rate, and the characteristics of the fluid
pumped. Modified Reynolds numbers in the range of 12-410
were investigated.

Pipe Size. This study was limited to the flow of
dilatant fluids in one type of conduit: 1-¼ inch, Schedule
40 galvanized pipe.

Fittings. Fittings studied included an 1-¼ inch gal-
vanized coupling; an 1-¼ inch galvanized, 90 degree standard
radius elbow; and a bronze globe valve.

Flow Curve Measurement. Flow curves were measured
with a cone and plate viscometer fabricated by adding cone
and plate components to a standard Stormer viscometer.

Recommendations

It is a natural consequence of an investigation of
any magnitude that more questions will arise as a result of
the investigation than will have been answered. It is the
purpose of this section to outline areas of investigation
that will be of value in further understanding the flow
of dilatant fluids.

Pipe-Flow of Dilatant Fluids. This investigation
has firmly established the experimental validity of the
Metzner-Reed correlation for dilatant, non-Newtonian fluids
in laminar pipe flow. Further work should be concerned

with flow in the transition and turbulent flow regions. It can be shown that fluids studied in this investigation can be used to attain high Reynolds numbers without encountering excessively high pressure drops.

It is unlikely that the present system of determining flow curves, i.e., the cone and plate viscometer, will be useful for characterizing dilatant fluids at the high shear rates expected for turbulent flow. For turbulent flow, fluids with very low K values will be employed, which may allow the capillary viscometer to be used for determining flow curves.

Pressure Drop Through Fittings. In view of the somewhat anomalous results obtained from the study of the flow of dilatant fluids through fittings, it would be of interest to broaden the study by taking additional measurements and by using other fitting types. In addition, any future study should include calibration of each fitting type with a Newtonian fluid so that comparisons with reported values are not mandatory.

Temperature Dependency of the Power Law Constants. The independency of temperature and the flow behavior index, n, is suggested from the results of this study. However, before such a conclusion can be made, several other dilatant fluids with different n values should be studied. In particular, a dilatant fluid employing an inorganic pigment, such as TiO_2, should be considered so that higher temperatures

can be studied. Higher degrees of dilatancy should also
be studied.

A point worth further investigation concerning the flow
consistency index, $\underline{K}$, is the apparent parallelism between
its behavior with temperature and the behavior of the sus-
pending medium. Tests designed to further explore this
parallelism would be of value in corroborating the proposed
mechanism of dilatancy.

Theory of Dilatancy. Of fundamental importance in
testing the proposed theory of dilatancy is the experimental
proof of adsorbed layers of solvent on the particles of the
dispersed phase in a dilatant suspension. Since no known
direct methods are available for detecting this adsorbed
layer, recourse must be made to indirect methods. A method
that suggests itself is that of calculating a hydrodynamical
particle radius from Einstein's dilute suspension theory
and viscometric measurements, and comparing this radius with
the known radius of the dispersed particles. Furthermore,
once this hydrodynamical radius has been found, the charact-
eristic distance between particles can be calculated and the
correctness of the dimensional analysis tested.

V. CONCLUSIONS

The conclusions drawn from the results found in the different phases of this investigation are presented in the following paragraphs.

Laminar Flow of Dilatant Fluids

It has been shown that for dilatant suspensions of starch in water, ethylene gylcol, and glycerine, with degrees of dilatancy of $n = 1.15-2.50$, flowing in a 1-¼ inch pipeline that:

1. The correlation method of Metzner-Reed satisfactorily correlates all the data to a single curve of friction factor versus modified Reynolds number.

2. Values for pressure drop across fittings were found to be different from those reported in the literature for Newtonian fluids, and were generally flow rate dependent.

The Power Law Parameters as a Function of Temperature

The determination of the flow curves of a dilatant starch/glycol/glycerine mixture in the proportion of 40/30/30 by weight, between the temperatures of 80-130°F, led to the following conclusions:

1. The flow behavior index, n, was independent of temperature over the range of temperature tested.

2. The flow consistency index, $\underline{K}$, was temperature dependent, with the data fitting an Arrhenius plot.

3. The activation energy for the flow of this fluid was found to be approximately equal to that of the solvent composition of the fluid.

Applicability of Power Law

These dilatant fluids were found to fit the Power Law Model over the limited range of shear rates studied, approximately $0.1-1000 \text{ sec}^{-1}$.

Viscometry

It was concluded from this investigation that the Stormer, capillary and Brookfield viscometers were not suited to the study of highly viscous dilatant fluids.

Mechanism of Dilatancy

A resolution of the reported discrepancies for the flow of dilatant fluids was made possible by postulating the existence of adsorbed layers of solvent on the surface of the dispersed phase. This proposed mechanism is not contradicted by any of the observed dilatant phenomena.

VI. SUMMARY

The purpose of this investigation was to test the existing methods of correlating pipe-line data on dilatant fluids in laminar flow, to gather pertinent physical properties of dilatant fluids, and to propose a theory for the mechanism of dilatancy.

In order that the correlation for flow of dilatant fluids in conduits could be tested it was necessary to build a flow apparatus from which pressure drops and flow rates could be measured, to develop viscometric equipment such that flow curves could be determined at shearing conditions similar to those in the flow tests, and to use the data from the two sources to calculate the variables of interest: the friction factor, f, and the modified Reynolds number, R_e'.

A flow apparatus suitable for the purpose outlined was constructed from 1-$\frac{1}{4}$ inch, Schedule 40 galvanized pipe with motive power provided by a Moyno pump, was provided with temperature control and calming sections, and was provided with a ten foot test section. Flow curves were determined independently with a specially constructed cone and plate viscometer. Provisions were made to determine pressure drop over the fittings: coupling, globe valve, and 90 degree elbow. Dilatant fluids consisting of corn starch suspended in the liquids water, ethylene glycol, and glycerine with

values of flow behavior index, $\underline{n}$, from 1.15-2.50 flowing in laminar flow between $\overset{\shortmid}{Re}$ of 12-410 were studied. Results of the investigation showed that the Metzner-Reed correlation method could be used in correlating dilatant, laminar flow. Equivalent resistances of fittings, expressed as equivalent diameters of pipe, were found not to match those found in the literature for Newtonian fluids, except that for the case of couplings the value was negligible for both fluid types. Rather, much lower values were found for the case of flow through a globe valve, and the value found for the 90 degree elbow was strongly dependent on the flow rate.

A cone and plate viscometer was used to study the dependency of the Power Law parameters on temperature for a starch suspension in glycerine and ethylene glycol. The parameter $\underline{n}$ was found to be independent of temperature over the 80-130°F range of temperature studied. Conversely, $\underline{K}$ varied with temperature in a manner described by an Arrhenius equation and its rate of change with temperature roughly paralleled that of the glycerine.

A theory of the basic mechanism responsible for the phenomenon of dilatancy was presented and discussed, and its relation to the Power Law Model established.

VII. BIBLIOGRAPHY

1. Bird, R.B., W.S. Stewart and E.N. Lightfoot: "Transport Phenomena", p.5, John Wiley and Sons, New York, N.Y., 1960. 1 ed.

2. Bogue, D.C.: Entrance Effects and Prediction of Turbulence in Non-Newtonian Flow, Ind. Eng. Chem., 51, 874-878 (1959).

3. Daniel, F.K.: India Rubber World, 102, no.4, 33-37 (1940).

4. de Bruijn, H. and P.G. Meerman: "Proceedings of the International Rheological Congress", p.160, Interscience Publishing Co., New York, N.Y., 1948. 1 ed.

5. Deryagin, B.V.: Transactions of the Faraday Society, 36, 203 (1940).

6. Deryagin, B.V., G. Strakhovskii and D. Malysheva: Acta Physicochim. URSS, 19, 541-52 (1944); C.A., 39, 2919-20 (1945).

7. de Waele, A.: Journal of the American Chemical Society, 48, 2772 (1926).

8. de Waele, A. and G. Lewis: Kolloid Z., 48, 126 (1929).

9. Dodge, D.W.: Turbulent Flow of Non-Newtonian Fluids in Smooth Round Pipes. Unpublished Ph.D. Thesis, University of Delaware, Newark, Delaware.

10. Dodge, D.W. and A.B. Metzner: Turbulent Flow of Non-Newtonian Systems, A.I.Ch.E. Journal, 5, no.2, 189-204 (1959).

11. Drew, T.B., et.al.: Flow of Fluids, "Chemical Engineer's Handbook" (J.H. Perry, Editor), p.389, McGraw-Hill Book Co., Inc., New York, N.Y., 1950.

12. Fischer, E.K.: "Colloidal Dispersions", p. 160-205, John Wiley and Sons, New York, N.Y., 1950. 1 ed.

13. ibid, p. 160-168.

14. ibid, p. 197.

15. ibid, p. 198.

16. ibid, p. 201.

17. ibid, p. 202.

18. ibid, p. 203-205.

19. Freundlich, H.: "Thixotropy", Hermann and Cie, Paris, France, 1935. 1 ed.

20. Freundlich, H. and A. Jones: Sedimentation Volume, Dilatancy, Thixotropic and Plastic Properties of Concentrated Suspensions, Journal of Physical Chemistry, 40, 1217-36 (1936).

21. Freundlich, H. and H.L. Roder: Dilatancy and Its Relation to Thixotropy, Trans. Faraday Soc., 34, 308-316 (1938).

22. Gallay, W. and I.E. Puddington: Canadian Journal of Research, 22B, 161-72 (1944).

23. Gunnerson, H.L. and J.P. Gallagher: Non-Newtonian Flow Behavior of Vinyl Resin Plastisols, Ind. Eng. Chem., 51, 854-855 (1959).

24. Hardy, W.: Transactions of the Royal Society (London), A230, 1-37 (1931).

25. Harkins, W.D. and G. Jura: Extension of the Attractive Energy of a Solid Into an Adjacent Liquid or Film, Am. Chem. Soc. J., 66, 923 (1944).

26. Jobling, A. and J.E. Roberts: Some Observations on Dilatancy and Thixotropy, "Rheology of Disperse Systems", (C.C. Mill, Editor), p. 127-138, Pergamon Press, New York, N.Y., 1959. 1 ed.

27. Krieger, I.M.: A Dimensional Approach to Colloid Rheology, Trans. Soc. Rheology, VII, 103 (1963).

28. Linford, A.: "Flow Measurement and Meters", E. and I. N. Spon, Ltd., London, 1961. 2 ed.

29. Markovitz, H. et. al.: Review of Scientific Instruments, 23, 430 (1952).

30. Mason, S. and W. Bartok: The Behavior of Suspended Particles in Laminar Shear, "Rheology in Disperse Systems", (C.C. Mill, Editor), p. 20, Pergamon Press, New York, N.Y., 1959. 1 ed.

31. ibid, p. 32.

32. ibid, p. 44.

33. McCabe, W.L. and J.C. Smith: "Unit Operations of Chemical Engineering", p. 912, McGraw-Hill Book Co., Inc., New York, N.Y., 1956. 1 ed.

34. ibid, p. 56.

35. ibid, p. 159.

36. Metzner, A. B.: Non-Newtonian Technology: Fluid Mechanics, Mixing and Heat Transfer, "Advances in Chemical Engineering", Vol. I (T.B. Drew and J.W. Hoopes, Jr., Editors), p. 77-153, Academic Press, Inc., New York, N.Y., 1956. 1 ed.

37. _____: Pipeline Design for Non-Newtonian Fluids, Chemical Engineering Progress, 50, 27-34 (1954).

38. Metzner, A.B. and R.E. Otto: Journal of the American Institute of Chemical Engineers, 3, 3 (1957).

39. Metzner, A.B. and J.C. Reed: Flow of Non-Newtonian Fluids: Correlation of the Laminar, Transition and Turbulent Flow Regions, A.I.Ch.E. Journal, 1, 434-440 (1955).

40. Metzner, A.B. and M. Whitlock: Flow Behavior of Concentrated (Dilatant) Suspensions, Trans. Soc. Rheology, Vol. II, p. 239-254, 1958.

41. ibid, p. 241-242.

42. ibid, p. 249-251.

43. ibid, p. 250.

44. Mooney, M.: Journal of Rheology, 2, 210 (1931).

45. Needs, S.J.: Transactions of the American Society of Mechanical Engineering, 62, 336-338 (1940).

46. Oka, S.: Principles of Rheology, "Rheology", Vol. 3, (F.R. Eirich, Editor), Academic Press, New York, N.Y., 1960. 1 ed.

47. Ostwald, W.: Kolloidzschr., 38, 261 (1926).

48. Pryce-Jones, J.: The Flow of Suspensions, Thixotropy and Dilatancy, Proc. Univ. Durham Phil. Soc., Vol. X, part 6, p. 427-67 (1948).

49. Rabinowitsch, B.: Z. Phys. Chem., A145, 1 (1929).

50. Reed, J.C.: Unpublished Ph.D. Thesis, University of Delaware, Newark, Delaware.

51. Reiner, M.: "Deformation and Flow", Lewis Co., London, 1949. 1 ed.

52. Reynolds, O.: Philosophical Magazine, 8, 20 (1885).

53. Segur, J.B. and H.E. Oberstar: Viscosity of Glycerol and Its Aqueous Solutions, Ind. Eng. Chem., 43, 2117-20 (1951).

54. Severs, E.T.: Molten Polymers, "Rheology of Polymers", p. 30, Reinhold Publishing Corp., New York, N.Y., 1962. 1 ed.

55. Sweeney, K. and R. Geckler: Rheology of Suspensions, J. Appl. Phys., 25, 1143 (1954).

56. Toms, B.A.: "Proceedings of the First International Congress on Rheology", Scheveningen, 1948.

57. Troskolanski, A.T.: "Hydrometry", Pergamon Press, London, 1960. 1 ed.

58. Verwey, E.J.W. and J. DeBoer: Rec. Tran. Chem., 57, 383 (1939).

59. Volkova, Z.: Acta Physicochim. URSS, 4, 635 (1936).

60. Weltman, Ruth N.: Ind. Eng. Chem., 48, 386 (1956).

61. Weltman, Ruth and T.A. Keller: N.A.C.A. Technical Note
No. 3889, 1957.

62. Wilkinson, W.L.: "Non-Newtonian Fluids", Pergamon
Press, New York, N.Y., 1960. 1 ed.

63. ibid, p. 4.

64. ibid, p. 28.

65. ibid, p. 32.

66. ibid, p. 66.

67. ibid, p. 76.

68. ibid, p. 121.

69. Williams, R.: J. Oil Coulor Chemists Association,
30, 116 (1922).

70. Williamson, R.V. and W.W. Heckart: Some Properties of
Dispersions of the Quicksand Type, Ind. Eng. Chem.,
23, 667-70 (1931).

71. Wilson, R. et. al.: Industrial and Engineering Chem-
istry, 14, 105 (1922).

VIII. ACKNOWLEDGMENTS

The two page vita has been removed from the scanned document. Page 1 of 2

X. APPENDIX A: VISCOMETRIC AND FLOW DATA

TABLE A1

Viscometric Data: Test No. 75

Test no.	Observed Results			Calculated Results		
	load gm	time sec	revolu- tions	rpm	$\dot{\gamma}$ sec^{-1}	τ lb$_f$/ft^2
75-1	600	30.9	30.0	58.2	210	0.878
-2	500	34.3	30.0	52.5	189	0.732
-3	400	39.0	30.0	46.1	166	0.586
-4	300	46.3	30.0	38.9	140	0.439
-5	200	39.3	20.0	30.6	111	0.293
-6	150	23.3	10.0	25.7	92.5	0.220
-7	100	30.6	10.0	19.6	70.5	0.146
-8	50	48.1	10.0	12.5	45.0	0.073

$n = n' = 1.60$

$K = 1.84 \times 10^{-4}$ lb$_f$-sec^n/ft^2

$K' = 1.57 \times 10^{-4}$ lb$_f$-sec^n/ft^2

Table A2

Flow Data: Test No. 75

	Observed Results						Calculated Results				
test no.	mass collected lb	time of collection sec	pressure drop in. CCl$_4$	pressure drop, ΔP lb$_f$/ft^2	mass flow rate lb/sec	average velocity, $\bar{V}$ ft/sec	$\bar{V}^2$ ft^2/sec^2	$\bar{V}^{2-n'}$ (ft/sec)$^{2-n'}$	$\Delta P/\bar{V}^2$ lb$_f$-sec^2/ft^4	f	Re'
75-1	25.0	17.8	33.5	82.8	1.404	1.760	3.100	1.254	26.7	0.0644	172.7
-2	25.0	21.7	26.4	65.2	1.150	1.440	2.075	1.157	31.4	0.0757	159.0
-3	25.0	23.6	22.8	56.4	1.059	1.324	1.754	1.119	32.2	0.0777	154.0
-4	25.0	25.3	20.8	51.4	0.988	1.237	1.530	1.089	33.6	0.0810	149.8
-5	30.0	31.9	19.4	47.9	0.940	1.176	1.383	1.067	34.7	0.0873	146.8
-6	25.0	31.1	15.8	39.0	0.804	1.006	1.013	1.000	38.6	0.0931	137.6
-7	20.0	27.3	14.2	35.1	0.732	0.918	0.837	0.965	42.0	0.1012	132.9
-8	20.0	29.7	12.5	30.9	0.673	0.845	0.711	0.934	43.5	0.1049	128.4
-9	20.0	31.6	11.0	27.2	0.633	0.795	0.627	0.911	43.5	0.1049	125.3
-10	15.0	25.4	9.8	24.2	0.590	0.740	0.545	0.886	44.4	0.1070	122.0
-11	20.0	37.1	8.4	20.8	0.539	0.675	0.455	0.855	45.7	0.1103	117.7
-12	20.0	39.8	7.6	18.8	0.502	0.628	0.394	0.830	47.7	0.1150	114.2
-13	25.0	18.2	35.0	86.5	1.373	1.720	2.958	1.242	29.2	0.0705	171.0
-14	20.0	18.2	24.6	60.8	1.100	1.376	1.894	1.136	32.2	0.0776	156.4
-15	20.0	24.5	16.6	41.0	0.816	1.022	1.046	1.010	39.0	0.0941	139.0
-16	20.0	30.6	11.8	29.2	0.654	0.818	0.670	0.922	43.5	0.1049	127.0

test fluid temperature: 96.0 °F
test fluid specific gravity: 1.231
manometer fluid: carbon tetrachloride (sp gr = 1.586)
manometer leads fluid: ethylene glycol (sp gr = 1.110)

Table A3

Flow Data: Test No. 81

Observed Results							Calculated Results				
test no.	mass collected lb	time of collection sec	pressure drop in. CCl4	pressure drop, ΔP lb$_f$/ft	mass flow rate lb/sec	average velocity, $\bar{V}$ ft/sec	$\bar{V}^a$ ft^a/sec^a	$\bar{V}^{a-n'}$ (ft/sec)$^{a-n'}$	$\Delta P/\bar{V}^a$ lb$_f$-sec^a/ft^4	f	Re'
81-3	20.0	13.50	32.4	60.2	1.481	1.870	3.496	1.870	17.2	0.0416	378
-5	20.0	15.40	29.2	54.3	1.299	1.642	2.700	1.642	20.2	0.0489	332
-7	20.0	30.50	15.3	28.5	0.655	0.827	0.684	0.827	41.7	0.1010	167
-9	20.0	20.80	21.4	39.8	0.961	1.214	1.473	1.214	26.9	0.0651	245
-11	25.0	22.70	25.0	46.5	1.100	1.391	1.936	1.391	24.0	0.0581	281
-13	25.0	30.10	19.2	35.7	0.831	1.050	1.103	1.050	32.5	0.0787	212
-15	20.0	19.60	22.2	41.3	1.020	1.290	1.665	1.290	24.9	0.0603	261
-17	20.0	40.00	10.5	19.5	0.500	0.632	0.400	0.632	48.8	0.1181	128
-19	20.0	27.80	16.0	29.8	0.719	0.909	0.826	0.909	36.1	0.0874	184

test fluid temperature: 92.0°F
test fluid specific gravity: 1.223
manometer fluid: carbon tetrachloride (sp gr = 1.581)
manometer leads fluid: test fluid

TABLE A4

Viscometric Data: Test No. 86

Test no.	Observed Results			Calculated Results		
	load gm	time sec	revolu- tions	rpm	$\dot{\gamma}$ sec^{-1}	τ lb$_f$/ft^2
86-24	200	60.3	60.0	59.7	215	0.293
-25	150	38.8	30.0	46.4	167	0.220
-26	100	55.6	30.0	32.4	117	0.146
-27	75	47.7	20.0	25.2	90.6	0.110
-28	50	67.6	20.0	17.8	64.0	0.073
-29	40	40.1	10.0	15.0	53.9	0.059
-30	30	54.3	10.0	11.1	39.8	0.044

$n = n' = 1.18$

$K = 5.22 \times 10^{-4}$ lb$_f$-sec^n/ft^2

$K' = 4.98 \times 10^{-4}$ lb$_f$-sec^n/ft^2

Table A5

Flow Data: Test No. 86

	Observed Results						Calculated Results				
test no.	mass collected lb	time of collection sec	pressure drop in. CCl$_4$	pressure drop, ΔP lb$_f$/ft^2	mass flow rate lb/sec	average velocity, $\bar{V}$ ft/sec	$\bar{V}^2$ ft^2/sec^2	$\bar{V}^{2-n'}$ (ft/sec)$^{2-n'}$	$\Delta P/\bar{V}^2$ lb$_f$-sec*/ft^4	f	Re'
86-2	15.0	10.60	18.0	54.3	1.415	1.784	3.180	1.607	17.1	0.0414	410
-3	10.0	14.20	7.1	21.4	0.705	0.889	0.789	0.915	27.1	0.0656	234
-5	15.0	10.90	16.4	49.5	1.376	1.735	3.010	1.571	16.4	0.0397	401
-6	15.0	13.10	14.0	42.3	1.144	1.442	2.080	1.350	20.4	0.0493	344
-8	15.0	13.30	13.2	39.8	1.128	1.421	2.020	1.334	19.6	0.0475	341
-9	10.0	13.80	6.9	20.8	0.725	0.914	0.837	0.929	24.8	0.0600	237
-11	10.0	10.40	11.7	35.4	0.962	1.212	1.470	1.172	24.1	0.0584	300
-12	10.0	11.90	10.3	31.1	0.840	1.058	1.120	1.047	27.8	0.0672	267
-14	10.0	12.00	10.4	31.4	0.833	1.050	1.103	1.041	28.6	0.0692	266
-15	10.0	12.30	9.8	29.6	0.813	1.023	1.046	1.019	28.3	0.0685	260
-17	10.0	14.75	5.9	17.8	0.678	0.855	0.730	0.876	24.4	0.0590	224
-18	10.0	12.80	7.5	22.6	0.782	0.985	0.970	0.988	23.3	0.0564	252

test fluid temperature: 96.0°F
test fluid specific gravity: 1.222
manometer fluid: carbon tetrachloride (sp gr = 1.586)
manometer leads fluid: water

TABLE A6

Viscometric Data: Test No. 87

	Observed Results			Calculated Results		
Test no.	load gm	time sec	revolu-tions	rpm	$\dot{\gamma}$ sec^{-1}	τ lb$_f$/ft^2
87-30	25	83.8	10.0	7.2	25.8	0.037
-31	35	66.2	10.0	9.1	32.7	0.051
-32	50	106.2	20.0	11.3	40.7	0.073
-33	75	83.6	20.0	14.4	51.7	0.110
-34	100	72.4	20.0	16.6	59.6	0.146
-35	150	57.9	20.0	20.7	74.6	0.220
-36	200	49.4	20.0	24.3	87.5	0.293
-37	300	39.7	20.0	30.2	109	0.439
-38	400	50.5	30.0	35.6	128	0.586
-39	500	44.3	30.0	40.7	147	0.732

$n = n' = 1.78$

$K = 10.22 \times 10^{-5}$ lb$_f$-sec^n/ft^2

$K' = 8.32 \times 10^{-5}$ lb$_f$-sec^n/ft^2

Table A7

Flow Data: Test No. 87

Observed Results   Calculated Results

test no.	mass collected lb	time of collection sec	pressure drop in. CCl_4	pressure drop, ΔP lb_f/ft^2	mass flow rate lb/sec	average velocity, $\bar{V}$ ft/sec	$\bar{V}^2$ ft^2/sec^2	$\bar{V}^{2-n'}$ $(ft/sec)^{2-n'}$	$\Delta P/\bar{V}^2$ $lb_f\text{-}sec^2/ft^4$	f	Re'
87-2	20.0	13.90	41.8	126.0	1.439	1.805	3.260	1.139	38.6	0.0930	138
-3	10.0	20.70	6.6	19.9	0.483	0.605	0.366	0.895	54.4	0.1310	108
-5	15.0	11.20	36.2	109.0	1.340	1.680	2.820	1.121	38.6	0.0930	136
-6	10.0	16.10	11.2	33.8	0.620	0.777	0.604	0.946	56.0	0.1350	115
-8	20.0	18.20	25.9	78.0	1.100	1.380	1.904	1.074	41.0	0.0988	130
-9	10.0	11.20	16.9	57.2	0.893	1.118	1.250	1.025	45.4	0.1094	124
-11	15.0	24.70	9.4	28.4	0.607	0.780	0.609	0.947	46.7	0.1126	115
-12	15.0	16.40	18.2	54.7	0.915	1.145	1.312	1.031	41.5	0.1000	125
-14	15.0	13.00	27.8	83.6	1.153	1.444	2.085	1.084	40.2	0.0970	131
-15	15.0	33.80	5.9	17.8	0.444	0.556	0.309	0.878	57.5	0.1388	106
-17	15.0	12.20	30.3	91.2	1.230	1.541	2.376	1.100	38.5	0.0928	133
-19	10.0	12.85	13.0	39.1	0.778	0.975	0.755	1.000	51.8	0.1250	121
-21	20.0	21.30	20.4	61.4	0.939	1.175	1.381	1.035	44.7	0.1080	125
-22	15.0	16.00	20.4	61.4	0.939	1.175	1.381	1.035	44.7	0.1080	125
-24	40.0	27.70	41.6	126.0	1.444	1.810	3.276	1.140	38.4	0.0925	138
-26	20.0	44.65	5.0	15.1	0.449	0.562	0.316	0.881	47.7	0.1150	107

test fluid temperature: 99.0°F
test fluid specific gravity: 1.230
manometer fluid: carbon tetrachloride (sp gr = 1.856)
manometer leads fluid: water

TABLE A8

<u>Viscometric Data: Test No. 88</u>

		Observed Results			Calculated Results	
Test no.	load gm	time sec	revolu-tions	rpm	$\dot{\gamma}$ sec^{-1}	τ lb$_f$/ft^2
88-10	50	52.4	10.0	11.4	41.2	0.073
-11	75	41.1	10.0	14.6	52.6	0.110
-12	100	69.4	20.0	17.3	62.3	0.146
-13	150	55.7	20.0	21.5	77.5	0.220
-14	200	47.7	20.0	25.2	90.7	0.293
-15	300	38.7	20.0	31.0	111.5	0.440
-16	400	33.1	20.0	36.3	130.7	0.586
-17	500	29.5	20.0	40.7	146.4	0.732

$n = n' = 1.79$

$K = 9.60 \times 10^{-5} \text{ lb}_f\text{-sec}^n/\text{ft}^2$

$K' = 7.80 \times 10^{-5} \text{ lb}_f\text{-sec}^n/\text{ft}^2$

Table A9

Flow Data: Test No. 88

	Observed Results						Calculated Results				
test no.	mass collected lb	time of collection sec	pressure drop in. CCl₄	pressure drop, ΔP lb_f/ft^2	mass flow rate lb/sec	average velocity, $\bar{V}$ ft/sec	$\bar{V}^2$ ft^2/sec^2	$\bar{V}^{2-n'}$ $(ft/sec)^{2-n'}$	$\Delta P/\bar{V}^2$ lb_f-sec^2/ft^4	f	Re'
88-2	30.0	21.50	48.0	145.0	1.395	1.739	3.020	1.122	48.4	0.1147	140.3
-4	15.0	35.70	5.8	17.5	0.420	0.523	0.274	0.873	63.9	0.1514	109.0
-6	15.0	25.40	11.0	33.2	0.591	0.735	0.540	0.937	61.5	0.1459	117.0
-8	30.0	24.30	37.9	114.0	1.234	1.537	2.365	1.094	48.7	0.1154	136.8
-10	30.0	27.60	30.0	90.5	1.088	1.355	1.837	1.067	48.9	0.1160	133.3
-12	20.0	24.65	17.4	52.5	0.811	1.010	1.020	1.000	51.5	0.1221	125.0

test fluid temperature: 104.0°F
test fluid specific gravity: 1.238
manometer fluid: carbon tetrachloride (sp gr = 1.856)
manometer leads fluid: water

TABLE   A10

Viscometric Data: Test No. 89

Test no.	Observed Results			Calculated Results		
	load gm	time sec	revolu- tions	rpm	$\dot{\gamma}$ sec^{-1}	τ lb$_f$/ft^2
89-10	50	51.5	10.0	11.6	41.6	0.073
-11	75	39.1	10.0	15.3	55.1	0.110
-12	100	67.3	20.0	17.8	64.3	0.146
-13	150	54.4	20.0	22.1	79.5	0.220
-14	200	46.7	20.0	25.7	92.5	0.293
-15	300	37.8	20.0	31.8	114.4	0.440
-16	400	32.9	20.0	36.5	131.4	0.586
-17	500	29.5	20.0	40.7	146.4	0.732

$n = n' = 1.82$

$K = 8.72 \times 10^{-5}$ lb$_f$-sec^n/ft^2

$K' = 7.00 \times 10^{-5}$ lb$_f$-sec^n/ft^2

TABLE A11

Viscometric Data: Test No. 90

Test no.	load gm	time sec	revolu- tions	rpm	$\dot{\gamma}$ sec^{-1}	τ lb$_f$/ft^2
		Observed Results			Calculated Results	
90-30	50	47.8	10.0	12.5	45.1	0.073
-31	75	39.0	10.0	15.4	55.4	0.110
-32	100	65.0	20.0	18.5	66.6	0.146
-33	150	52.5	20.0	22.9	82.5	0.220
-34	200	45.3	20.0	26.5	95.5	0.293
-35	300	37.0	20.0	32.4	116.5	0.440
-36	400	32.1	20.0	37.4	134.5	0.586
-37	500	28.8	20.0	41.7	150.0	0.732

$n = n' = 1.87$

$K = 5.99 \times 10^{-5}$ lb$_f$-sec^n/ft^2

$K' = 4.75 \times 10^{-5}$ lb$_f$-sec^n/ft^2

Table A12

Flow Data: Test No. 89&90

	Observed Results						Calculated Results				
test no.	mass collected lb	time of collection sec	pressure drop in. CCl_4	pressure drop, ΔP lb_f/ft^2	mass flow rate lb/sec	average velocity, $\bar{V}$ ft/sec	$\bar{V}^2$ ft^2/sec^2	$\bar{V}^{2-n'}$ $(ft/sec)^{2-n'}$	$\Delta P/\bar{V}^2$ $lb_f\text{-}sec^2/ft^4$	f	Re'
(test no. 89; fluid temperature: 106.2°F)											
89-2	25.0	17.65	41.8	126.3	1.417	1.764	3.110	1.110	40.6	0.0964	134.5
-4	15.0	34.10	5.7	17.2	0.440	0.548	0.300	0.897	57.3	0.1358	108.7
-6	30.0	24.70	32.5	98.1	1.214	1.512	2.285	1.078	42.9	0.1016	130.7
-8	20.0	22.90	17.6	53.1	0.873	1.087	1.182	1.015	45.0	0.1067	123.0
-10	20.0	22.35	18.9	57.1	0.895	1.114	1.240	1.024	46.0	0.1090	124.2
-12	15.0	21.30	12.2	36.8	0.705	0.878	0.772	0.977	47.8	0.1133	118.4
-14	25.0	25.50	23.0	69.5	0.980	1.220	1.489	1.037	46.7	0.1107	125.7
(test no. 90; fluid temperature: 110.2°F)											
90-2	25.0	17.75	35.0	105.7	1.408	1.752	3.070	1.076	34.4	0.0815	156.0
-4	15.0	30.85	6.1	18.4	0.486	0.605	0.366	0.937	50.3	0.1192	135.8
-6	15.0	13.45	23.9	72.1	1.114	1.388	1.926	1.044	37.4	0.0886	151.4
-8	20.0	24.10	14.0	42.2	0.830	1.033	1.066	1.000	39.4	0.0834	145.0
-10	30.0	24.10	28.6	86.3	1.245	1.550	2.403	1.059	36.0	0.0854	153.4

test fluid specific gravities: 1.238
manometer fluids: carbon tetrachloride (sp gr = 1.856)
manometer leads fluid: water

TABLE A13

Viscometric Data: Test No. 93

| | Observed Results | | | Calculated Results | | |
Test no.	load gm	time sec	revolu- tions	rpm	$\dot{\gamma}$ sec^{-1}	τ lb$_f$/ft*
93-40	600	27.3	30.0	65.9	237	0.878
-41	500	31.2	30.0	57.8	208	0.732
-42	400	35.8	30.0	50.3	181.0	0.586
-43	300	44.0	30.0	40.9	147.4	0.439
-44	250	49.2	30.0	36.6	131.8	0.366
-45	200	39.0	20.0	30.8	110.6	0.293
-46	150	47.2	20.0	25.4	91.5	0.220
-47	100	62.5	20.0	19.2	69.1	0.146
-48	50	76.0	20.0	15.8	57.0	0.110

$n = n' = 1.45$

$K = 3.15 \times 10^{-4}$ lb$_f$-sec^n/ft*

$K' = 2.80 \times 10^{-4}$ lb$_f$-sec^n/ft*

Table A14

Flow Data: Test No. 93

	Observed Results							Calculated Results				
test no.	mass collected lb	time of collection sec	pressure drop in. CCl_4	pressure drop, ΔP lb_f/ft^2	mass flow rate lb/sec	average velocity, $\bar{V}$ ft/sec	$\bar{V}^2$ ft^2/sec^2	$\bar{V}^{2-n'}$ $(ft/sec)^{2-n'}$	$\Delta P/\bar{V}^2_2$ lb_f-sec^2/ft^4	f	Re'
93-2	30.0	21.30	34.3	103.5	1.408	1.750	3.063	1.360	33.8	0.0798	199
-4	15.0	34.80	6.0	18.2	0.431	0.535	0.286	0.708	63.6	0.1500	103
-6	15.0	35.80	6.0	18.2	0.419	0.520	0.270	0.698	67.4	0.1590	102
-8	30.0	22.60	31.7	95.7	1.328	1.650	2.725	1.318	35.2	0.0830	192
-10	25.0	20.45	26.5	80.0	1.222	1.513	2.286	1.256	34.9	0.0824	183
-12	25.0	22.00	23.1	69.7	1.136	1.410	1.990	1.208	35.0	0.0826	176
-14	20.0	18.50	22.1	66.7	1.180	1.340	1.796	1.175	37.0	0.0873	172
-16	20.0	21.95	17.7	53.4	0.910	1.130	1.278	1.070	41.7	0.0985	156
-18	20.0	23.55	16.1	48.6	0.849	1.054	1.112	1.029	43.8	0.1035	150
-20	20.0	25.75	14.4	43.5	0.776	0.964	0.929	0.980	46.9	0.1107	143
-22	15.0	20.35	13.1	39.6	0.737	0.914	0.835	0.952	47.4	0.1119	139
-24	15.0	25.70	11.0	33.2	0.603	0.724	0.524	0.837	63.4	0.1496	122
-26	15.0	25.60	10.1	30.5	0.605	0.726	0.527	0.838	57.9	0.1367	122
-28	15.0	26.00	9.5	28.7	0.577	0.715	0.511	0.832	56.1	0.1324	121
-32	15.0	34.80	5.9	17.8	0.445	0.535	0.286	0.709	62.2	0.1469	103
-34	20.0	19.70	20.9	63.1	1.015	1.260	1.590	1.135	39.7	0.0937	166

test fluid temperature: 99.5°F
test fluid specific gravity: 1.235
manometer fluid: carbon tetrachloride (sp gr = 1.586)
manometer leads fluid: water

TABLE A15

Viscometric Data: Test No. 98

| Test no. | Observed Results | | | Calculated Results | | |
	load gm	time sec	revolu- tions	rpm	$\dot{\gamma}$ sec^{-1}	τ lb$_f$/ft*
98-30	200	37.1	5.0	8.1	29.1	0.293
-31	1000	47.8	20.0	25.1	90.4	1.464
-32	800	42.4	15.0	21.2	76.4	1.170
-33	600	52.6	15.0	17.1	61.5	0.879
-34	500	40.2	10.0	14.9	53.6	0.732
-35	400	47.4	10.0	12.7	45.7	0.586
-36	300	58.1	10.0	10.3	37.1	0.439

$n = n' = 1.37$

$K = 3.08 \times 10^{-3}$ lb$_f$-sec^n/ft*

$K' = 2.80 \times 10^{-3}$ lb$_f$-sec^n/ft*

Table A16

Flow Data: Test No. 98

	Observed Results							Calculated Results			
test no.	mass collected lb	time of collection sec	pressure drop in. CCl_4	pressure drop, ΔP lb_f/ft^2	mass flow rate lb/sec	average velocity, $\bar{V}$ ft/sec	$\bar{V}^2$ ft^2/sec^2	$\bar{V}^{2-n'}$ $(ft/sec)^{2-n'}$	$\Delta P/\bar{V}^u$ lb_f-sec^u/ft^4	f	Re'
98-2	20.0	14.7	9.1	595	1.360	1.595	2.550	1.342	233	0.524	29.2
-4	10.0	31.2	1.2	78	0.320	0.376	0.141	0.540	556	1.250	11.8
-6	15.0	19.1	4.0	262	0.785	0.920	0.846	0.949	310	0.696	20.7
-8	15.0	12.7	6.8	445	1.180	1.383	1.910	1.227	233	0.524	26.8
-10	10.0	19.0	2.3	151	0.526	0.617	0.380	0.738	398	0.895	16.1
-12	15.0	11.8	7.2	471	1.270	1.490	2.220	1.286	212	0.477	28.0
-14	10.0	21.6	2.0	131	0.463	0.543	0.295	0.680	445	1.000	14.9
-16	15.0	14.4	5.8	380	1.040	1.220	1.490	1.133	255	0.573	24.7
-18	10.0	17.6	2.4	157	0.566	0.665	0.442	0.733	356	0.800	16.9
-20	10.0	8.9	5.6	367	1.123	1.319	1.740	1.190	211	0.475	26.0
-22	10.0	15.6	2.8	183	0.641	0.752	0.565	0.835	324	0.728	18.2

test fluid temperature: 110.1°F
test fluid specific gravity: 1.305
manometer fluid: mercury (sp gr = 13.6)
manometer leads fluid: water

TABLE A17

Viscometric Data: Test No. 99

| | Observed Results | | | Calculated Results | | |
Test no.	load gm	time sec	revolu- tions	rpm	$\dot{\gamma}$ sec^{-1}	τ lb$_f$/ft*
99-30	200	24.4	5.0	12.2	44.1	0.293
-31	1000	45.1	30.0	40.0	144	1.464
-32	800	35.6	20.0	33.7	121	1.170
-33	600	44.5	20.0	27.0	97.2	0.879
-34	500	51.0	20.0	23.5	84.6	0.732
-35	400	30.2	10.0	19.9	71.6	0.586
-36	300	36.7	10.0	16.3	58.7	0.439

$n = n' = 1.35$

$K = 1.83 \times 10^{-3}$ lb$_f$-sec^{n}/ft*

$K' = 1.67 \times 10^{-3}$ lb$_f$-sec^{n}/ft*

Table A18

Flow Data: Test No. 99

	Observed Results					Calculated Results					
test no.	mass collected lb	time of collection sec	pressure drop in. $C_2H_2Br_4$	pressure drop, ΔP lb_f/ft^2	mass flow rate lb/sec	average velocity, $\bar{V}$ ft/sec	$\bar{V}^2$ ft^2/sec^2	$\bar{V}^{2-n'}$ $(ft/sec)^{2-n'}$	$\Delta P/\bar{V}^2$ lb_f-sec^2/ft^4	f	Re'
99-2	15.3	11.1	33.4	341	1.378	1.645	2.710	1.382	126	0.286	53.6
-4	10.0	32.2	4.0	40.8	0.310	0.370	0.137	0.524	298	0.676	20.3
-6	15.0	17.8	15.6	159	0.844	1.008	1.020	1.000	156	0.354	38.8
-8	8.0	21.0	7.0	71.5	0.381	0.455	0.207	0.600	345	0.785	23.3
-10	20.0	15.5	28.2	288	1.290	1.540	2.370	1.374	121	0.276	53.4
-12	15.0	13.2	24.0	245	1.136	1.356	1.850	1.222	132	0.300	47.5
-14	20.0	20.8	20.4	208	0.965	1.152	1.320	1.096	157	0.357	42.5
-16	20.0	22.8	17.6	180	0.880	1.050	1.100	1.032	164	0.373	40.0
-18	10.0	14.6	12.6	129	0.685	0.818	0.670	0.878	193	0.439	34.1
-20	15.0	24.9	10.6	108	0.602	0.719	0.517	0.807	209	0.475	31.3
-22	10.0	22.3	7.6	77.5	0.448	0.535	0.286	0.666	271	0.616	25.8
-24	10.0	32.0	5.2	53.1	0.312	0.373	0.139	0.527	382	0.868	20.4
-26	20.0	14.3	33.2	339	1.400	1.670	2.780	1.395	122	0.277	54.1

test fluid temperature: 114.2°F
test fluid specific gravity: 1.283
manometer fluid: tetrabromoethane (sp gr = 2.964)
manometer leads fluid: water

TABLE   A19

Viscometric Data: Test No. 100

	Observed Results			Calculated Results		
Test no.	load gm	time sec	revolu- tions	rpm	$\dot{\gamma}$ sec^{-1}	τ lb$_f$/ft^2
100-30	50	40.8	5.0	7.4	26.5	0.073
-31	800	37.8	40.0	63.5	229	1.170
-32	600	35.9	30.0	50.1	180	0.879
-33	400	32.9	20.0	36.5	131	0.586
-34	300	41.4	20.0	29.0	104	0.439
-35	200	56.0	20.0	21.4	77.0	0.293
-36	100	47.5	10.0	12.6	45.4	0.146

$n = n' = 1.29$

$K = 1.08 \times 10^{-3}$ lb$_f$-sec^n/ft^2

$K' = 1.00 \times 10^{-3}$ lb$_f$-sec^n/ft^2

Table A20

Flow Data: Test No. 100

	Observed Results							Calculated Results			
test no.	mass collected lb	time of collection sec	pressure drop in. $C_2H_2Br_4$	pressure drop, ΔP lb_f/ft^2	mass flow rate lb/sec	average velocity, $\bar{V}$ ft/sec	$\bar{V}^2$ ft^2/sec^2	$\bar{V}^{2-n'}$ $(ft/sec)^{2-n'}$	$\Delta P/\bar{V}^2$ $lb_f\text{-}sec^2/ft^4$	f	Re'
100-2	25.0	17.6	14.6	149.0	1.420	1.759	3.090	1.494	48.2	0.118	124.0
-4	15.0	36.4	3.1	31.6	0.412	0.510	0.260	0.620	121.5	0.286	51.4
-6	20.0	17.4	11.8	120.3	1.150	1.423	2.025	1.285	59.5	0.140	106.4
-8	15.0	15.2	9.6	98.0	0.987	1.221	1.491	1.152	65.7	0.154	95.6
-10	15.0	18.3	7.6	77.6	0.820	1.015	1.030	1.011	75.4	0.177	84.0
-12	20.0	25.4	7.2	73.5	0.788	0.975	0.950	0.982	77.4	0.182	81.4
-14	15.0	22.5	5.9	60.2	0.677	0.826	0.682	0.873	88.3	0.208	72.4
-16	15.0	32.2	4.2	42.9	0.466	0.576	0.331	0.676	129.6	0.307	56.0
-18	15.0	37.0	2.9	29.6	0.405	0.501	0.251	0.612	118.0	0.278	50.6
-20	20.0	14.3	14.6	149.0	1.400	1.733	3.004	1.478	49.6	0.117	122.4
-22	20.0	15.9	12.4	126.7	1.258	1.558	2.425	1.370	52.3	0.123	113.6
-24	20.0	21.5	8.8	89.8	0.930	1.151	1.325	1.105	67.8	0.159	91.6

test fluid temperature: 102.0°F
test fluid specific gravity: 1.260
manometer fluid: tetrabromothane (sp gr = 2.964)
manometer leads fluid: water

TABLE   A21

Viscometric Data: Test No. 114

| | Observed Results | | | Calculated Results | | |
Test no.	load gm	time sec	revolu- tions	rpm	$\dot{\gamma}$ sec^{-1}	τ lb$_f$/ft^2
114-50	50	30.0	5.0	10.0	36.0	0.073
-51	400	29.5	30.0	61.0	220.0	0.586
-52	300	31.8	25.0	47.2	170.0	0.439
-53	250	37.4	25.0	40.2	144.8	0.366
-54	200	36.2	20.0	33.1	119.2	0.293
-55	150	35.2	15.0	25.6	92.2	0.220
-56	100	33.0	10.0	18.2	65.5	0.146

$n = n' = 1.15$

$K = 1.19 \times 10^{-3}$ lb$_f$-sec^n/ft^2

$K' = 1.14 \times 10^{-3}$ lb$_f$-sec^n/ft^2

Table A22

Flow Data: Test No. 114

test no.	fitting type	mass collected lb	time of collection sec	pressure drop in. CCl₄	mass flow rate lb/sec	average velocity ft/sec	$\bar{V}^a$ ft^a/sec^a	$\bar{V}^{a-n'}$ (ft/sec)$^{a-n'}$	$(\Delta P)_{obs.}$ press. drop lb$_f$/ft^a	Re	$(f)_{calc.}$ friction factor	$(\Delta P/ft)_{calc.}$ lb$_f$/ft^3
114-2	valve	20.0	13.9	18.2	1.439	1.810	3.277	1.655	55.1	212.6	0.0752	10.30
-4	"	15.0	27.6	4.5	0.544	0.685	0.469	0.725	13.6	93.2	0.1717	3.36
-6	"	20.0	16.6	15.7	1.204	1.516	2.300	1.425	47.4	183.2	0.0874	8.40
-8	"	15.0	14.4	13.4	1.045	1.314	1.729	1.262	40.5	162.3	0.0986	7.11
-10	"	15.0	15.8	10.8	0.946	1.190	1.418	1.159	32.6	149.0	0.1074	6.36
-12	"	15.0	18.3	8.4	0.820	1.031	1.065	1.026	25.4	131.9	0.1212	5.40
-14	"	15.0	20.6	8.2	0.728	0.916	0.839	0.928	24.8	119.3	0.1340	4.69
-16	"	15.0	22.2	7.2	0.675	0.850	0.722	0.871	21.8	112.0	0.1430	4.31
-21	coupling	20.0	13.8	6.4	1.450	1.825	3.330	1.668	19.3	214.3	0.0747	10.40
-23	"	10.0	18.8	1.4	0.530	0.667	0.445	0.708	3.9	91.0	0.1760	3.26
-25	"	15.0	12.0	5.0	1.250	1.573	2.478	1.470	15.1	189.0	0.0846	8.75
-27	"	20.0	20.4	3.7	0.979	1.230	1.512	1.193	11.2	153.4	0.1044	6.60
-29	"	15.0	18.8	2.7	0.796	1.000	1.000	1.000	8.2	128.5	0.1245	5.20
-34	elbow	20.0	13.6	11.9	1.470	1.850	3.420	1.687	33.4	216.6	0.0739	10.54
-36	"	10.0	19.6	6.0	0.510	0.641	0.411	0.685	18.1	88.0	0.1820	3.12
-38	"	15.0	21.6	7.3	0.695	0.875	0.765	0.893	22.0	114.7	0.1396	4.46
-40	"	15.0	13.5	9.8	1.110	1.397	1.950	1.328	29.6	170.7	0.0938	7.64
-42	"	10.0	11.8	8.6	0.843	1.060	1.123	1.051	26.0	135.1	0.1183	5.55
-44	"	10.0	19.9	6.7	0.502	0.632	0.399	0.677	20.2	87.0	0.1840	3.07

test fluid temperature: 97.2°F
test fluid specific gravity: 1.240
manometer fluid: carbon tetrachloride (sp gr = 1.856)
manometer leads fluid: water

TABLE A23

Viscometric Data: Test No. 115

	Observed Results				Calculated Results	
Test no.	load gm	time sec	revolu- tions	rpm	$\dot{\gamma}$ sec^{-1}	τ lb$_f$/ft^2
(98.2°F)						
115-50	50	33.9	5.0	8.8	31.8	0.073
-51	600	32.9	30.0	54.7	197	0.878
-52	500	37.5	30.0	48.0	173	0.732
-53	400	29.2	20.0	41.1	148	0.586
-54	300	36.1	20.0	33.2	119	0.439
-55	200	36.1	15.0	24.9	89.6	0.293
-56	100	40.3	10.0	14.9	53.6	0.146
(96.5°F)						
-70	50	38.7	5.0	7.8	27.9	0.073
-71	600	35.1	30.0	51.3	185	0.878
-72	500	40.1	30.0	45.0	162	0.732
-73	400	31.4	20.0	38.2	137	0.586
-74	300	38.5	20.0	31.2	112	0.439
-75	200	38.6	15.0	23.4	84.3	0.293
-76	100	43.0	10.0	14.0	50.3	0.146

$n = n' = 1.36$

$K(96.5°F) = 7.51 \times 10^{-4}$ lb$_f$-sec^n/ft^2

$K'(96.5°F) = 6.86 \times 10^{-4}$ lb$_f$-sec^n/ft^2

$K(98.2°F) = 6.73 \times 10^{-4}$ lb$_f$-sec^n/ft^2

$K'(98.2°F) = 6.15 \times 10^{-4}$ lb$_f$-sec^n/ft^2

Table A24

Flow Data: Test No. 115

		Observed Results							Calculated Results			
test no.	fitting type	mass collected lb	time of collection sec	pressure drop in. CCl$_4$	mass flow rate lb/sec	average velocity ft/sec	$\bar{V}^2$ ft²/sec²	$\bar{V}^{2-n'}$ (ft/sec)$^{2-n'}$	$(\Delta P)_{obs.}$ press. drop lb$_f$/ft²	Re'	$(f)_{calc.}$ friction factor	$(\Delta P/ft)_{calc.}$ lb$_f$/ft³
115-2	elbow	20.0	14.0	11.3	1.430	1.792	3.215	1.456	34.1	132.0	0.1211	16.30
-3	"	12.0	26.4	5.5	0.455	0.571	0.326	0.697	16.6	63.2	0.2530	3.46
-5	"	20.0	16.0	9.6	1.250	1.568	2.456	1.336	29.0	121.0	0.1322	13.50
-6	"	10.0	12.7	6.5	0.787	0.987	0.973	1.000	19.6	90.6	0.1766	7.20
-8	"	15.0	13.6	8.3	1.106	1.387	1.924	1.235	25.0	112.0	0.1429	11.50
-9	"	15.0	17.0	7.3	0.882	1.106	1.223	1.067	22.0	96.7	0.1654	8.48
-12	coupling	20.0	14.2	9.2	1.403	1.760	3.100	1.440	27.8	130.4	0.1226	15.94
-13	"	12.0	24.6	2.2	0.488	0.612	0.374	0.728	6.6	66.0	0.2122	3.80
-15	"	20.0	15.8	7.6	1.270	1.593	2.540	1.350	22.9	122.4	0.1307	13.91
-16	"	22.0	17.7	5.8	1.242	1.560	2.435	1.332	17.5	120.8	0.1324	13.50
-18	"	15.0	16.3	5.1	0.920	1.153	1.330	1.096	15.4	99.3	0.1611	9.00
-19	"	15.0	23.7	3.3	0.633	0.794	0.630	0.862	10.0	78.1	0.2048	5.41
-20	"	10.0	22.2	2.2	0.450	0.564	0.318	0.691	6.6	62.6	0.2556	3.40
-22	valve	20.0	14.4	22.7	1.390	1.742	3.040	1.430	68.5	144.5	0.1108	14.10
-23	"	10.0	25.7	4.8	0.389	0.488	0.238	0.630	15.4	63.7	0.2510	2.50
-25	"	15.0	12.2	18.7	1.233	1.547	2.392	1.325	56.5	134.0	0.1194	12.00
-26	"	15.0	14.3	12.3	1.050	1.318	1.737	1.185	37.1	119.8	0.1335	9.71
-28	"	10.0	14.8	9.1	0.674	0.845	0.714	0.897	27.4	90.6	0.1766	5.28
-29	"	10.0	21.6	6.3	0.463	0.581	0.338	0.705	19.0	71.2	0.2248	3.19
-30	"	27.0	18.5	22.5	1.460	1.831	3.360	1.477	68.0	149.2	0.1072	15.10

test fluid specific gravity: 1.243
manometer leads fluid: water

TABLE A25

Viscometric Data: Test No. 116

Test no.	load gm	time sec	revolutions	rpm	$\dot{\gamma}$ sec^{-1}	τ lb$_f$/ft^2
	Observed Results			Calculated Results		
116-30	50	21.0	5.0	14.3	51.5	0.073
-31	600	34.5	30.0	52.2	188.0	0.879
-32	500	36.7	30.0	49.1	177.0	0.732
-33	400	27.3	20.0	44.0	158.4	0.586
-34	300	31.5	20.0	38.1	137.0	0.439
-35	200	19.3	10.0	31.1	112.0	0.293
-36	100	27.8	10.0	21.6	77.8	0.146

$n = n' = 2.50$

$K = 2.85 \times 10^{-6}$ lb$_f$-sec^n/ft^2

$K' = 2.42 \times 10^{-6}$ lb$_f$-sec^n/ft^2

Table A26

Flow Data: Test No. 116

	Observed Results						Calculated Results				
test no.	mass collected lb	time of collection sec	pressure drop in. CCl_4	pressure drop, ΔP lb_f/ft^2	mass flow rate lb/sec	average velocity, $\bar{V}$ ft/sec	$\bar{V}^2$ ft^2/sec^2	$\bar{V}^{2-n'}$ $(ft/sec)^{2-n'}$	$\Delta P/\bar{V}^2$ $lb_f\text{-}sec^2/ft^4$	f	Re'
116-2	25.0	16.6	25.0	75.5	1.504	1.880	3.535	1.000	21.3	0.0507	212
-4	12.0	21.8	5.2	15.7	0.549	0.686	0.471	1.000	33.3	0.0793	212
-5	20.0	19.4	14.4	43.5	1.033	1.290	1.665	1.000	26.1	0.0621	212
-7	20.0	18.2	16.2	48.9	1.100	1.374	1.890	1.000	25.9	0.0616	212
-8	20.0	32.8	6.5	19.6	0.610	0.762	0.580	1.000	33.8	0.0805	212
-10	20.0	17.8	17.1	51.6	1.120	1.400	1.960	1.000	26.3	0.0625	212
-11	10.0	15.2	7.2	21.8	0.660	0.825	0.681	1.000	32.0	0.0762	212
-13	20.0	24.0	10.2	30.8	0.833	1.042	1.087	1.000	28.3	0.0674	212
-15	10.0	16.4	6.6	19.9	0.608	0.760	0.578	1.000	34.4	0.0819	212
-17	20.0	24.6	9.3	28.1	0.811	1.014	1.030	1.000	27.3	0.0650	212
-18	10.0	11.1	10.2	30.8	0.901	1.127	1.270	1.000	24.2	0.0576	212
-20	20.0	21.2	11.8	35.6	0.944	1.180	1.392	1.000	25.6	0.0610	212
-21	25.0	19.2	18.8	56.8	1.300	1.625	2.640	1.000	21.5	0.0511	212

test fluid temperature: 97.0°F
test fluid specific gravity: 1.226
manometer fluid: carbon tetrachloride (sp gr = 1.856)
manometer leads fluid: water

TABLE A27

Viscometric Data: Test No. 117

	Observed Results			Calculated Results		
Test no.	load gm	time sec	revolu- tions	rpm	$\dot{\gamma}$ sec^{-1}	τ lb$_f$/ft^2
117-30	100	33.1	10.0	18.1	65.2	0.146
-31	800	43.5	30.0	41.4	149	1.170
-32	600	32.8	20.0	36.6	132	0.879
-33	500	36.1	20.0	33.2	120	0.732
-34	400	41.9	20.0	28.6	103	0.586
-35	300	36.6	15.0	24.6	88.6	0.439
-36	200	29.3	10.0	20.5	73.9	0.293

$n = n' = 2.50$

$K = 4.38 \times 10^{-6} \text{ lb}_f\text{-sec}^n/\text{ft}^2$

$K' = 2.92 \times 10^{-6} \text{ lb}_f\text{-sec}^n/\text{ft}^2$

Table A28

Flow Data: Test No. 117

	Observed Results						Calculated Results				
test no.	mass collected lb	time of collection sec	pressure drop in. CCl4	pressure drop, ΔP lb$_f$/ft^2	mass flow rate lb/sec	average velocity, $\bar{V}$ ft/sec	$\bar{V}^2$ ft^2/sec^2	$\bar{V}^{2-n'}$ (ft/sec)$^{2-n'}$	$\Delta P/\bar{V}^2$ lb$_f$-sec^2/ft^4	f	Re'
117-2	25.0	20.7	26.7	80.6	1.208	1.496	2.240	1.223	36.0	0.0850	133.5
-4	10.0	22.75	3.5	10.6	0.440	0.545	0.297	0.738	35.7	0.0842	221.2
-5	20.0	26.9	9.7	29.3	0.744	0.921	0.848	0.960	34.5	0.0814	170.2
-7	50.0	39.4	26.5	80.0	1.270	1.572	2.472	1.254	32.4	0.0765	129.9
-8	15.0	22.8	7.7	23.2	0.659	0.815	0.644	0.903	35.0	0.0826	181.1
-10	15.0	12.0	28.9	87.3	1.250	1.548	2.397	1.244	36.4	0.0859	131.4
-12	15.0	30.0	4.5	13.6	0.500	0.619	0.283	0.787	48.1	0.1134	207.4
-14	15.0	26.0	5.9	17.8	0.577	0.715	0.511	0.846	34.9	0.0824	193.2
-16	15.0	23.2	6.9	20.8	0.647	0.801	0.641	0.895	32.5	0.0767	182.6
-18	15.0	21.0	9.7	29.3	0.715	0.885	0.784	0.941	37.4	0.0882	173.9
-19	15.0	19.6	11.3	34.1	0.765	0.947	0.896	0.973	38.0	0.0897	168.2
-21	20.0	22.0	18.7	56.5	0.910	1.127	1.270	1.062	44.5	0.1050	154.0
-22	28.0	28.8	22.9	69.2	0.972	1.204	1.450	1.098	47.7	0.1124	149.0
-23	30.0	35.9	15.1	45.6	0.835	1.034	1.070	1.017	42.6	0.1004	160.8

test fluid temperature: 102.0°F
test fluid specific gravity: 1.238
manometer fluid: carvon tetrachloride (sp gr = 1.586)
manometer leads fluid: water

TABLE   A29

<u>Viscometric Data: Test No. 118</u>

Test no.	Observed Results			Calculated Results		
	load gm	time sec	revolutions	rpm	$\dot{\gamma}$ sec^{-1}	τ lb$_f$/ft^2
118-1	100	84.2	5.0	3.56	12.8	0.146
-2	200	41.9	5.0	7.16	25.8	0.293
-3	300	29.1	5.0	10.30	37.1	0.439
-4	400	42.0	10.0	14.30	51.5	0.586
-5	500	33.4	10.0	17.95	64.6	0.732
-6	600	56.0	20.0	21.4	77.0	0.878
-7	800	42.2	20.0	28.4	102.2	1.171
-8	1000	33.9	20.0	35.4	127.5	1.464

XI. APPENDIX B

The Mixing of Dilatant Fluids

Details concerning attempts to test the validity of using the Power Number correlation for the mixing of dilatant fluids are presented.

Introduction. While outlining methods for studying the flow of dilatant fluids in conduits, note was taken of the great similarity between the methods of correlating pipe flow data and of correlating mixing data. At that time, it was uncertain whether any data would be forthcoming from the study of the flow of dilatant fluids through conduits. Since such an apparent analogy between the two situations seemed to exist, it was decided to perform mixing experiments with the idea of obtaining some insight into the behavior that might be expected in flow experiments. A literature survey was made to aid in designing the experiments.

Literature Survey. Rushton[5] has reviewed the basic parameters of mixing and has concluded that they are too complex to treat mathematically. The use of the method of dimensional analysis to correlate the variables involved in the agitation of a singe-phase fluid in a baffled mixer leads to:

$$\frac{P\, g_c}{N^3 D^5} = \frac{C\, \rho\, N\, D^2}{g_c\, \mu_a}$$

where: P = power expended in mixing, ft-lb$_f$

ρ = density of fluid, lb$_m$/ft^3

N = stirrer speed, revolutions per second

D = stirrer diameter, ft

C = constant

μ_a = apparent viscosity of fluid, lb$_f$-sec/ft^2

g_c = gravitational constant, lb$_m$-ft/lb$_f$-sec

The expression on the left is dimensionless and is known as the power number, N_{po}. The expression on the right is, of course, a form of the Reynolds number, Re.

This method of correlation can be extended to non-Newtonian fluids by defining the apparent viscosity, μ_a, after Metzner and Otto[4]:

$$\mu_a = K\, (13N)^{n-1}$$

where: K = flow consistency index, lb$_f$-sec^n/ft^2

n = flow behavior index, dimensionless

This treatment assumes that the average shear rate near the impeller is equal to 13N. Calderbank and Moo-Young[1,2], in extending the work of Metzner and Otto found that the shear rate was more properly given by 12.8N x $(D_i/D_t)^{\frac{1}{2}}$, where D_i and D_t were impeller and tank diameters,

respectively. The curve of Rushton for Newtonian fluids
and that of Metzner and Otto for non-Newtonians is pre-
sented in Figure B-1. Foresti and Liu[3] have also
presented data on the mixing of dilatant fluids.

Experimental. A Chemineer Model ELB mixer/dynamometer
was used for this study; a picture of the apparatus is
given in Figure B-2. The ten inch torque arm of the dyna-
mometer was allowed to bear on the pan of an Ohaus beam
balance (not shown in Figure B2), thus transmitting the
torque imparted to the mixer from the mixing operation to
the balance. A Strobotac was used to measure the angular
velocity of the mixing shaft. Flow curves were determined
with a cone and plate viscometer.

The experimental procedure consisted of the measure-
ment of mixer speeds and corresponding weight readings. The
weight readings were based on a tare weight found by taking
the torque reading with mixer revolving in air. The value
of this tare reading was found to be independent of mixer
speed. The fluids tested were premixed in another container
and allowed to age for at least 15 hours before testing.
Samples of the test fluids were removed immediately after
testing and were used to establish flow curves at the same
temperature at which the mixing test was performed. In all
tests, the same total amount of fluid was agitated in the
twelve inch diameter mixing tank. Several impeller types
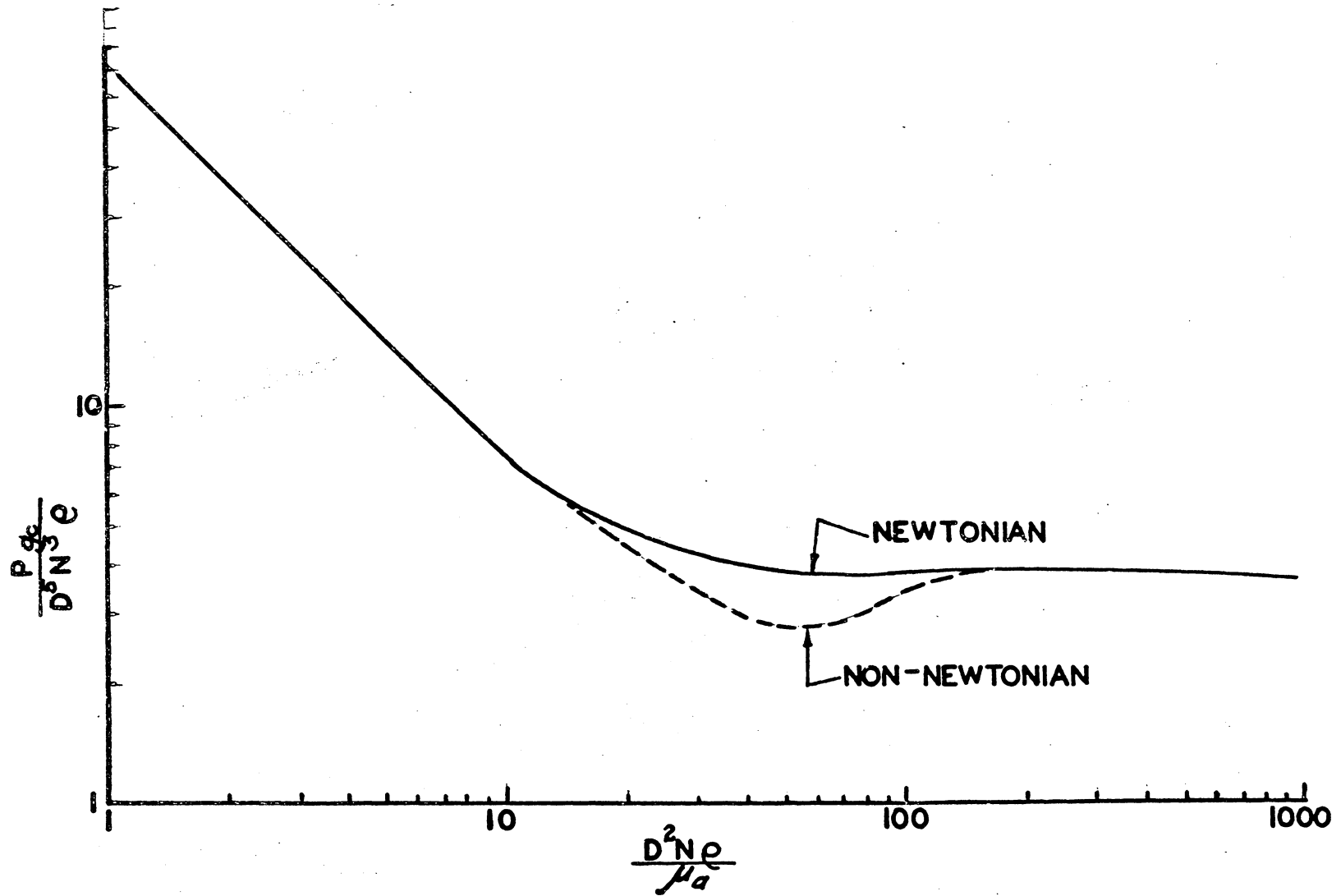and sizes were investigated for each fluid.

Figure B1   Comparison of Power Number Reynolds Number Correlations for New-
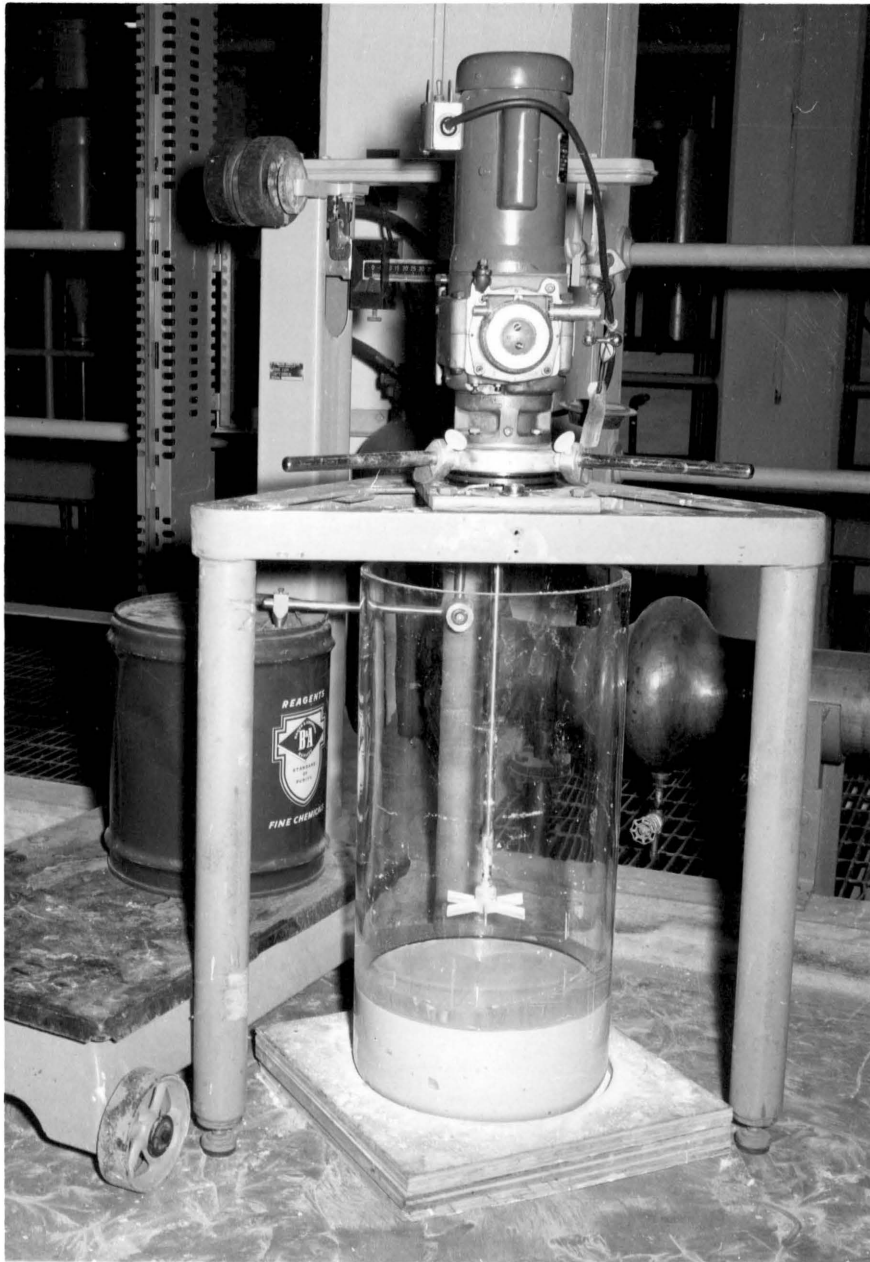tonian and Non-Newtonian Mixing Data

Figure B2   Mixing Test Apparatus

Results. Representative results of this investigation are presented in Figure B-3 as a plot of Power Number versus Reynolds Number; the solid line on that plot is the curve of Metzner and Otto for non-Newtonian fluids. It can be seen that the points do not fit the line.

Discussion. From the results of this investigation, as shown in Figure B-3, it can be concluded that the proposed correlation fails for the dilatant fluids tested here. Although many of the data points approach the theoretical curve, the preponderance of them do not.

Some insight into the cause of this discrepancy can be gained by plotting the torque (or load) readings against the stirrer speed on log-log coordinates for a given test and comparing the value obtained for the slope of such a line with the value of n obtained viscometrically. In order that the data truly fit the correlating line, the value of n determined in these two separate ways must be nearly identical. However, a plot of Tests 67 and 70, Figure B-4, shows that the data actually give a curved line on a log-log plot and only in the lower shear rate region is there any correspondence between n as measured in this manner and that measured viscometrically.

A special bob was made to use in these mixing studies since such a bob/mixer combination would represent a viscometer of the type classified as a bob rotating in an infinite
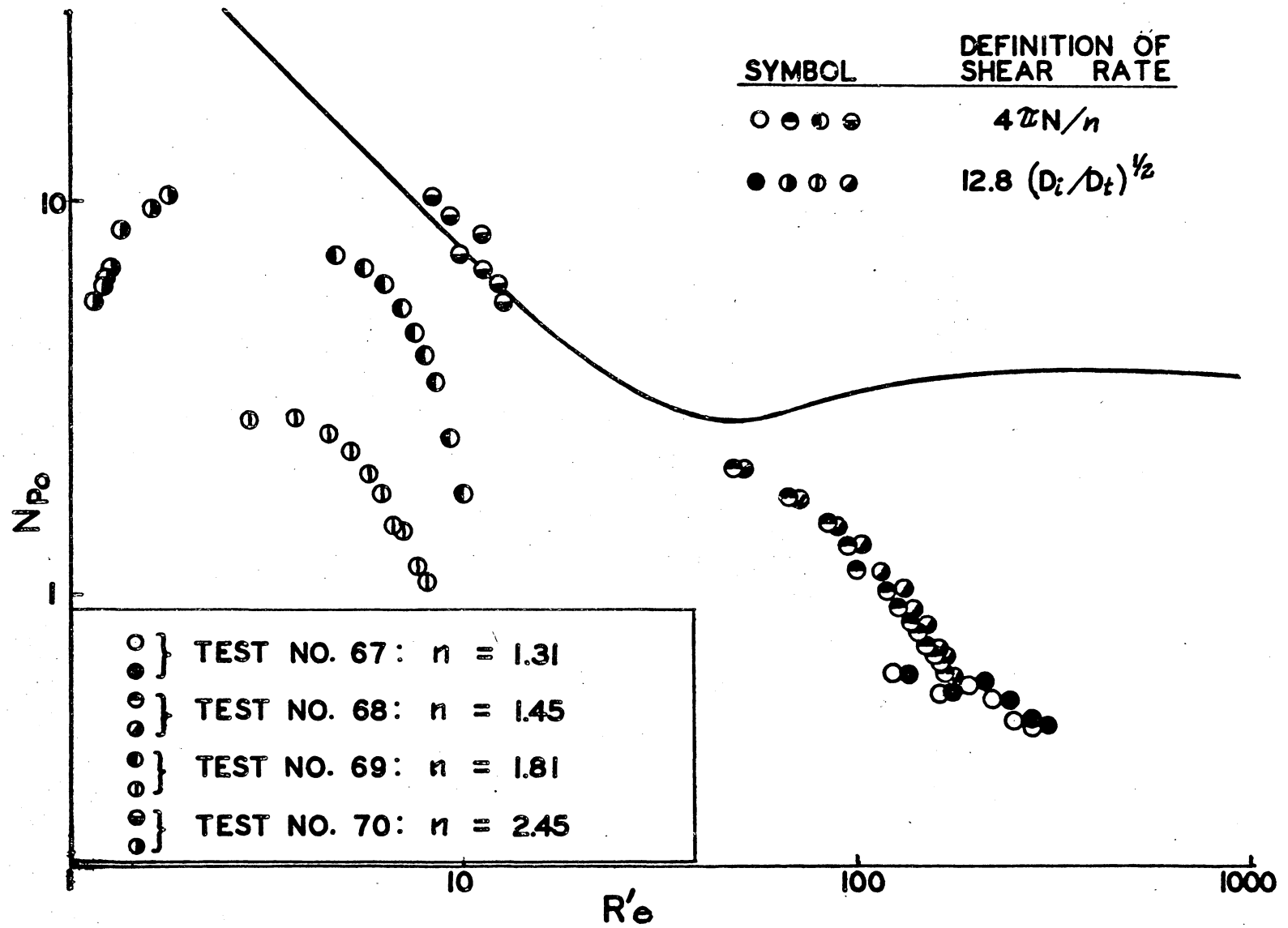
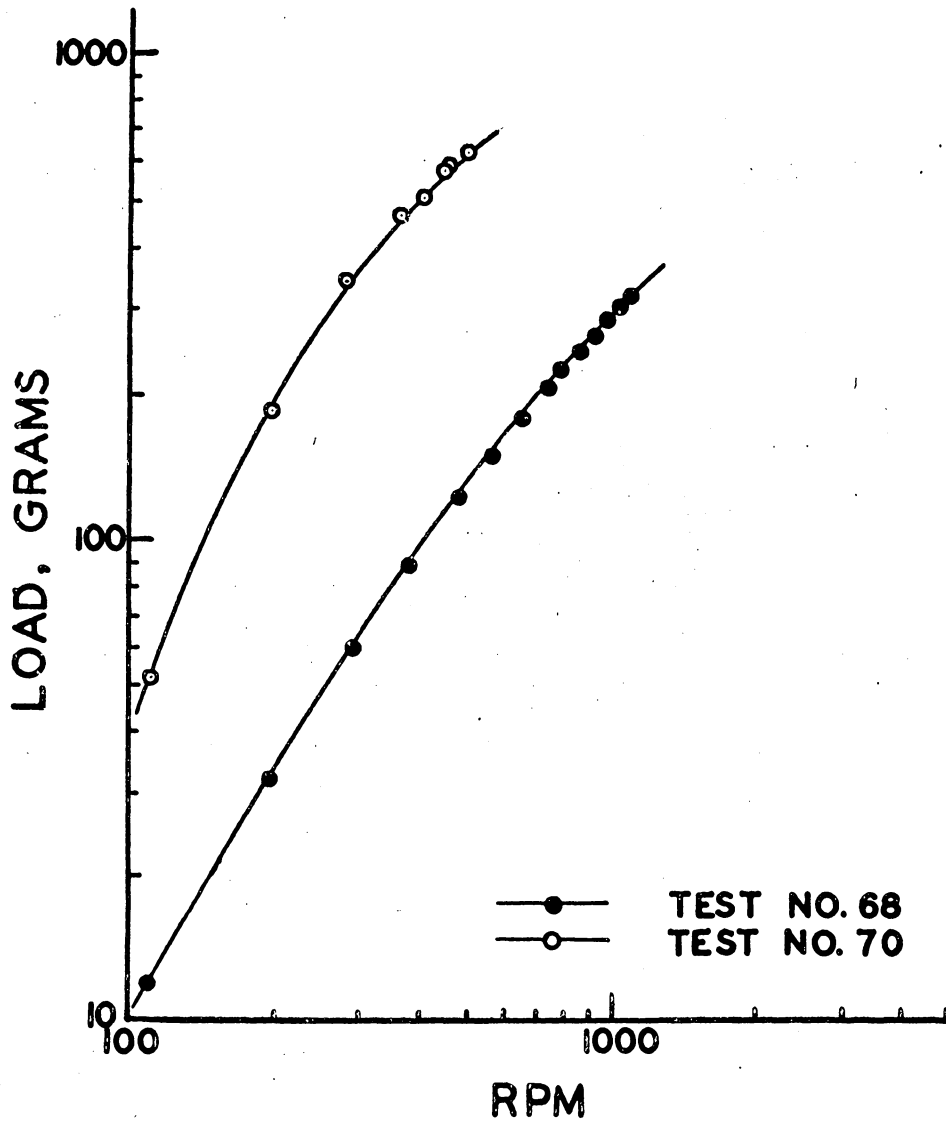Figure B3   Comparison of Experimental Data to Theoretical Curve.

Figure B4   Use of Mixing Data to Test Power Number
Reynolds Number Correlation

fluid. Wilkinson[6] has summarized the equations for the rate of shear and the shear stress at the bob surface:

$$\tau = G/2\pi R^2$$

$$\dot{\gamma} = \frac{4\pi N}{n}$$

where: τ = shear stress at bob surface, lb_f/ft^2

G = moment per unit height acting on bob, lb_f

$\dot{\gamma}$ = shear rate at bob, sec^{-1}

N = angular velocity of bob, revolutions per second

n = slope of log-log plot of torque versus speed

Using these relationships it should be possible to test the correlation with the bob data to see whether the variables included in the Reynolds Number and the Power Number are sufficient to correlate data from the mixing of dilatant fluids.

Subsequent agitation studies concerning dilatant fluids should be directed toward establishing what other parameters are of importance, with the object of finding a new correlation that will satisfactorily fit the data.

Mixing Bibliography

1. Calderbank, P.H. and M.B. Moo-Young: The Prediction of Power Consumption in the Agitation of Non-Newtonian Fluids, Trans. Inst. Chem. Engrs., 37, 31 (1959)

2. _____: The Power Characteristics of Agitators for the Mixing of Newtonian and Non-Newtonian Fluids, Trans. Inst. Chem. Engrs., 39, 22 (1961)

3. Foresti, R., Jr. and T. Liu: Agitation of Non-Newtonian Liquids, Industrial and Engineering Chemistry, 51, 860 (1959)

4. Metzner, A.B. and R.E. Otto: Journal of the American Institute of Chemical Engineers, 3, 3 (1957)

5. Rushton, J.H.: Chemical Engineering Progress, 54, 587 (1954)

6. Wilkinson, W.L.: "Non-Newtonian Fluids", p.26, Pergamon Press, London, 1960. 1 ed.

ABSTRACT

"A Fundamental Study of the Flow of Dilatant Fluids"

Richard G. Green

The purpose of this investigation was to test the existing methods of correlating pipe-line data on dilatant fluids in a laminar flow, to gather pertinent physical properties of dilatant fluids, and to propose a theory for the mechanism of dilatancy.

In order that the correlation for flow of dilatant fluids in conduits could be tested it was necessary to build a flow apparatus from which pressure drops and flow rates could be measured, to develop viscometric equipment such that flow curves could be determined at shearing conditions similar to those in the flow tests, and to use the data from the two sources to calculate the variables of interest: the friction factor, $\underline{f}$, and the modified Reynolds number, R_e'.

A flow apparatus suitable for the purpose outlined was constructed from 1-1/4 inch, Schedule 40 galvanized pipe with motive power provided by a Moyno pump, was provided with temperature control and calming sections, and was provided with a ten foot test section. Flow curves were determined independently with a specially constructed cone and plate viscometer. Provisions were made to determine pressure drop over the fittings: coupling, glove valve, and 90 degree elbow. Dilatant fluids consisting of corn starch suspended in the liquids water,

ethylene glycol, and glycerine with values of flow behavior index,

n, from 1.15-2.50 flowing in laminar flow between R'_e of 12-410 were studied. Results of the investigation showed that the Metzner-Reed correlation method could be used in correlating dilatant, laminar flow. Equivalent resistances of fittings, expressed as equivalent diameters of pipe, were found not to match those found in the literature for Newtonian fluids, except that for the case of couplings the value was negligible for both fluid types. Rather, much lower values were found for the case of flow through a globe valve, and the value found for the 90 degree elbow was strongly dependent on the flow rate.

A cone and plate viscometer was used to study the dependency of the Power Law parameters on temperature for a starch suspension in glycerine and ethylene glycol. The parameter n was found to be independent of temperature over the 80-130° F range of temperature studied. Conversely, K varied with temperature in a manner described by an Arrhenius equation and its rate of change with temperature roughly paralleled that of the glycerine.

A theory of the basic mechanism responsible for the phenomenon of dilatancy was presented and discussed, and its relation to the Power Law Model established.